

FOR REFERENCE

NOT TO BE TAKEN FROM THIS ROOM

FATIGUE CRACK PROPAGATION  
UNDER  
VARIABLE AMPLITUDE LOADING

by

Sami KAYA

Bogazici University Library



14

39001100315996

Submitted to the Faculty of the Engineering  
In Partial Fulfillment of the Requirements  
for the Degree of

MASTER OF SCIENCE

IN

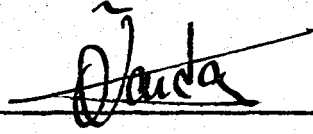
MECHANICAL ENGINEERING

BOĞAZIÇI UNIVERSITY

1983

THIS THESIS HAS BEEN APPROVED BY:

Doç.Dr.Öktem VARDAR  
(Thesis Supervisor)

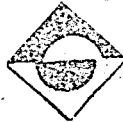
: 

Doç.Dr.M.Başar CIVELEK

: M. Başar Civelek

Dr.Sabri ALTINTAŞ

: S. Altıntaş



## ACKNOWLEDGEMENTS

I would like to express my gratitude and sincere thanks to Assoc.Prof.Öktem VARDAR, thesis supervisor, for his kind interest and guidance in the production of this work.

I am also indebted to Turkish Air Force who gave me opportunity to get my entire graduate education in the Faculty of Engineering at Boğaziçi University.

Sami KAYA

## ABSTRACT

In this thesis, the use of crack growth rate data and analytical retardation models in predicting crack growth under variable amplitude loading is reviewed. The effective stress model developed by Willenborg, et al. is described in detail, including the mathematical formulation. Comparison of test data and predictions for various loading programs are shown in figures.

All tests are carried out in an MTS fatigue testing machine with a maximum capacity of 10 tons. During each test, cycling is interrupted periodically to measure crack length (with a Gaertner Travelling Microscope, X10) and to note the associated number of applied cycles.

Compact tension specimen made of 2024-T4 aluminum alloy, are used throughout the tests. All tests are performed under ambient laboratory conditions. Eleven specimens are used to obtain the experimental data.

The results of the experimental program are used to review existing crack growth prediction models. In the logarithmic scale, crack growth rate vs. stress intensity factor range are plotted.

## ÖZET

Bu çalışmada, çatlak ilerleme hızı verileri ve analitik gecikme modellerinin, değişken genlikli yüklemeler altında çatlak ilerleme tahminindeki kullanılması gözden geçirilmiştir. Willenborg ve arkadaşları tarafından geliştirilen etkin gecikme modeli, matematik formülasyonunda dahil olmak üzere ayrıntılı olarak açıklanmıştır. Çeşitli yükleme programlarına ait deney ve analitik verilerin karşılaştırılması şekillerde gösterilmiştir.

Deneyler 10 ton kapasiteli, kapalı devre yorulma cihazında (MTS) gerçekleştirilmiş olup, deney esnasında periyodik olarak yüklemeye ara verilip, o andaki çatlak uzunluğu ve buna karşı gelen çevrim sayısı kaydedilmiştir. Deneylerde 2024-T4 alüminyum alaşımından hazırlanmış, çentikli "ufak çekme numunesi" kullanılmıştır. 11 numune üzerinde çatlak ilerleme çalışmaları yapılmış, çatlak uzunluğu ve çevrim sayısı ilişkileri saptanmıştır.

Deney sonuçları değerlendirilmiş ve logaritmik skalada çatlak ilerleme hızı, gerilme şiddet çarpanı aralığı ilişkileri gösterilmiştir.

## TABLE OF CONTENTS

LIST OF FIGURES	i
LIST OF TABLES	v
LIST OF SYMBOLS	vi
1. INTRODUCTION	1
2. FATIGUE CRACK PROPAGATION	3
2.1. Fatigue Crack Growth and the Stress Intensity Factor	3
2.2. Related Studies	9
3. FATIGUE CRACK PROPAGATION UNDER VARIABLE AMPLITUDE LOADING	14
3.1. Different Types of Variable Amplitude Loading	14
3.2. Delay in Fatigue Crack Growth	17
3.3. Retardation Models	20
3.3.1. The Wheeler Model	20
3.3.2. The Nelson and Fuchs Model	22
3.4. Other Prediction of Crack Growth Under Variable-Amplitude Loading	22
3.4.1. The RMS Model	22
3.4.2. The Crack Closure Model	23
3.5. The Willenborg Model	25
4. EXPERIMENTAL WORK	32
4.1. Test Materials	32
4.2. Specimen Geometry	33
4.3. Set-Up	36

4.4.Experimental Procedure	37
4.5.Test Results	47
4.5.1.Group I Test Results	47
4.5.2.Group II Test Results	51
4.5.3.Group III Test Results	54
4.5.4.Group IV Test Results	57
4.5.5.Groqp V Test Results	59
4.5.6.Group VI Test Results	67
4.6.Discussion of Results	68
4.6.1.Constant Amplitude Test Results	68
4.6.2.Single Overload Test Results	69
4.6.3.Constant Amplitude Load, at Displacement Control	71
5.CONCLUSIONS	73
REFERENCES	74
APPENDIX-A :The Data Obtained from the Experiments	81
APPENDIX-B :Fracture Toughness Test Procedure	99

LIST OF FIGURES

	<u>PAGE</u>
FIGURE 2.1 : Variable stress and stress intensity factor	5
FIGURE 2.2 : Results in one scatter band [1]	6
FIGURE 2.3 : Schematic representation of fatigue crack growth	7
FIGURE 2.4 : "m" vs. fracture toughness curve	8
FIGURE 3.1 : Stationary and non-stationary variable amplitude loading	15
FIGURE 3.2 : Several simple types of VA-Loading	15
FIGURE 3.3 : Several types of complex fatigue load histories	16
FIGURE 3.4 : Schematic illustration of delay in fatigue crack growth and definition of $N_D$	18
FIGURE 3.5 : Typical $da/dN$ versus " $\Delta a$ " results	19
FIGURE 3.6 : Yield zone due to overload ( $r_{po}$ )	21
FIGURE 3.7 : Illustration of crack closure	24
FIGURE 3.8 : Illustration of crack tip plastic zones and the plastic envelope left in the wake of a growing crack	24
FIGURE 3.9 : Effective stress intensity range as proposed by Elber	25



FIGURE 3.10:	Development of WILLENBORG MODEL	27
FIGURE 3.11:	Formulation of Willenborg Model	29
FIGURE 3.12:	Development of Willenborg Model-Modes of retardation	31
FIGURE 4.1 :	The compact specimen geometry	34
FIGURE 4.2 :	Envelope for crack starter notch	34
FIGURE 4.3 :	The experimental set-up for fatigue crack propagation test	36
FIGURE 4.4 :	Specimen 7 in mounted position	38
FIGURE 4.5 :	The loading program of specimen 2	43
FIGURE 4.6 :	The loading program of specimen 3	43
FIGURE 4.7 :	The loading program of specimen 5	45
FIGURE 4.8 :	The experimental set-up for Fracture Toughness Testing	46
FIGURE 4.9 :	Crack length vs. number of cycles (CTS 1)	47
FIGURE 4.10:	Crack length vs. number of cycles (CTS 11)	48
FIGURE 4.11:	Fracture surfaces of specimen 1	49
FIGURE 4.12:	Fracture surfaces of specimen 11	49
FIGURE 4.13:	Crack growth rate as a function of stress intensity factor range for constant amplitude tests	50

FIGURE 4.14:	Fracture surfaces of specimen 2	51
FIGURE 4.15:	Fracture surfaces of specimen 3	51
FIGURE 4.16:	Crack length vs. applied cycles (CTS 2)	52
FIGURE 4.17:	Crack length vs. applied cycles (CTS 3)	54
FIGURE 4.18:	Fatigue crack growth rate vs. stress intensity factor range for Group II	53
FIGURE 4.19:	Fracture surfaces of specimen 4 (at displacement control)	55
FIGURE 4.20:	Crack length vs. applied cycles (CTS 4)	55
FIGURE 4.21:	Fatigue crack growth rate vs. stress intensity factor range (CTS 4)	56
FIGURE 4.22:	Fracture surfaces of specimen 5 (single overload test)	57
FIGURE 4.23:	Crack length vs. applied cycles (CTS 5)	58
FIGURE 4.24:	Crack growth rate vs. stress intensity factor range (CTS 5)	58A
FIGURE 4.25:	Crack length vs. applied cycles for overload test; O/L=1.5 (CTS 6)	60
FIGURE 4.26:	Crack length vs. applied cycles for overload test; O/L=1.25 (CTS 8)	61
FIGURE 4.27:	Crack length vs. applied cycles for overload test; O/L=2.0 (CTS 9)	62

FIGURE 4.28:	Fracture surfaces of specimen 6	63
FIGURE 4.29:	Fracture surfaces of specimen 8	63
FIGURE 4.30:	Fracture surfaces of specimen 9	63
FIGURE 4.31:	Fracture surfaces of three specimens (6, 8 and 9, respectively)	64
FIGURE 4.32:	Crack length vs. applied cycles for Group V specimens	65
FIGURE 4.33:	Crack growth rate vs. stress intensity factor range for overload tests	66
FIGURE 4.34:	Fracture surfaces of specimen 7 (after Fracture Toughness Test)	67
FIGURE 4.35:	A graph for $g(a/W)$ at displacement control	72

LIST OF TABLES

TABLE 4.1	Chemical Composition of 2024 Aluminum Alloy
TABLE 4.2	Mechanical Properties of 2024-T4 Al-Alloy
TABLE 4.3	Crack Initiation Data
TABLE 4.4	Summary of Tests on 2024-T4 Al-Alloy
TABLE 4.5	Constant Amplitude Test Program
TABLE 4.6	Group II Specimens Test Program
TABLE 4.7	Single Overload Test Plan for Specimen 5

LIST OF SYMBOLS

a	Crack length for compact tension specimen
a	Crack length increment
a/W	Crack length-the width of specimen ratio
B	Thickness of specimen
C	Material constant in Paris Equation
da/dN	Crack growth rate ( $\mu\text{m}/\text{cycle}$ )
K	Stress intensity factor
$K_I$	Stress intensity factor for Mode I
$K_{IC}$	Fracture toughness ( $\text{kg}\cdot\text{mm}^{-3/2}$ )
K	Stress intensity factor range, $K_{\text{max}} - K_{\text{min}}$
$K_{\text{eff}}$	Effective stress intensity range
$K_{\text{th}}$	Stress intensity range threshold at which the crack growth rate is apparently zero
$K_{\text{max}}$	Maximum stress intensity factor
$K_{\text{min}}$	Minimum stress intensity factor
$K_{\text{maxOL}}$	Maximum stress intensity factor at overload
N	Cycles of load
$N_D$	Number of delay cycles
$N_O$	Cycle at which an overload(s) is applied
$N_f$	Cycle count at which fracture is occurred
$N_i$	Number of crack initiation cycles

n	Material constant
P	Applied load, also maximum applied baseline load
$P_{OL}$	Overload, maximum applied load
$P_{max}$	Maximum applied baseline load
$P_{min}$	Minimum applied baseline load
R	Stress or load ratio, $S_{min}/S_{max}$ or $P_{min}/P_{max}$
$r_y$	Plastic zone size (Irwin)
$r_{y_{OL}}$	Overload affected plastic zone
$S_{max}$	Maximum stress
$S_{min}$	Minimum stress
$S_y$	Material yield stress
O/L	Overload ratio, ratio of $P_{OL}$ to P. (or $P_{OL}/P_{max}$ ) also $K_{max_{OL}} / K_{max}$

## CHAPTER I

### INTRODUCTION

One of the most remarkable successes in recent fatigue studies has been the application of the Linear Elastic Fracture Mechanics (LEFM) methods to fatigue crack propagation problems. Good correlation between crack propagation rate and range of stress intensity factor has generally been established for various materials and is widely used in many fields of engineering applications. However, it is known that this correlation sometimes conflicts in some details with experimentally observed phenomena of fatigue crack propagation. Some examples of disagreement may be found in the nonpropagating fatigue crack problem and also in acceleration and retardation of fatigue crack propagation rate under variable amplitude loads.

According to the recent advances in Linear Elastic Fracture Mechanics, it is known that the stress intensity factor of a crack generated at a notch or a stress raiser always increases, or at least does not decrease with increasing crack length.

If a unique monotonous relation is assumed between crack propagation rate and range of stress intensity factor, the crack should always propagate at an increasing speed until final fracture.

An extensive review of the research done on the fatigue crack propagation under constant amplitude loading is given in Chapter II. Also theoretical explanation of the problem has been made through the linear elastic fracture mechanics and it is presented in Chapter II.

Most of the research on fatigue crack propagation under variable amplitude load behaviour has been theoretical, because experimental methods for observing crack propagation and studying their individual properties, have been recently developed, and it is still difficult to utilize these techniques. These techniques are presented in Chapter III.

Experimental work including test results and discussion of result is given in Chapter IV.

Chapter V presents the conclusions of test results.

The data obtained from the experiments and standard  $K_{IC}$  test procedure are placed in Appendices.



## CHAPTER II

### FATIGUE CRACK PROPAGATION

#### 2.1. Fatigue Crack Growth and the Stress Intensity Factor

In the elastic case, the stress intensity factor is a sufficient parameter to describe the whole stress field at the tip of a crack. When the size of the plastic zone at the crack tip is small compared to the crack length, the stress intensity factor may still give a good indication of the stress environment of the crack tip. If two different cracks have the same environment, i.e. the same stress intensity factor, they behave in the same manner and show equal rates of growth. This implies [1]

Similar Conditions applied to the Same System will cause  
Similar Consequences

$$\left( \begin{array}{l} \text{Same K values} \\ \text{Same environment} \end{array} \right) + \left( \begin{array}{l} \text{Same materials} \\ \text{in crack tip area} \end{array} \right) \rightarrow \text{Same Crack Rat}$$

The crack growth rate, usually denoted as  $da/dN$  (= slope of crack growth curve), should be considered to be the crack extension  $\Delta a$  of a crack length  $a$  occurring in one cycle

$$\frac{da}{dN} = \Delta a$$

- It will be clear that  $\Delta a$  will depend on;
- the cyclic stress on the crack tip area
  - the (cyclic) elasto-plastic response of the material in the same area
  - the environment
  - some fracture criterion

From the definition of stress intensity factor  $K = CS\sqrt{\pi a}$  a cyclic variation of stress ( $S$ ) will cause similarly a cyclic variation of  $K$ . The stress intensity in the crack tip area will be characterized by  $K_{max}$  and  $K_{min}$ . (Figure 2.1)

The similarity approach predicts

$$\frac{da}{dN} = f(K_{min}, K_{max})$$

where

$$K_{max} = \frac{\Delta K}{1-R}$$
$$K_{min} = \frac{R \Delta K}{1-R}$$

$$\frac{da}{dN} = f(\Delta K, R)$$

or

$$\frac{da}{dN} = f_R(\Delta K)$$

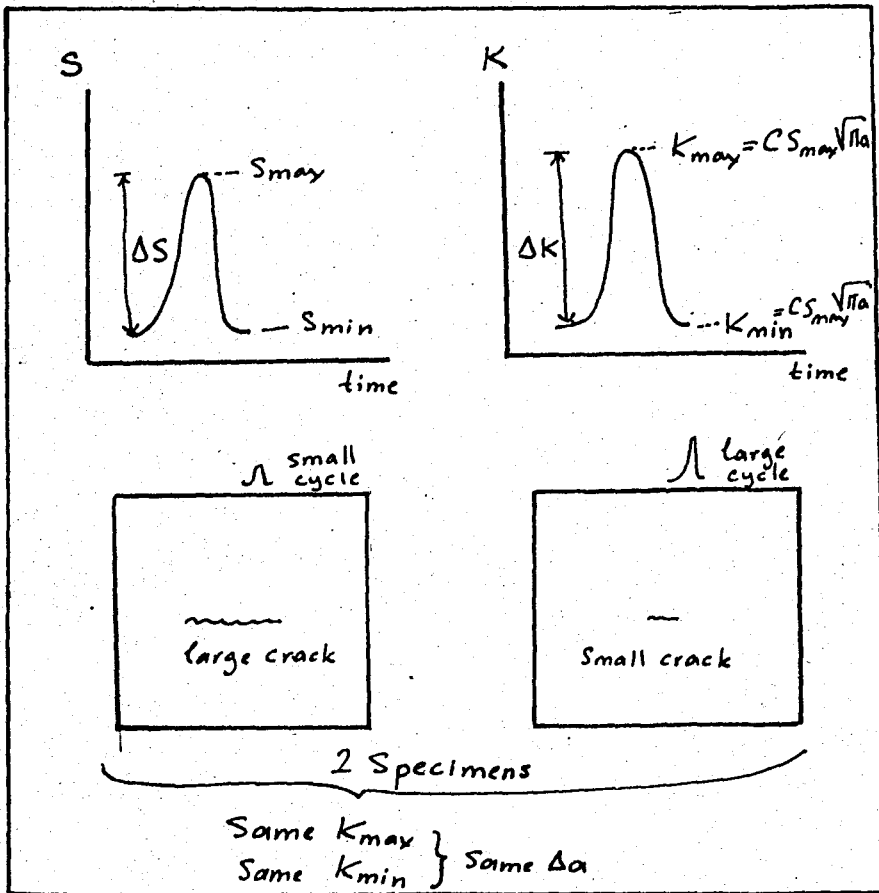


Figure 2.1: Variable stress and stress intensity factor

A formulae proposed by Paris is

$$\frac{da}{dN} = C (\Delta K)^m$$

Figure 2.2 gives an illustration of the applicability of K to the comparison between crack growth results from specimens with end loading and specimens with crack edge loading [1]. For crack edge loading the K-factor is decreasing for increasing crack length.

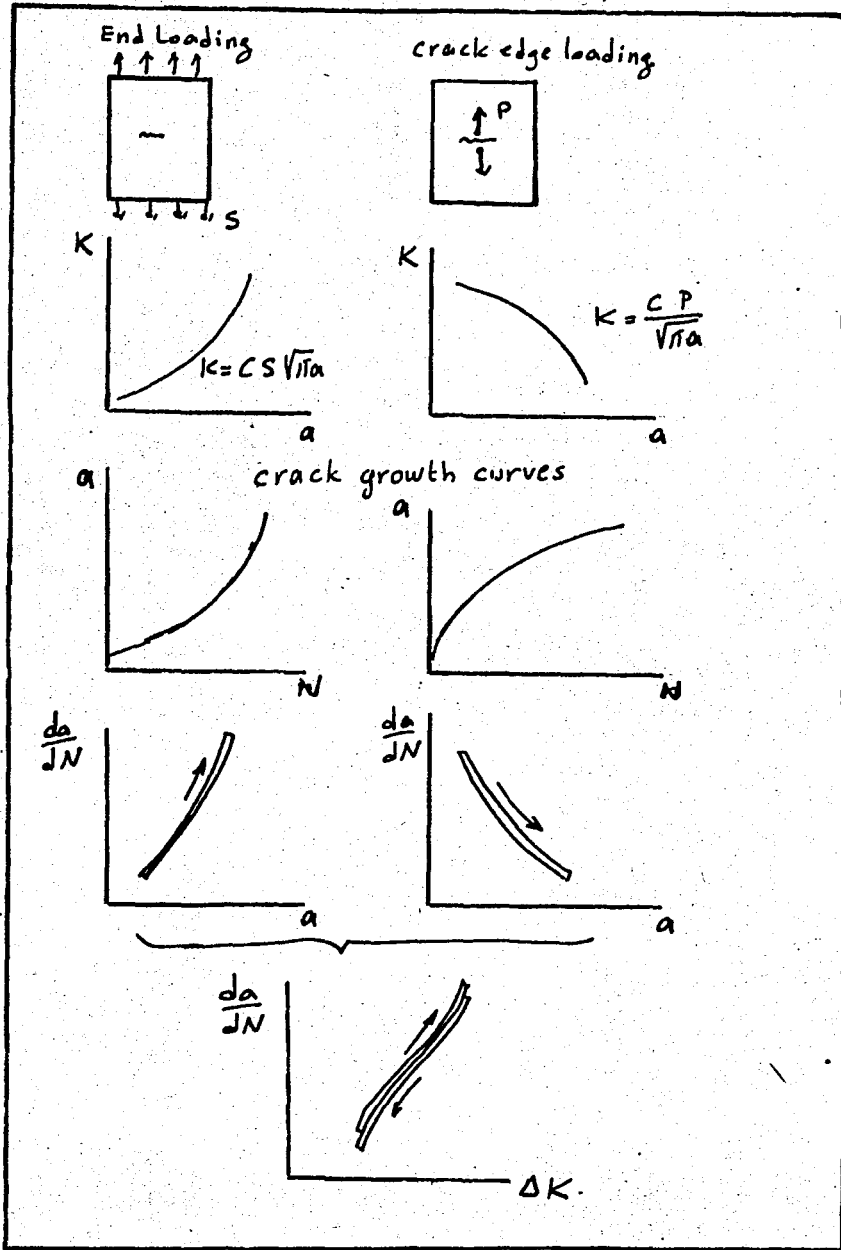


Figure 2.2: Results in one scatter band [1]

Various  $a$  versus  $N$  curves can be generated by varying the magnitude of the cyclic-load fluctuation and/or the size

of the initial crack. These curves reduce to a single curve when the data are presented in terms of crack growth rate per cycle of loading,  $da/dN$ , and the fluctuation of the stress intensity factor,  $\Delta K$ , because  $\Delta K$  is a single-term parameter that incorporates the effect of changing crack length and cyclic load magnitude.

The most commonly used presentation of fatigue crack growth data is a log-log plot of the rate of fatigue crack growth per cycle of load fluctuation and the fluctuation of the stress intensity factor. The fatigue crack propagation behaviour for metals can be divided into three regions. (Figure 2.3)

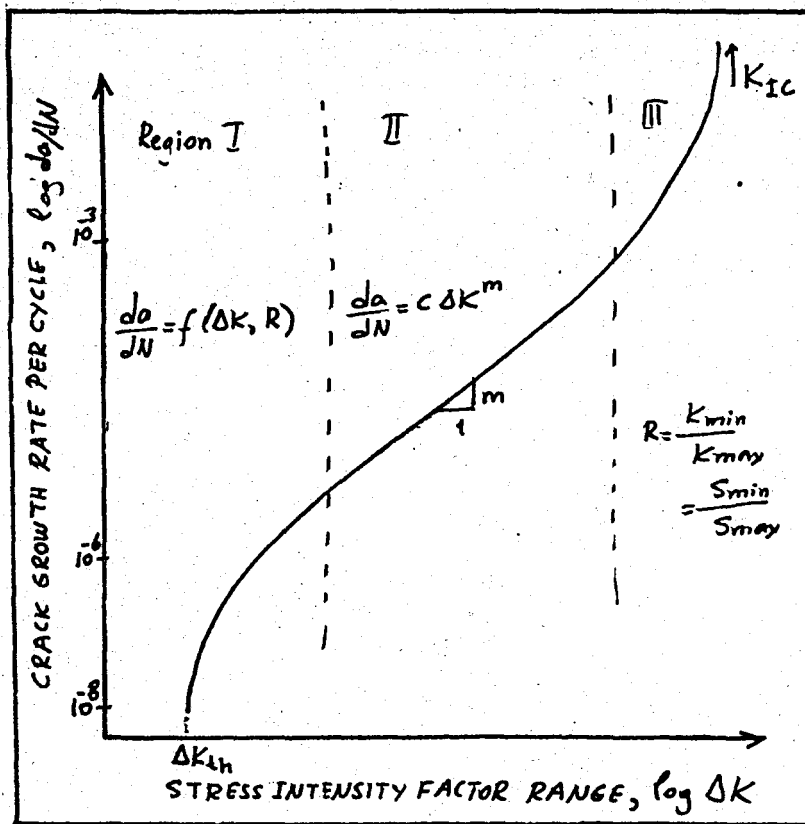


Figure 2.3: Schematic representation of fatigue crack growth

The behaviour in Region I exhibits a "fatigue threshold" cyclic stress intensity factor fluctuation,  $\Delta K_{th}$ , below which cracks do not propagate under stress fluctuations.

$$\frac{da}{dN} = f(\Delta K, R) \quad (\text{sensitivity of } R)$$

An analysis of experimental results, published in the literature on non-propagating fatigue cracks in various metals, has been conducted by Harrison [2].

Region II represents the fatigue crack propagation behaviour above  $\Delta K_{th}$  which can be represented by

$$\frac{da}{dN} = C \Delta K^m \quad (\text{Paris and Erdoğan})$$

$m$  has a value 2 to 10. High values of  $m$  are obtained only in materials of low toughness, and in high toughness materials  $m$  has a value close to 2. [3] (Figure 2.4)

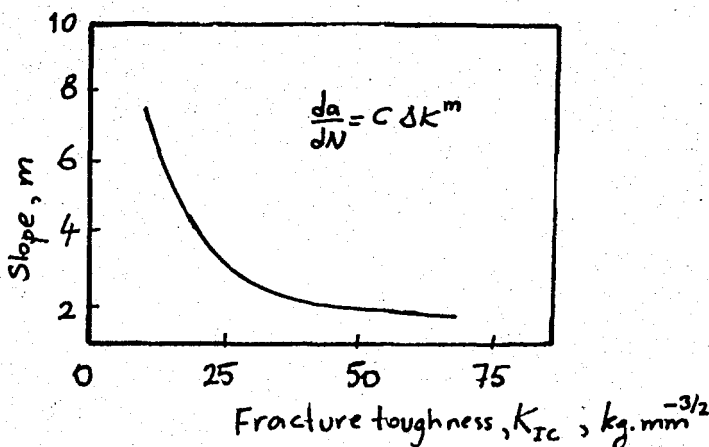


Figure 2.4: "m" versus fracture toughness curve

In Region III, the fatigue crack growth per cycle is higher than predicted for Region II. Region III is not so important, in that it has a relatively small effect on the total crack propagation life. We are interested, from a fail-safe viewpoint, in improving crack propagation resistance over 2-2.5 decades from about  $0.1 \mu\text{m}/\text{cycle}$  upwards.

## 2.2. Related Studies

After the end of the Second World War, the problem of brittle fracture has been studied extensively. Because these low-stress (compared to the yield stress of the material) fractures always originate at flaws or cracks of various types, the fracture mechanics approach has proved useful in problems of materials development, design and failure analysis. This approach, to the residual static strength in the presence of a crack, makes use of the concept of the stress intensity factor  $K_I$  and was explained in previous section. Generally  $K_I$  describes the stress field at a crack tip and values of  $K_I$  are known for a wide range of cracked configurations [7,8] when  $K_I$  reaches a critical value  $K_C$  the crack extends, usually catastrophically. In view of its success in dealing with static fracture problems, it is logical to use a similar general approach to analyse fatigue crack growth data. The availability of a master curve for a particular material relating fatigue

crack growth rate and range of stress intensity factor can enable a designer to predict growth rates for any cracked body configuration and he would not be limited to situations similar to those pertaining to the cracked specimen geometry used to generate the original data.

During the last twenty-five years, numerous "laws" of fatigue crack growth have been published [9]. All of them are equally valid in the sense that they accurately represent a set of fatigue crack growth data, notwithstanding these data were restricted to a limited range of specimen and crack length geometries and stress levels. For example, Frost and coworkers [10] obtained fatigue crack growth data for a wide variety of metallic materials using 10 in. wide panels about 0.1 in. thick, subjected to tensile stress cycle, cracks being grown from both ends of a small transverse central slit. They expressed the rate of growth of cracks by the equation theoretically,

$$\frac{da}{dN} = A \sigma^3 a$$

where  $a$  = average half crack length measured  
from the center of the sheet

$A$  = material constant



Paris and Erdoğan [11] argued that the growth rate should be a function of the stress intensity factor  $K$  and that this factor is defined by the elastic stress field around the crack tip. They found that a large body of data could be fitted by an expression of the form;

$$\frac{da}{dN} = C (\Delta K)^m$$

where  $C$  = material constant

$m$  = an exponent (has the values between 2 and 4)

$\Delta K$  = the stress intensity factor range

And this formula accounts neither for mean stress effects, nor for  $K_{th}$ , nor for  $K_C$ . In 1967, Forman and coworkers [12] published an improved Paris equation,

$$\frac{da}{dN} = C \frac{\Delta K^n}{(1-R) K_C - \Delta K}$$

where  $R$  = stress ratio ( $S_{min}/S_{max}$  or  $K_{min}/K_{max}$ )

$K_C$  = critical stress intensity factor

$C, n$  = material constants

in which at least mean stress effects and  $K_C$  were incorporated. This formula has been proved by many laboratories to

give a reasonable approximation to crack propagation test results for many different materials. Some examples are presented in reference [13].

Forman equation does not contain  $\Delta K_{th}$  "fatigue-threshold" cyclic stress intensity factor below which cracks do not propagate under cyclic stress fluctuations and therefore implies fatigue crack propagation even at infinitely small  $\Delta K$ . Klesnil and Lukas [14] modified the original Paris equation in the following way;

$$\frac{da}{dN} = C (\Delta K^n - \Delta K_{th}^n)$$

While Hartman and Schijve [15] suggested a slightly different version;

$$\frac{da}{dN} = C (\Delta K - \Delta K_{th})^n$$

In [16] the IABG incorporated both proposals into the Forman equation and found the Klesnil and Lukas solution,

$$\frac{da}{dN} = \frac{C (\Delta K^n - \Delta K_{th}^n)}{(1-R) K_C - \Delta K}$$

to be a better fit to the experimental data available. However, the numerical values for  $\Delta K_{th}$  must be determined

experimentally.

Other formulae for calculation crack propagation under constant amplitude loading have been published. See references [17 - 24]

Crack growth retardation models are explained in Chapter III.

## CHAPTER III

### FATIGUE CRACK PROPAGATION UNDER VARIABLE AMPLITUDE LOADING

#### 3.1. Different Types of Variable Amplitude Loading

In the previous chapter, we have seen that K-concept was quite successful in correlating crack growth data obtained under constant amplitude loading. The K-concept can be again useful for variable amplitude loading, if this type of loading has a stationary character.

As mentioned in the above explanation variable amplitude loading should be defined in two categories:

1. Stationary VA-loading
2. Non-stationary VA-loading

Simple examples of both categories are shown in Figure 3.1. A survey of several types of loading applied in test series, reported in the literature, are given in Fig. 3.2 and 3.3. The more simple ones are presented in Figure 3.2. The number of variables is small and the variables can easily be defined. For the more complex load-time histories

shown in Fig.3.3, a statistical description of the loads has to be given.

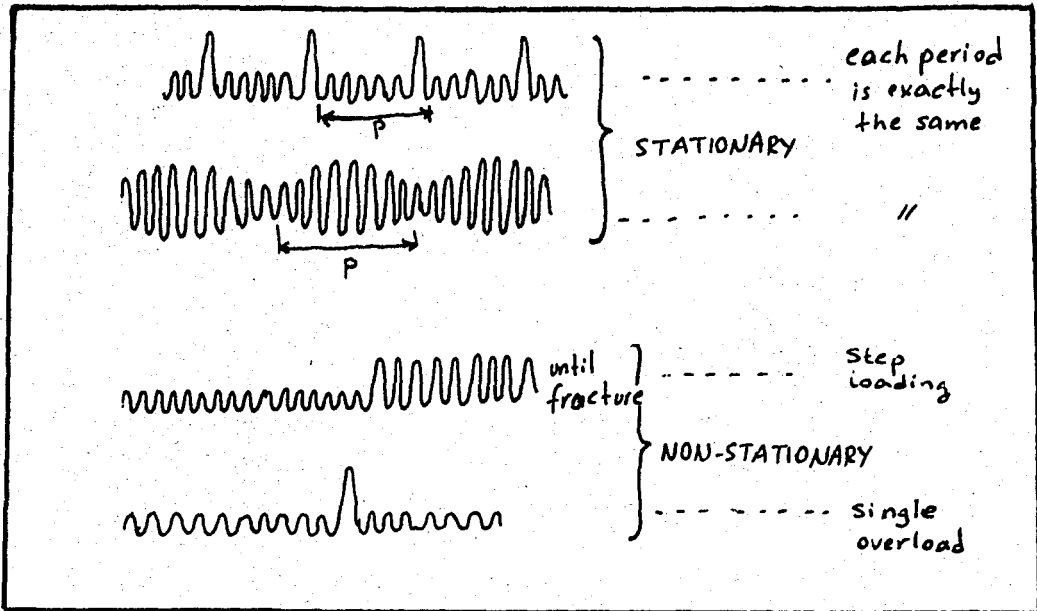


Figure 3.1: Stationary and non-stationary VA-Loading

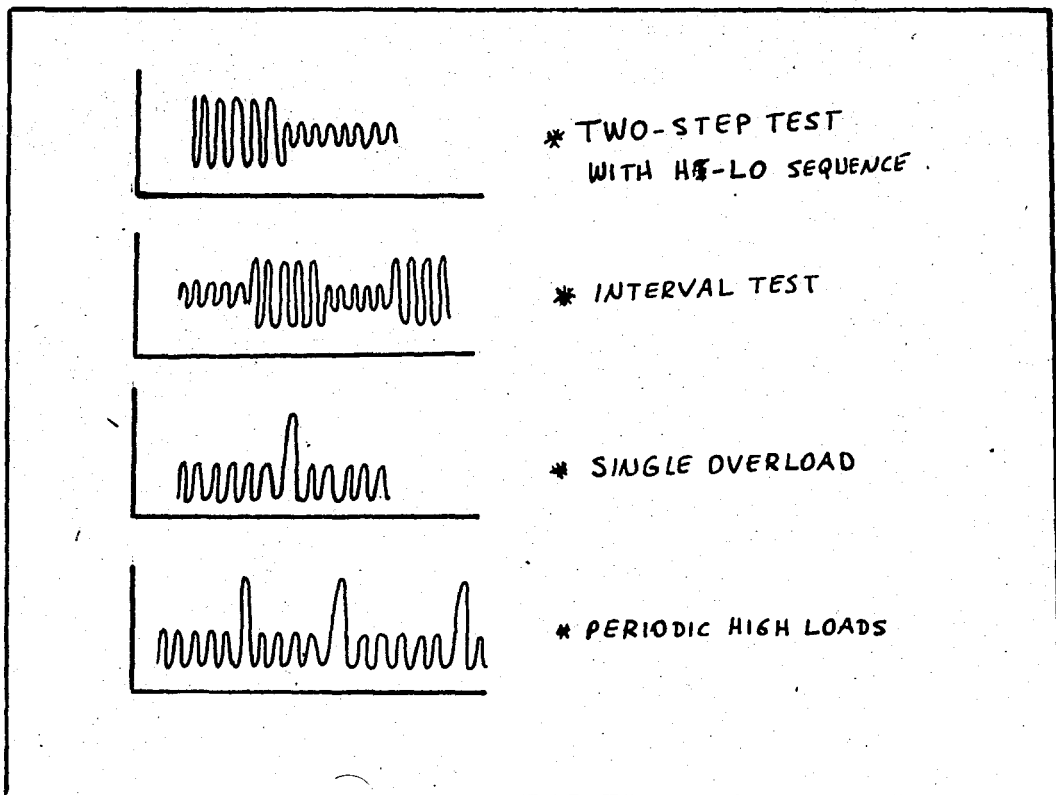


Figure 3.2: Several simple types of VA-Loading

This may be the distribution function of the load amplitudes. The function may be a stepped one, as for instance for the program loading F and the randomized block loading G in Figure 3.3.

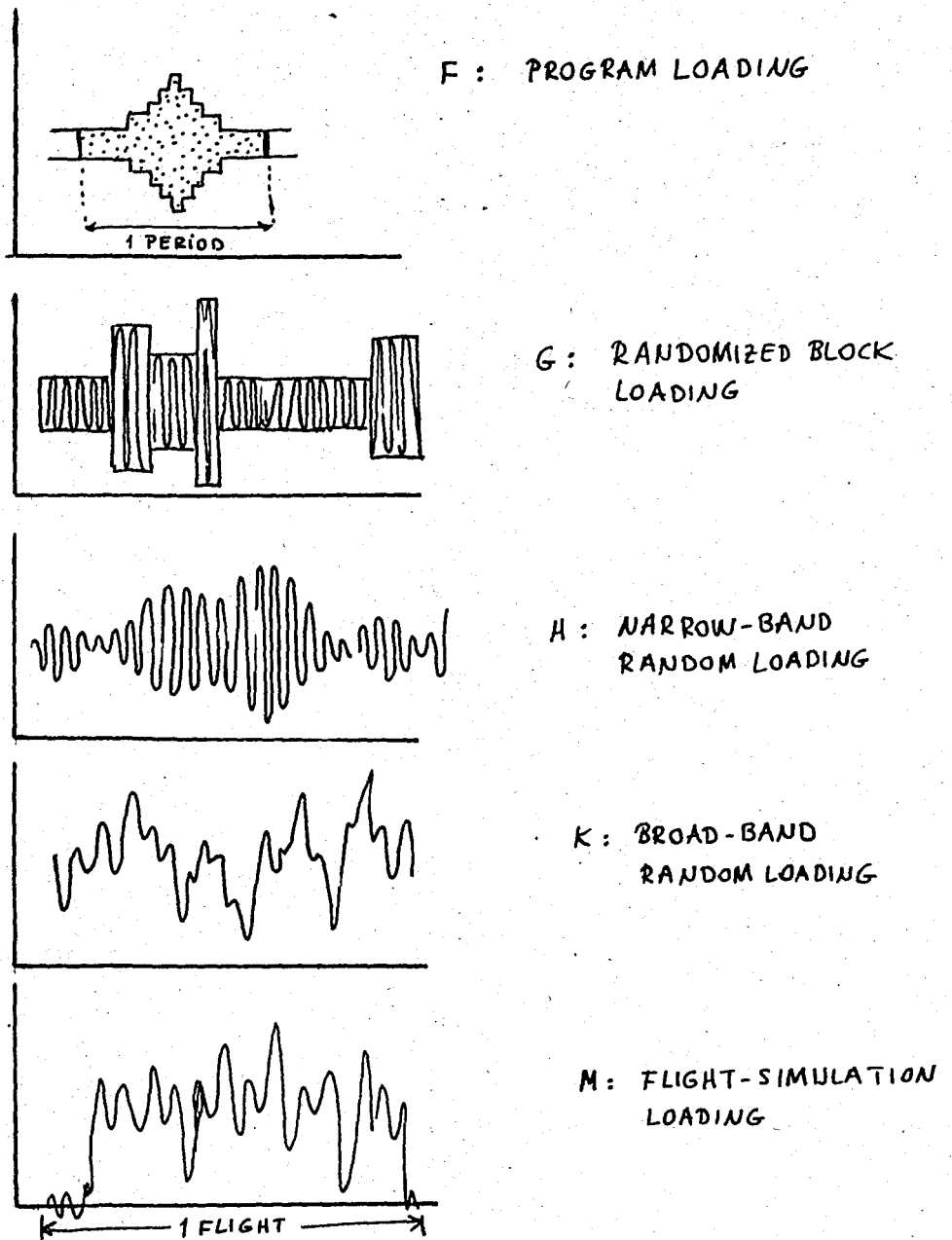


Figure 3.3: Several types of complex fatigue load histories

### 3.2. Delay in Fatigue Crack Growth

The importance of delay ( or retardation in the rate of fatigue crack growth) produced by load interactions in variable amplitude, on the accurate prediction of fatigue lives and/or inspection intervals for engineering structures has been well recognized for sometime. Therefore, only a few simple loading combinations or spectra have been examined systematically. In a recent exploratory study, Jonas and Wei [25] showed that the phenomenon of delay is very complex and can depend on a broad range of variables. This and other investigations have shown that the effects of delay can be quite large, and need to be taken into consideration in the development of improved analysis procedures for fatigue of engineering structures [26 - 30].

Several models have been proposed recently to account for the effects of delay. These models, while successful in predicting trends in fatigue crack growth under randomized load spectra, break down for ordered spectra. The lack of quantitative success may be attributed to:

1. a lack of physical and phenomenological understanding of the effects of load interactions on fatigue crack growth [25, 28-30], and of the simpler problem of fatigue growth in itself; and

2. inadequacies in stress analysis to account for the types of loading, crack geometry and residual stresses [7, 8].

Delay properly refers to the period of abnormally low rate, or zero rate, of fatigue crack growth between a decrease in load level and the establishment of a rate of growth commensurate with that for constant amplitude loading at a prevailing (lower) load. It is usually measured in terms of the number of elapsed load cycles. For experimental accuracy and potential engineering utility, however it is more convenient to define delay  $N_D$  artificially as a period of zero crack growth as illustrated in Figure 3.4, by extrapolation of the constant amplitude growth curve to zero-growth line.

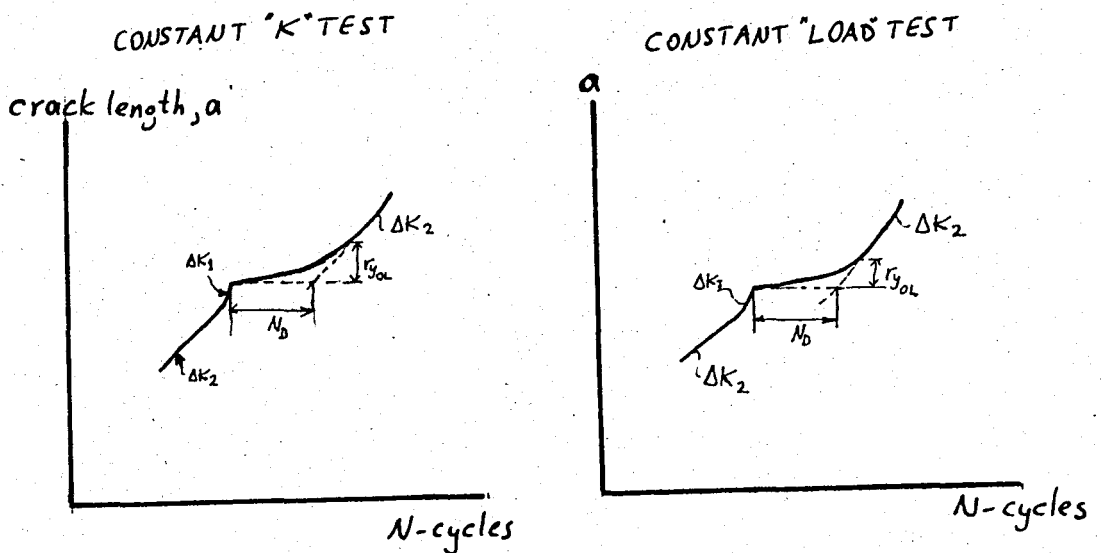


Figure 3.4: Schematic illustration of delay in fatigue crack growth and definition of  $N_D$  [25]



Figure 3.4 also shows the method of defining the extend of the overload affected plastic zone,  $r_{y_{OL}}$ , and the number of delay cycles,  $N_D$ . Figure 3.5 shows typical  $da/dN$  versus  $a$  results. This phenomenon has been termed "Crack Retardation". If a tensile overload is sufficiently large, crack arrest can occur.

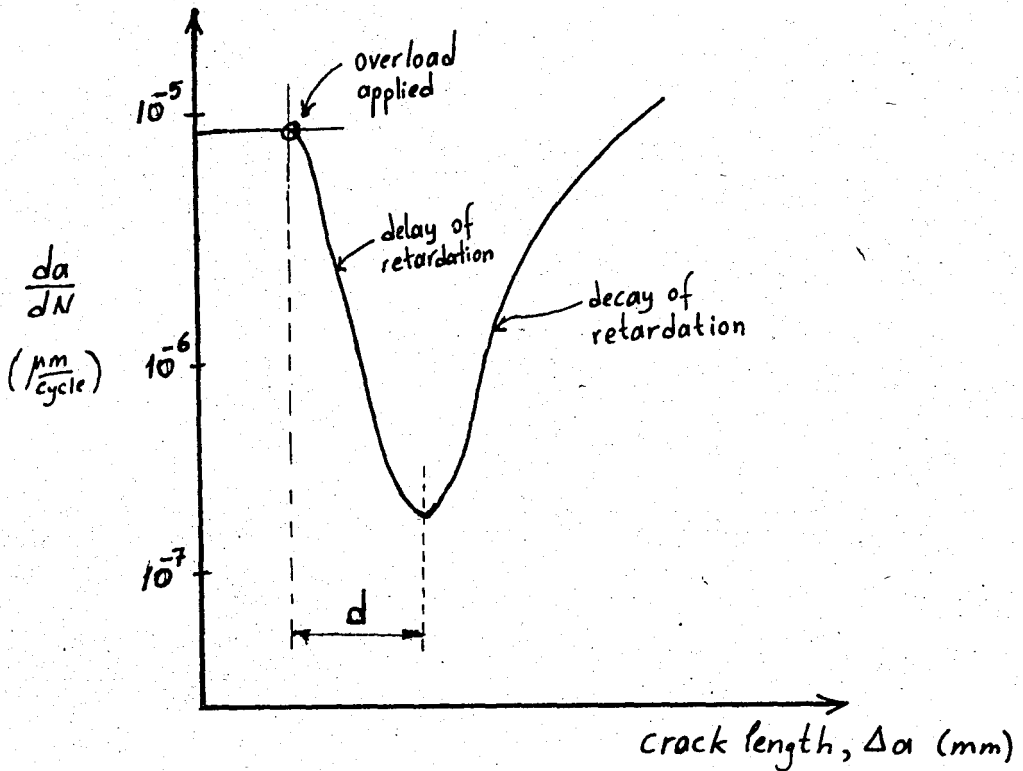


Figure 3.5: Typical  $da/dN$  versus "a" results

### 3.3. Retardation Models

#### 3.3.1. The Wheeler Model

The Wheeler model [26] is a relative damage accumulation hypothesis. Tests under a realistic load sequence are used to determine a factor "m" which is used to fit the prediction to the actual crack propagation life.

Wheeler summed crack growth cycle-by-cycle according to

$$a_r = a_o + \sum_{i=1}^r (da/dN)_i$$

where  $a_o$  = initial crack length

$(da/dN)_i$  = growth due to cycle i

$a_r$  = crack length after r cycles

To account for the effects of retardation, Wheeler proposed that retarded growth rate could be represented by

$$\left( \frac{da}{dN} \right)_{ret} = C_p f(\Delta K)$$

where  $f(\Delta K)$  is the usual crack growth function ( $= C \Delta K^m$ ) and  $C_p$  is "retardation factor" as shown below (Fig. 3.6)

$$C_p = \left( \frac{r_{pi}}{a_o - r_{po} - a_i} \right)^m = \left( \frac{r_{pi}}{s - a_i} \right)^m$$

where  $r_{pi}$  = current plastic zone generated i-th cycle  
 $a_i$  = current crack size  
 $r_{po}$  = size of the plastic zone generated by a previous overload  
 $m$  = retardation exponent

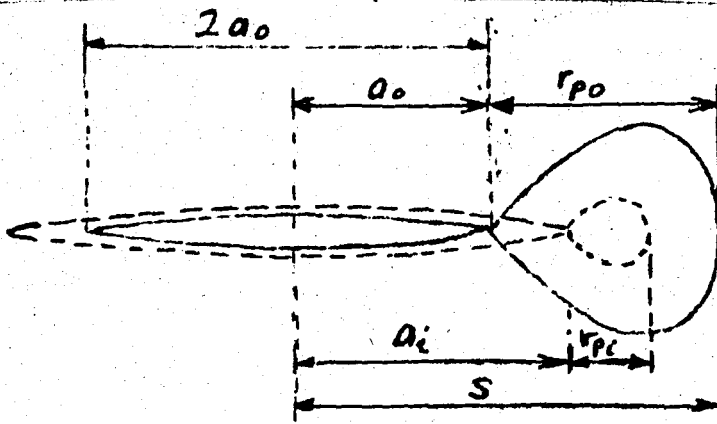


Fig.3.6: Yield zone due to overload ( $r_{po}$ ), crack size at overload ( $a_o$ ), current yield zone ( $r_{pi}$ ) and current crack size ( $a_i$ )

$C_p$  can take on values from 0 to 1, indicating crack arrest or no retardation at the extremes. Wheeler was able to make good predictions of crack growth by properly choosing  $m$  (retardation exponent) values to fit experimental data.

Another retardation model is the Willenborg Model. The Willenborg model makes use of an effective stress intensity factor. It is described in section 3.3 in detail.

Development of fatigue crack growth models to account not only for the effects of retardation but also the effects of compressive loading and low-to-high load sequences is now underway at a number of aircraft companies, government research labs and universities.

### 3.3.2. The Nelson and Fuchs Model

Nelson and Fuchs, in addition to their check on the Forman model mentioned in section 2.2, developed their own model [32]. The model uses an effective  $\Delta K$  ( $\Delta K_{\text{eff}}$ ).

To account for the following possible load sequence effects:

1. Crack retardation
2. The decrease of retardation by sufficiently large compressive overloads
3. The acceleration of crack growth rate by cross yielding in compression (but not in tension)

### 3.4. Other Prediction of Crack Growth Under VA-Loading

#### 3.4.1. The RMS Model

The basic idea of this method is to find a constant stress amplitude  $\Delta K_{\text{equ}}$  which is equivalent (with regard to crack propagation) to the variable realistic stress amplitudes. The root mean square (r.m.s.) of the realistic sequence was thought to be that equivalent. It is clear that no interaction effect can be accounted for in this way. For example, rare high stress peaks will not influence the r.m.s.-value appreciably, but they do influence crack growth.

Barsom [33] has found that the average crack growth rate for the random loadings, could be correlated well with with the relation;

$$\frac{da}{dN} = C (\Delta K_{\text{rms}})^n$$

where  $\Delta K_{\text{rms}}$  = the root mean square stress intensity range for a load sequence

Swanson et al. [34] have also obtained good correlations with similar spectrum characterizations for random loadings. In these studies of random-loading crack growth, stress spectra were all represented by a continuous, unimodal distribution, in particular, by a Rayleigh Distribution Function. The use of an r.m.s. type of characterization to predict fatigue crack growth should be restricted to load histories which can be described by such distributions and in which sequence effects are not expected to be significant

#### 3.4.2. The Crack Closure Model

Traditionally, it has been assumed that under cycling loading, a crack tip would open and close at zero load. In 1968, Elber [27] observed that during constant amplitude cycling, fatigue cracks actually close when the load is still tensile and do not open again until a sufficiently high tensile load is reached on the next cycle as illustrated in Figure 3.7. Elber found that the opening/closing stress levels were nearly the same and equal to about one half on the maximum applied stress for  $R=0$  loading.

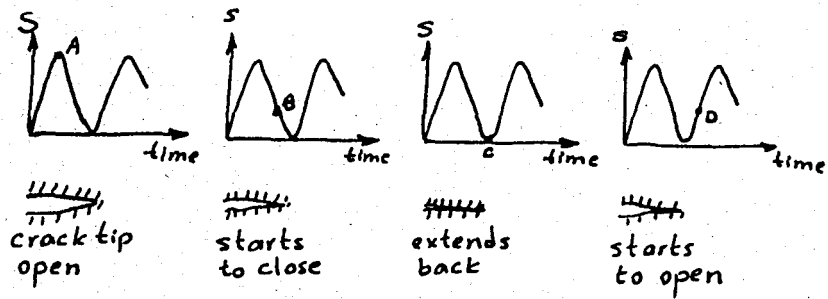


Figure 3.7: Illustration of crack closure

The physical reason for crack closure behaviour can be explained as follows. A plastic zone is always present surrounding a crack tip as shown in Figure 3.8.

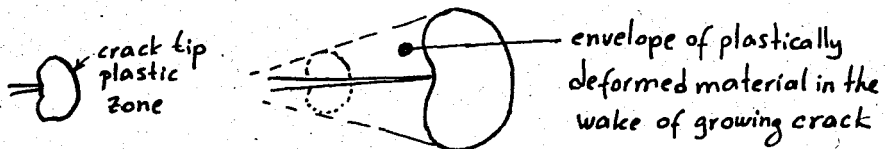


Fig. 3.8: Illustration of crack tip plastic zones

As the crack grows through a succession of these zones (which increase in size with crack length), an envelope of plastically deformed material is left in the wake of the crack. Residual tensile deformations with corresponding residual compressive stresses are present in this envelope. These residual tensile deformations cause a crack to close while still subjected to tensile loading is applied again.

Elber has proposed that, since a crack is open for only a portion of a tensile load cycle, then crack growth rate should more appropriately be correlated with an effective stress intensity range,  $\Delta K_{\text{eff}} = K_{\text{max}} - K_{\text{op}}$ , as shown

in Figure 3.9, rather than the total  $\Delta K$ , as has been customary.

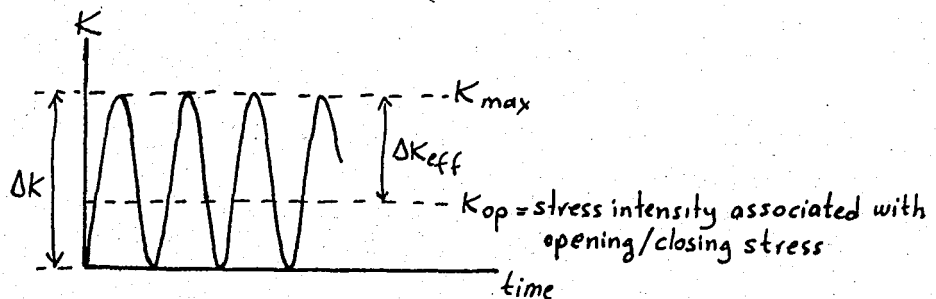


Fig.3.9: Effective stress intensity range as proposed by Elber

### 3.5. The Willenborg Model

Current predictive analysis techniques for crack propagation under cycling loading rely on the interaction of basic constant amplitude growth rate data derived from laboratory tests on standard specimens. Such an automated procedure is contained in reference [35] and [36].

Variations between predicted and actual growth lives have been noted for cases of variable amplitude spectrum loading due to the interaction of the stress applications [37,38]. The occurrence of a tensile overload will retard growth below that is normally expected. Neglecting these interaction effects results in grossly conservative prediction of crack growth life.

Several attempts at developing mathematical models for growth retardation have been made [26,27].

In reference [26], Wheeler calculates a retardation factor  $C_p$  which operates directly by reducing growth rate  $da/dN$ . The procedure requires previous spectrum growth data to derive a retardation exponent "m". Moderate success has been achieved by the author in fitting existing spectrum data.

In the current study, retardation is accounted for by operating directly on the crack growth driving function  $\Delta K$ . An effective value of the stress intensity factor range is computed by assuming a form of the residual crack tip stress present after the application of the overload. Once obtained, the modified  $\Delta K$  is used in conjunction with ordinary constant growth rate data and the CRACKS computer routine [35,36] to calculate life. No other empirical data or factors are required.

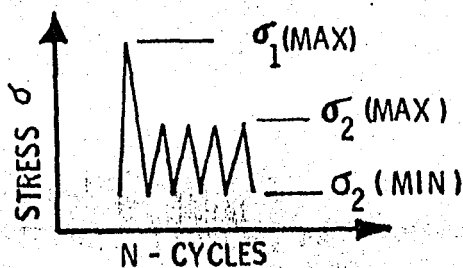
Using as the basis the yield zone concepts proposed by Wheeler, the model is developed under the following assumptions;

1. Retarded growth occurs when the maximum cycling stress is reduced.
2. Retardation is proportional to the amount that the maximum stress is reduced.
3. The length of retarded growth is that zone caused by the overload (i.e. the approximate yield zone  $R_y$  caused by the overload)



4. A new condition of retardation is produced each time a load is applied which is larger than the original overload.

To illustrate the mathematical development and the operation of the model, the case of a single overload is considered. Figures 3.10, 3.11 and 3.12 summarize the development steps of the model.



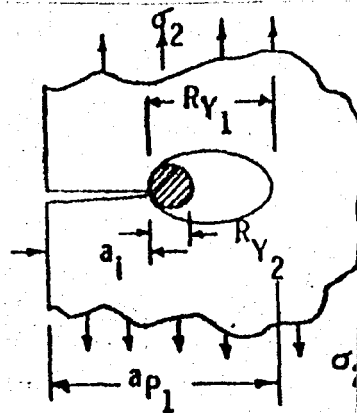
LOADING

- $\sigma_1$  RETARDS  $da/dN$  FOR  $\Delta \sigma_2$
- $R_{Y1}$  = SIZE OF YIELD ZONE DUE TO  $\sigma_1$
- $a_i$  = INITIAL CRACK LENGTH
- $a_c$  = CRACK LENGTH AT ANYTIME FOLLOWING OVERLOAD
- $a_{p1}$  = TOTAL AFFECTED CRACK LENGTH =  $a_i + R_{Y1}$

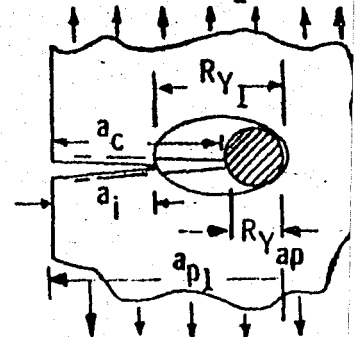
$$= \frac{(K_1)^2}{2\pi(\sigma_Y)^2} + a_i$$

• FOR ANY GENERAL CRACK LENGTH  $a_c$  FOLLOWING THE OVERLOAD, THE STRESS  $\sigma_{ap}$  REQUIRED TO PRODUCE A YIELD ZONE  $R_{Yap}$  SUCH THAT RETARDATION WOULD BE TERMINATED IS DETERMINED AS FOLLOWS:

$$a_p = a_c + R_{Yap} = a_c + \frac{(\sigma_{ap} \sqrt{\pi a_c})^2}{2\pi(\sigma_Y)^2}$$



YIELD ZONE IMMEDIATELY FOLLOWING OVERLOAD APPLIED  $\sigma_2$



YIELD ZONE CONDITION FOLLOWING  $\sigma_1$  FOR  $K_{ap} = \sigma_{ap} \sqrt{\pi a_c}$ ; RE

Figure 3.10: Development of Willenborg Model

Following the single overload, the crack continues to grow under cyclic loading,  $\Delta \sigma_2$ . The growth, however, is retarded as long as no subsequent maximum stress greater than  $\sigma_2(\max)$  is applied and as long as growth remains within the zone of plasticity caused by the overload,  $\sigma_1(\max)$ .

For the latter condition, it is presumed that the "current" crack length,  $a_c$ , plus the length of "current" yield zone,  $R_{yc}$ , is less than the value of  $a_p$ , that is the yield zone caused by the overload. Irwin's yield zone model is used in the model where

$$R_y = \text{yield zone size} = \frac{1}{2\pi} \left( \frac{K_I}{S_y} \right)^2 \quad (\text{for plane stress})$$

In the example (Fig. 3.10) the plane stress assumption is illustrated. Although a single two level stress spectrum is considered here, assume a third stress level  $\sigma_3 = \sigma_{ap}$  (less than  $\sigma_1$ ) occurs following the last cycle of  $\sigma_2$ , and assume also that growth has not completely progressed through the yield zone caused by the overload,  $\sigma_1$ .

For the previously established conditions of retardation, it can be presumed that retardation will be terminated when the value of  $\sigma_{ap}$  is large enough ( $\sigma_{ap} \ll \sigma_1$ ), and the current crack length,  $a_c$ , is of such extent that the below condition exists;

$$a_c + R_{yap} = a_{pl}$$

where  $R_{yap}$  = yield zone caused by general stress  $\sigma_{ap}$  at crack length  $a_c$

$$= \frac{(K_{ap})^2}{2\pi (S_y)^2} = \frac{1}{2} \left( \frac{\sigma_{ap}}{S_y} \right)^2$$

therefore, the value of general stress  $\sigma_{ap}$  is as follows:

$$\sigma_{ap} = S_y \sqrt{\frac{2(a_p - a_c)}{a_c}} \quad (\text{plane stress})$$

Further illustration of  $\sigma_{ap}$  is indicated in Fig. 3.11, where it is plotted against the increment of crack growth following the overload,  $\sigma_1$ .

$$a_p - a_c = 1/2 \left( \frac{\sigma_{ap}}{\sigma_y} \right)^2 - a_c$$

$$\sigma_{ap} = \sigma_y \sqrt{2 \frac{(a_p - a_c)}{a_c}}$$

- $\sigma_{red}$  = EFFECTIVE RESIDUAL STRESS CAUSED BY OVERLOAD, VARIABLE WITH  $a_c$  AND DEPENDENT UPON  $\sigma_2$

$$\sigma_{red} = \sigma_{ap} - \sigma_2$$

FOLLOWING OVERLOAD:  $\sigma_2(\text{MAX})$ ,  $\sigma_2(\text{MIN})$ , R

ARE REDUCED BY AMOUNT  $\sigma_{red}$

$$\sigma_{2(\text{MAX})\text{EFF}} = \sigma_{2(\text{MAX})} - \sigma_{red}$$

$$\sigma_{2(\text{MIN})\text{EFF}} = \sigma_{2(\text{MIN})} - \sigma_{red}$$

$$R_{\text{EFF}} = \frac{\sigma_{2(\text{MIN})\text{EFF}}}{\sigma_{2(\text{MAX})\text{EFF}}}$$

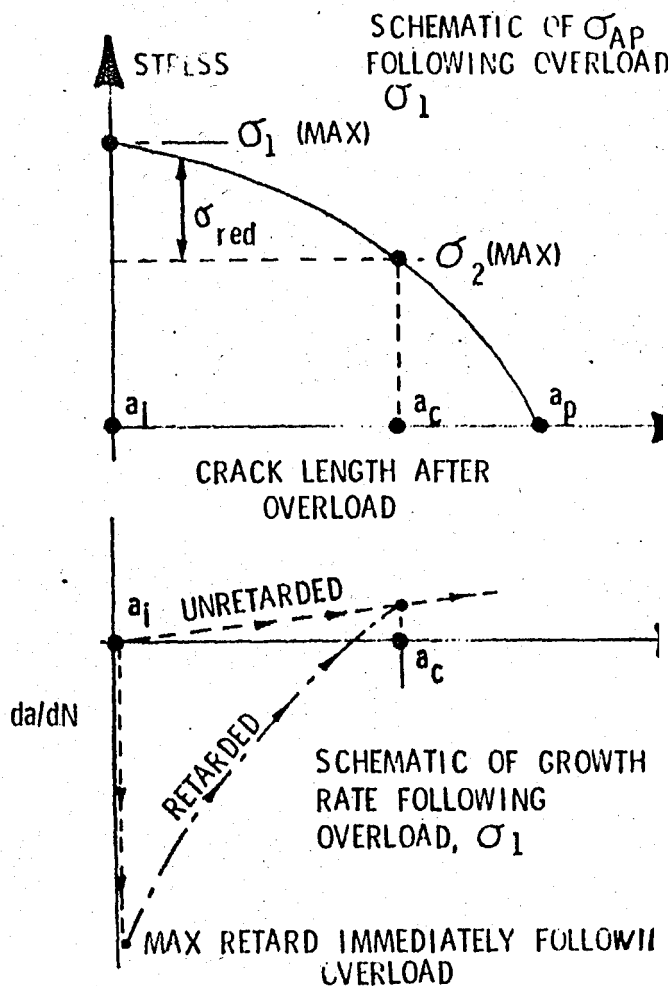


Figure 3.11: Formulation of Willenborg Model

Note that  $\sigma_{ap}$  is bounded by values  $\sigma_{ap} = \sigma_1$  and  $\sigma_{ap} = 0$  over the increment  $(a_i - a_p)$ . In a physical sense,  $\sigma_{ap}$  may be thought of as the effective portion of  $\sigma_1$  which is capable of causing retardation for stress  $\sigma_2 < \sigma_{ap}$  at a crack length still within the plastic zone caused by the overload,  $\sigma_1$ . Because it is assumed that retardation is proportional to the differences in applied stresses, the amount that  $\sigma_2$  is retarded should be the difference  $\sigma_{ap} - \sigma_2(\max)$  at any crack length. (Note that  $\sigma_2 - \sigma_1(\max) = \sigma_1(\max) - \sigma_2(\max)$  immediately following the overload.)

$$\begin{aligned}\sigma_{red} &= \text{the amount of "residual stress" caused by} \\ &\quad \text{the overload available to retard } \sigma_2 \\ &= \sigma_{ap} - \sigma_2(\max)\end{aligned}$$

The relationship between  $\sigma_{red}$  and  $\sigma_{ap}$  is illustrated in Figure 3.11 for the specific example.

In the computation of reduced growth due to  $\sigma_2$  loading, both  $\sigma_2(\max)$  and  $\sigma_2(\min)$  are reduced by the amount  $\sigma_{red}$  as illustrated in Fig. 3.11. Negative values are set equal to zero. Effective values of  $\Delta K_2$ ,  $R_2$  are computed with  $R_2$  always being equal to or greater than zero. The effective  $\Delta K$  and  $R$  are then used to compute a new and reduced growth rate.

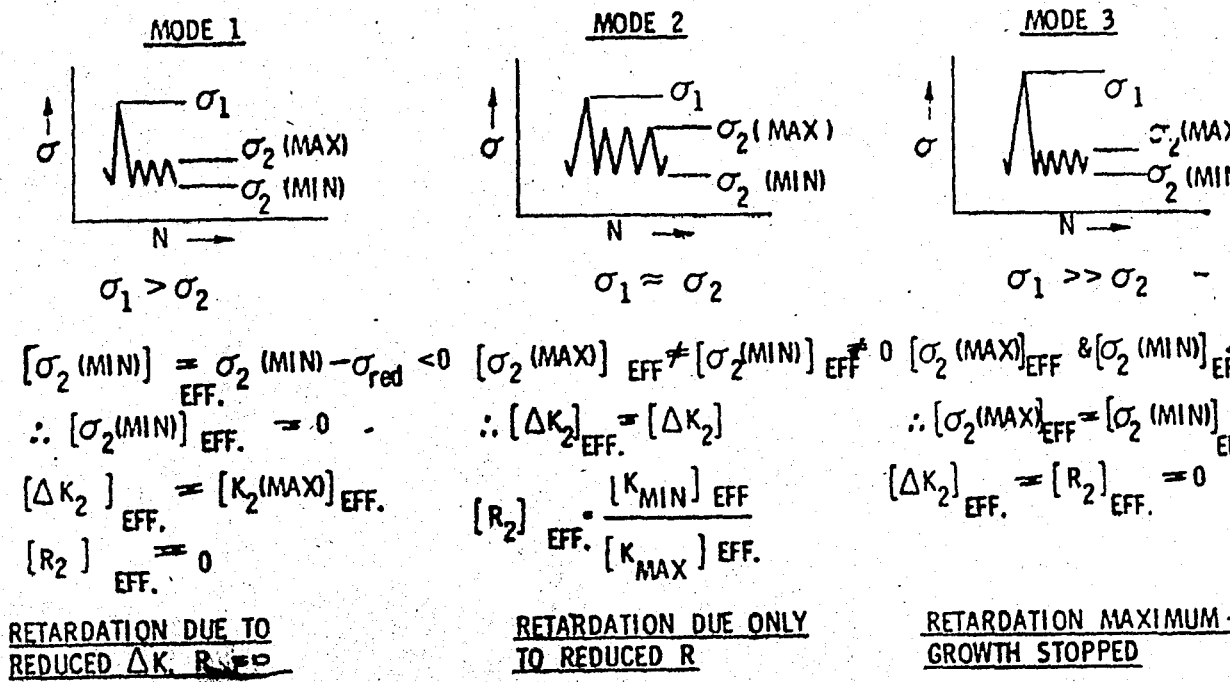


Figure 3.12: Development of Willenborg Model-Modes of retardation

There are three distinct modes of retardation possible within the model: (Figure 3.12)

1. Retardation is due to both a reduced  $\Delta K$  and  $R = 0$
2. Retardation is due to the reduction of  $R$  only,  $R > 0$ ,  
 $\Delta K_{eff} = \Delta K$
3. Maximum retardation occurs when both  $\Delta K_{eff}$  and  $R$  are equal to zero.

Note that condition (3) occurs at  $R = 0$  for the case when  $(\sigma_1 / \sigma_2)_{max} \geq 2.0$

The model and procedure has been programmed for ease of computation into the program CRACKS [35]. Schematically the rate of growth versus the increment of crack growth for the single overload case is illustrated in Fig. 3.11. Maximum retardation is seen to occur immediately following overload and recovery to normal or unretarded rate occurs within the yield zone as shown.

## CHAPTER IV

### EXPERIMENTAL WORK

#### 4.1. Test Materials

The material used in the experiments is aluminum alloy 2024 in the T4 condition which is received in plate form ( 0.625 in. thick) from Reynolds Al. Company, U.S.A. The chemical composition and mechanical properties are given in Table 4.1 and Table 4.2, respectively. The fracture toughness property is determined in accordance with present ASTM standards.

	Cu	Mg	Mn	Cr	Si	Fe	Ti	Zn	Ni	Sn	Al
2024	4.73	1.58	0.61	0.01	0.13	0.23	0.03	0.04	0.01	0.01	rest

Table 4.1: Chemical Composition of 2024 Al-alloy [39]

Ultimate Tensile Stress	Tensile Yield Stress	Elongation $\epsilon$ %	Modulus of Elasticity $E$	Shear Modulus, $G$
62 ksi 43.6 kg/mm <sup>2</sup>	44 ksi 30.9 kg/mm <sup>2</sup>	8	$10.5 \times 10^6$ psi	$4.0 \times 10^6$ psi

Table 4.2: Mechanical Properties of 2024-T4 Aluminum Alloy [39]

All specimens are oriented with the load line parallel to the rolling direction so that the crack grows parallel to the rolling direction.

#### 4.2. Specimen Geometry

Fatigue crack growth tests are performed with the compact tension specimen (CTS). In the CTS,  $K$  as a function of crack length is well characterized. The specimens are prepared according to ASTM E 399-74, with a valid crack growth range of  $a/W = 0.3$  to  $a/W = 0.7$ .

The compact tension specimen is single-edge notched and pin loaded in tension. It has been assumed to be one of the standard specimens of ASTM described in "Standard Test for Plane-Strain Fracture Toughness of Metallic Materials", E - 399 [40]. In Fig. 4.1, the CTS is shown.

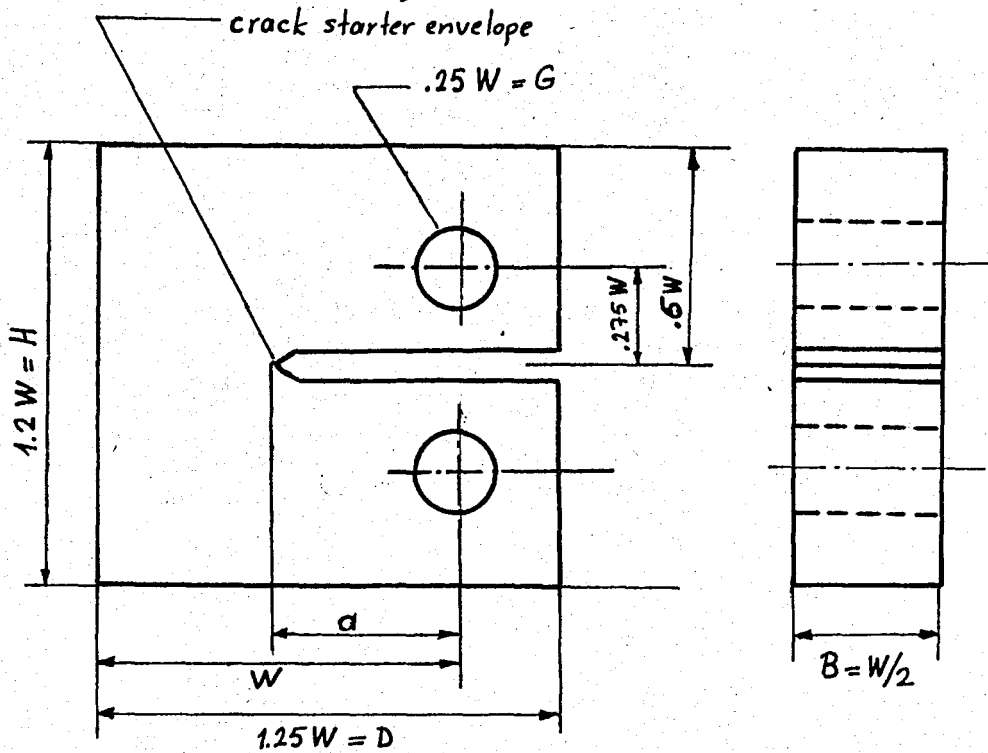


Figure 4.1: The compact tension specimen

The crack-starter notch has been chosen to be the keyhole (Figure 4.2). All data are taken after the crack has propagated by 1.5 mm's.

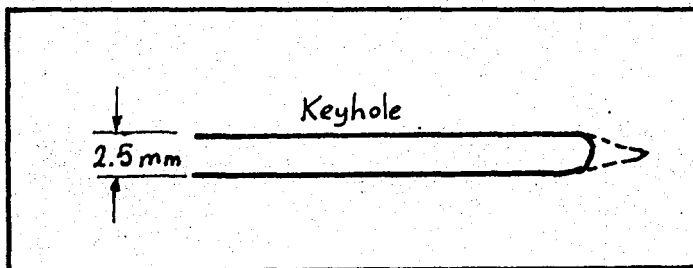


Figure 4.2: Envelope for crack starter notch



The compact tension specimen requires the least amount of material and is relatively inexpensive to test. It must be precracked in tension-to-tension fatigue test [41].

It is not only a standard configuration for toughness testing but also a common specimen for fatigue crack growth experiments. The requirement that the thickness (B) should be half of the specimen width (W/2) is relaxed in fatigue tests.

In the experiments, Dimensions are chosen such as ;

$$W = 100 \text{ mm}$$

$$a = 45 \text{ mm}$$

$$H = 120 \text{ mm}$$

$$G = 12 \text{ mm}$$

$$D = 125 \text{ mm}$$

$$B = 15 \text{ mm}$$

#### 4.3.Set-Up

Figure 4.3 shows the experimental set-up for fatigue crack propagation tests. Tests are conducted on electro-hydraulic closed loop ( MTS 812 ) fatigue testing machine with a maximum capacity of 10 tons.

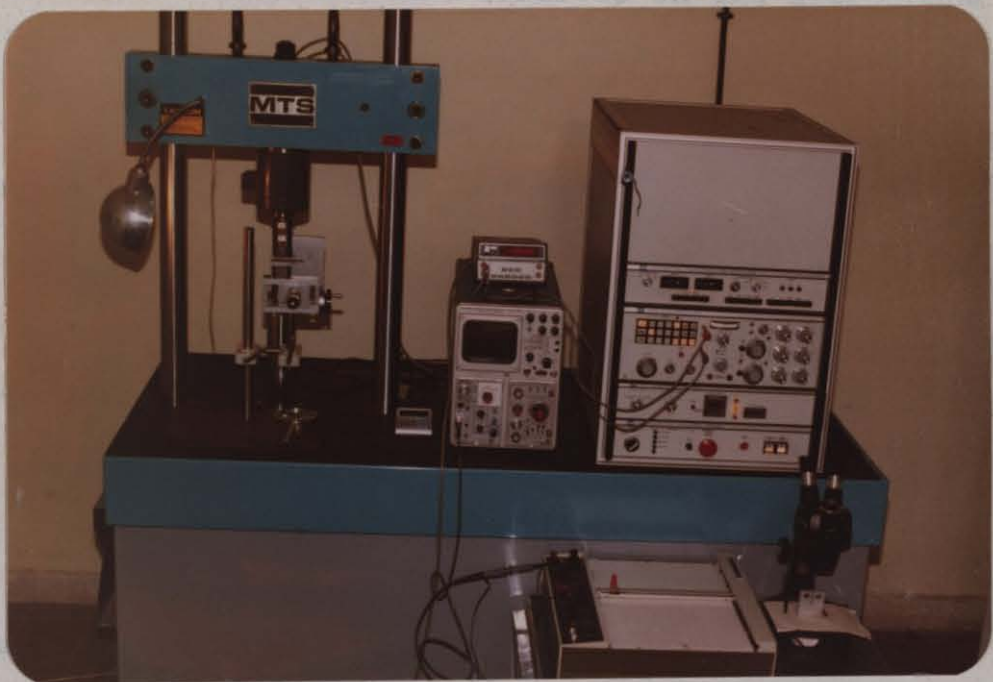


Figure 4.3: The experimental set-up for FCP test

Tests may be conducted on load control, displacement control or strain control. Load is measured by a conventional load-cell, which has an accuracy of  $\pm 1\%$ . Displacement is measured by means of a "clip-gauge" mounted across the open mouth of the stress concentrator.

Load and displacement are plotted as the ordinate and abscissa respectively on an X - Y recorder. ( Hewlett-Packard X-Y Recorder)

Crack length measurements are taken at every 1000 cycles with a Gaertner Travelling Microscope (10 X ) And fracture surfaces are observed on the microscope ( 30 X ) seen in Figure 4.3 at right.

The magnifying glass is used to observe the crack length existing in the specimens.

Applied loads are observed on the digital multimeter (Hewlett-Packard, 40072 Display) and the oscilloscope (Textronix).

#### 4.4. Experimental Procedure

First the specimens have been precracked in zero-to-tension fatigue loading. The conditions necessary for a sharp, flat crack normal to the specimen edges are completely met by MTS (namely, load distribution be symmetrical with relation to the notch in planes normal to the thickness direction and the maximum value of the stress intensity in the fatigue cycle be known with an error of not more than 5% ) [40].

To initiate fatigue crack, specimens have been mounted to the testing device. In order to accelerate the initiation the notch root is scratched with a sharp knife. A total of eleven specimens have been precracked in tension-to-tension fatigue with various baseline loads. To determine whether fatigue cracking was completed within desired limits observation of the traces of the crack on the side surfaces of the specimens was sufficient. (Figure 4.4)

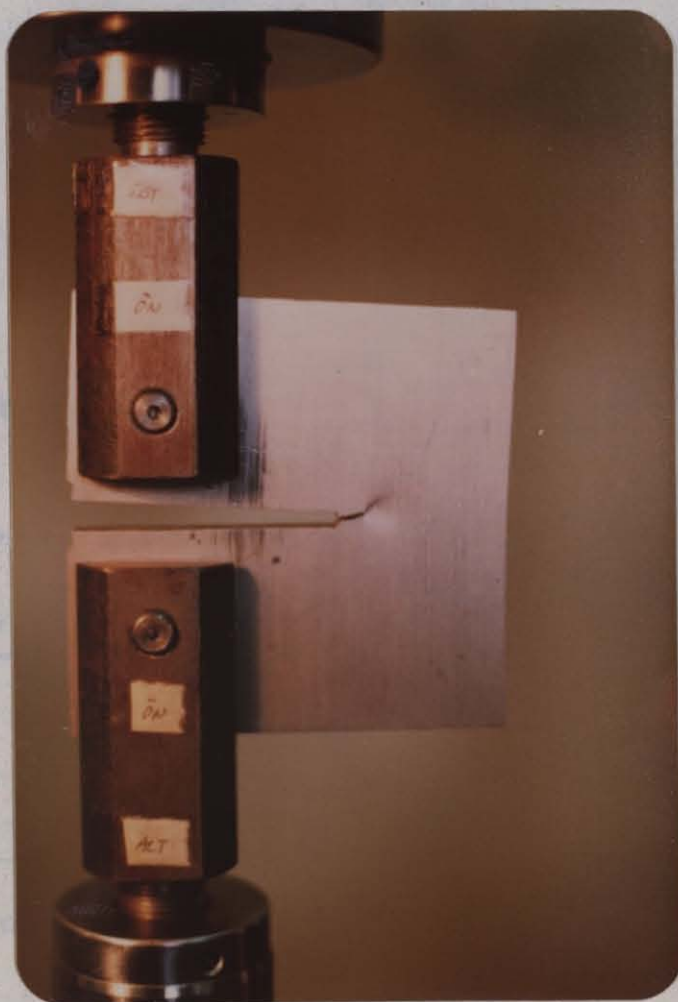


Figure 4.4: Specimen 7 in mounted position. The crack propagating at the notch can be easily seen

The relevant data of crack initiation is summarized in Table 4.3. As an addition the nominal stress at the notch root <sup>x</sup> has been calculated and listed.

Specimen	$\frac{a}{W}$	$\Delta P$ (kgf)	$N_i$ (cycles)	$\Delta a$ (mm)	$a_i$ (mm)	$\Delta \sigma_{notch}$ (kg/mm <sup>2</sup> )	$\Delta K$ (kg.mm <sup>-3/2</sup> )
1	0.50	1000-50	30000	5	50	13.3	73.6
2	"	"	28000	5.5	50.5	16	61.5
3	"	1200-50	10800	3.61	48.61	"	70.5
4	"	"	31070	2	47	"	68
5	"	"	19200	5	50	"	73.6
6	"	"	7360	1.5	46.50	"	66.7
7	"	"	13000	5.5	50.50	"	74.8
8	"	1000-50	12150	2	47	13.3	56.2
9	"	"	12170	2.12	47.12	"	56.5
10	"	"	19850	2.5	47.50	"	63
11	"	"	24000	3.35	48.35	"	57.6

Table 4.3: Crack Initiation Data

<sup>x</sup> Stress at notch root is given by;

$$\sigma = \frac{P}{A} + \frac{MC}{I} = \frac{P}{BW} \frac{2(2+a/W)}{(1-a/W)^2}$$

The frequency -although not critical in this case- is held at 3 Hz. All tests were performed in a laboratory environment at ambient temperature and relative humidity.

The data obtained from the experiments are the crack length versus cycles to failure, ( a - N ) curve. These a-N curves from actual tests are compared with the predicted ones obtained using the Willenborg Model. The raw a-N data are included in Appendix A in detail.

During the tests, crack length measurement are taken at every 1000 cycles with a Gaertner Travelling Microscope ( 10X).

All tests are summarized in Table 4.4. The fracture surfaces are shown in figures 4.11, 4.12, 4.14, 4.15, 4.19, 4.22, 4.28, 4.29, 4.30, 4.31, 4.34.

Tests are divided into 6 groups:

Group I : (Constant Amplitude Loading)

Constant amplitude fatigue crack tests were performed to characterize the steady-state crack growth behaviour of the 2024-T4 aluminum alloy. Table 4.5 shows the constant amplitude test plan.

Specimen	Loading Type	Load/displacement control	number of overloads	$\Delta P$ (kgf)	Overload ratio, %
1	CONSTANT AMPLITUDE	Load Control	—	550	—
2)	"	"	Several load range	900, 700, 520, 500, 300	—
3	"	"	" " "	950, 750, 550, 350, 250	—
4	"	Displacement Control	—	—	—
5	SINGLE OVERLOAD	Load Control	4 times overload	550	1.5, 1.75
6	"	"	3 " "	550	1.5
7	FRACTURE TOUGHNESS	Displacement Control	—	—	—
8	SINGLE OVERLOAD	Load Control	3 times overload	550	1.25
9	"	"	3 " "	550	2.0
10	FRACTURE TOUGHNESS	Displacement Control	—	—	—
11	CONSTANT AMPLITUDE	Load Control	—	700	—

Table 4.4 : Summary of <sup>tests</sup> Mon 2024-T4 Al-alloy

Specimen	Specimen type	Thickness B (mm)	Stress (Load) Ratio, R	$\Delta P$ (kgf.)
1	CTS	15	0.083	550
11	CTS	15	0.066	700

Table 4.5: Constant Amplitude Test Program

It is known [42] that varying the stress ratio has a strong effect on crack growth rates. The stress ratio, R, is defined as the ratio of the minimum applied stress or load to the maximum applied stress or load.

Two different stress ratios were tested. Since it was desired to obtain  $da/dN$  data over the range  $10^{-7}$  to  $10^{-4}$  mm/cycle, the allowable stress (or load) ranges were limited.

The specimens were loaded in tension loads. It was found [43] that the compact tension specimen produced erroneous results when subjected to compression loads.

Group II : (Block Loading with Hi-Lo Sequence)

In this group, two specimens (No:2 and No:3) were subjected to block loading with Hi-lo sequence. Figure 4.5 and 4.6 show the loading program in Group II.



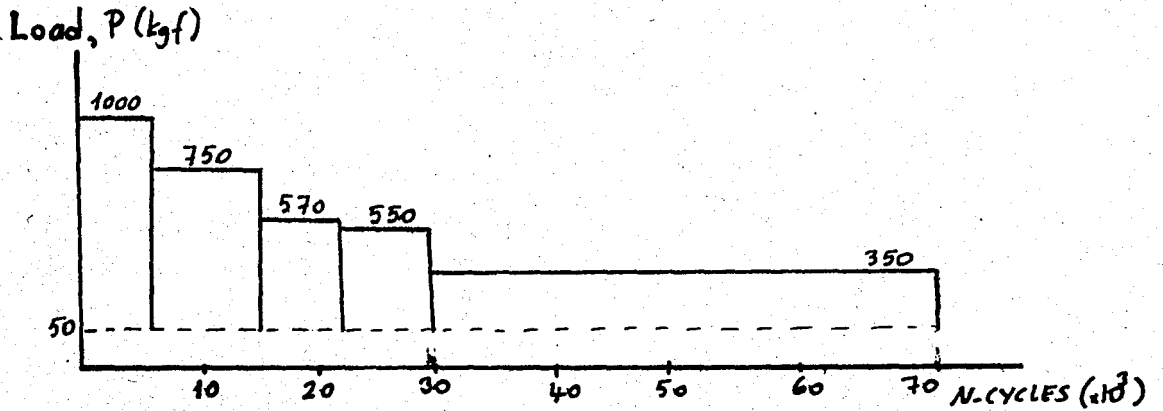


Figure 4.5: The loading program of specimen no:2

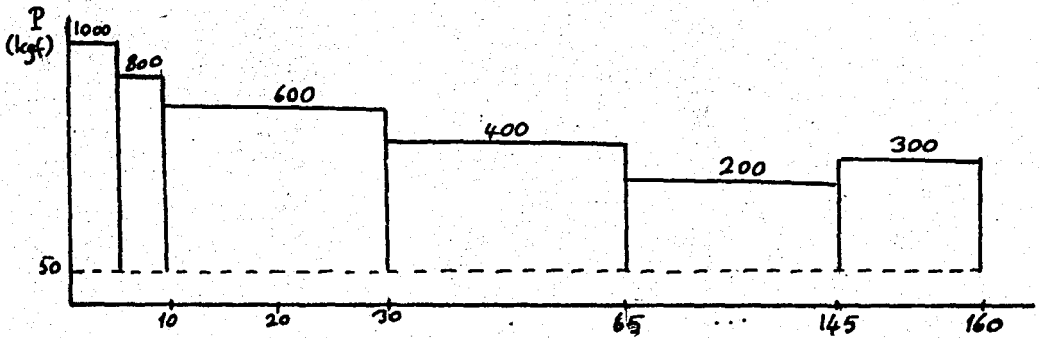


Figure 4.6: The loading program of specimen no:3

Table 4.6 shows the loading program in Group II, including stress ratio and stress intensity factor range.

CTS #2					
$N \times 10^3$	$\sum \Delta a$ (mm)	$a$ (mm)	$\Delta P$ (kgf)	$R$	$\Delta K$ (kg/mm <sup>3/2</sup> )
0-5	4.6	55.10	1000-50	0.050	71.5
5-15	9.81	60.31	750-50	0.066	63.5
15-22	12.15	60.25	570-50	0.087	52
23-30	17.04	67.54	550-50	0.090	63
30-69	30.46	80.96	350-50	0.142	74.8
Precrack: $\Delta P = 1000-50$ , $a_i = 50.5$ mm, $N_f = 69230$ cycles					
CTS #3					
$N \times 10^3$	$\sum \Delta a$ (mm)	$a$ (mm)	$\Delta P$ (kgf)	$R$	$\Delta K$ (kg/mm <sup>3/2</sup> )
0-5	4.17	52.76	1000-50	0.050	66.5
5-10	6.78	55.37	800-50	0.062	56.6
10-30	14.50	63.18	600-50	0.083	56.6
30-65	23.29	71.95	400-50	0.125	55.3
65-145	23.75	72.40	200-50	0.250	24.3
145-160	33.86	82.51	300-50	0.166	72
Precrack: $\Delta P = 1200-50$ , $a_i = 48.61$ mm, $N_f = 160320$ cycles					

Table 4.6: Group II: Specimens Test Program

Group III: (Constant Amplitude, at Displacement Control)

In this group, only one specimen was tested under displacement control. The loading program is shown in Appendix-A in detail.

Group IV: (Single Overload, at different overload ratios)

Specimen no:5 was tested with 4 single overloads at two different overload ratios and different baseline loads. Table 4.7 and Figure 4.7 show the loading program for specimen no:5.

CTS #5					
Precrack: $\Delta P = 1200-50$ , $a_i = 50$ mm, $N_f = 40560$ cycles					
$N \times 10^3$	$\Sigma \Delta a$	$a$ (mm)	$\Delta P$ (kgf)	R	$\Delta K$ (kgf. $mm^{-3/2}$ )
0-10	2.40	52.40	800-50	0.062	51.5
* $\%L = 1.5$	-	-	1200-50	0.041	-
10-20	10.54	60.54	800-50	0.062	68.8
* $\%L = 1.5$	-	-	1200-50	0.041	-
20-23.5	17.02	67.02	800-50	0.062	91.5
23.5-28.5	18.49	68.49	533-50	0.093	62.8
* $\%L = 1.5$	-	-	800-50	0.062	-
28.5-32	23.92	73.92	533-50	0.093	85.3
* $\%L = 1.75$	-	-	630-50	0.079	-
32-40.5	28.66	78.66	360-50	0.138	70.63

Table 4.7: Single Overload Test Plan for Specimen 5

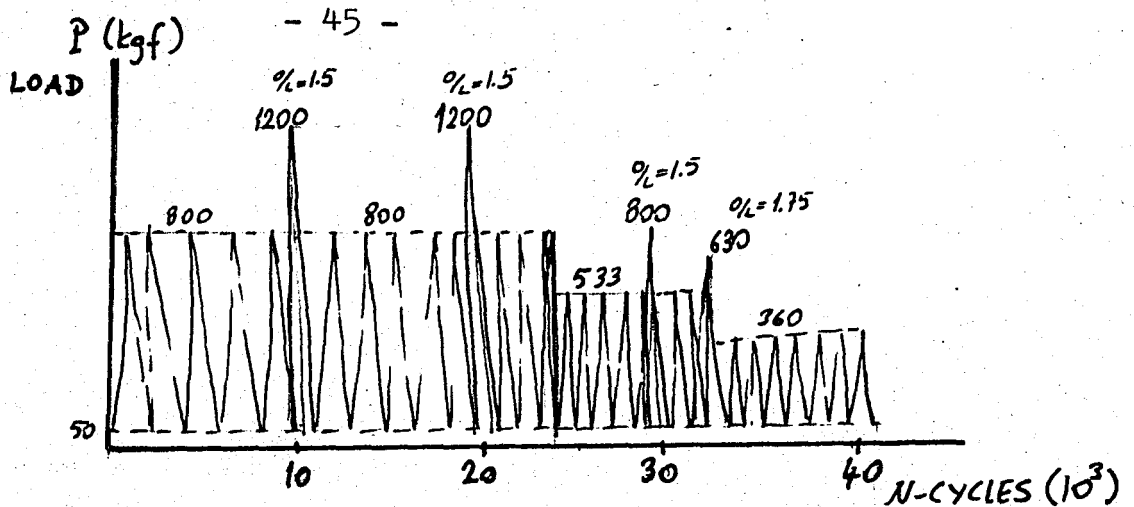


Figure 4.7: The loading program of specimen 7

Group V: (Single Overload Tests,  $O/L = 1.25, 1.5, \text{ and } 2.0$ )

In this group (specimens 6, 8 and 9), the effects on subsequent crack growth of single overloads were examined. The crack was propagated under constant amplitude loading conditions, a single overload cycle was applied, and the crack was then loaded under constant amplitude loading until steady-state growth rate was again reached.

Three compact tension specimens (6, 8 and 9) were subjected to single overloads with overload ratios of 1.25, 1.5 and 2.0. The overload ratio,  $O/L$ , is defined as the overload stress (or load) divided by the maximum baseline stress ( $S_{OL}/S$ ) or load ( $P_{OL}/P$ ).

Single overload cycles were applied at same crack length to discuss the effects of various overload ratios.

Group VI: (Fracture Toughness Tests)

4.5.1 The fracture toughness properties were performed in accordance with present ASTM standards [40]. Figure 4.8 shows the experimental set-up for fracture toughness testing. The standard  $K_{IC}$  test procedure is added to Appendix-B.

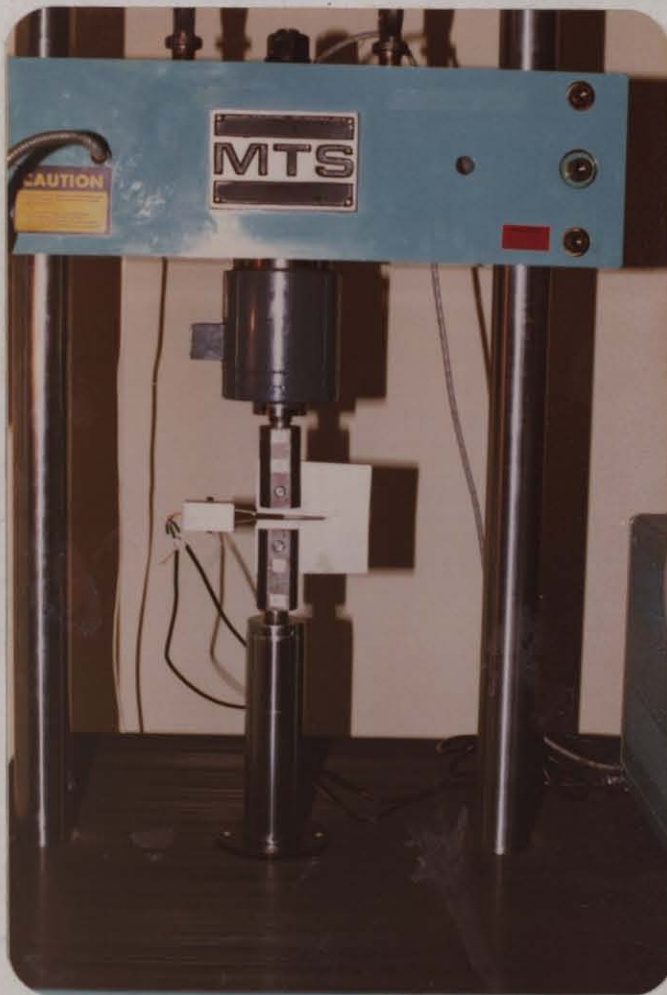


Figure 4.8: The experimental set-up for Fracture Toughness Testing

#### 4.5. Test Results

##### 4.5.1. Group I test results

Figure 4.9 and 4.10 show the a-N curves for specimen 1 and 11, respectively.

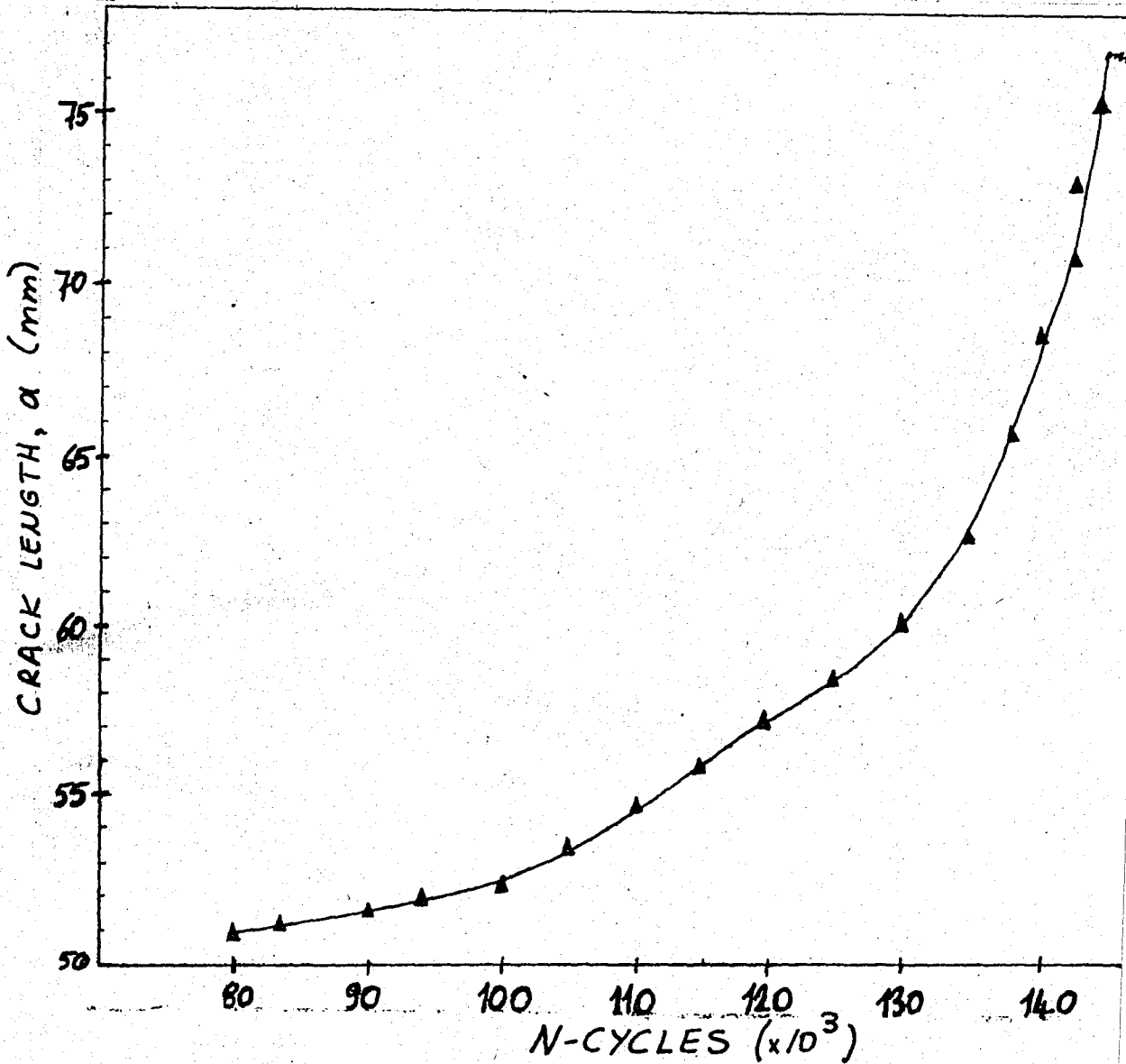


Figure 4.9: Crack length vs. number of cycles (CTS 1)

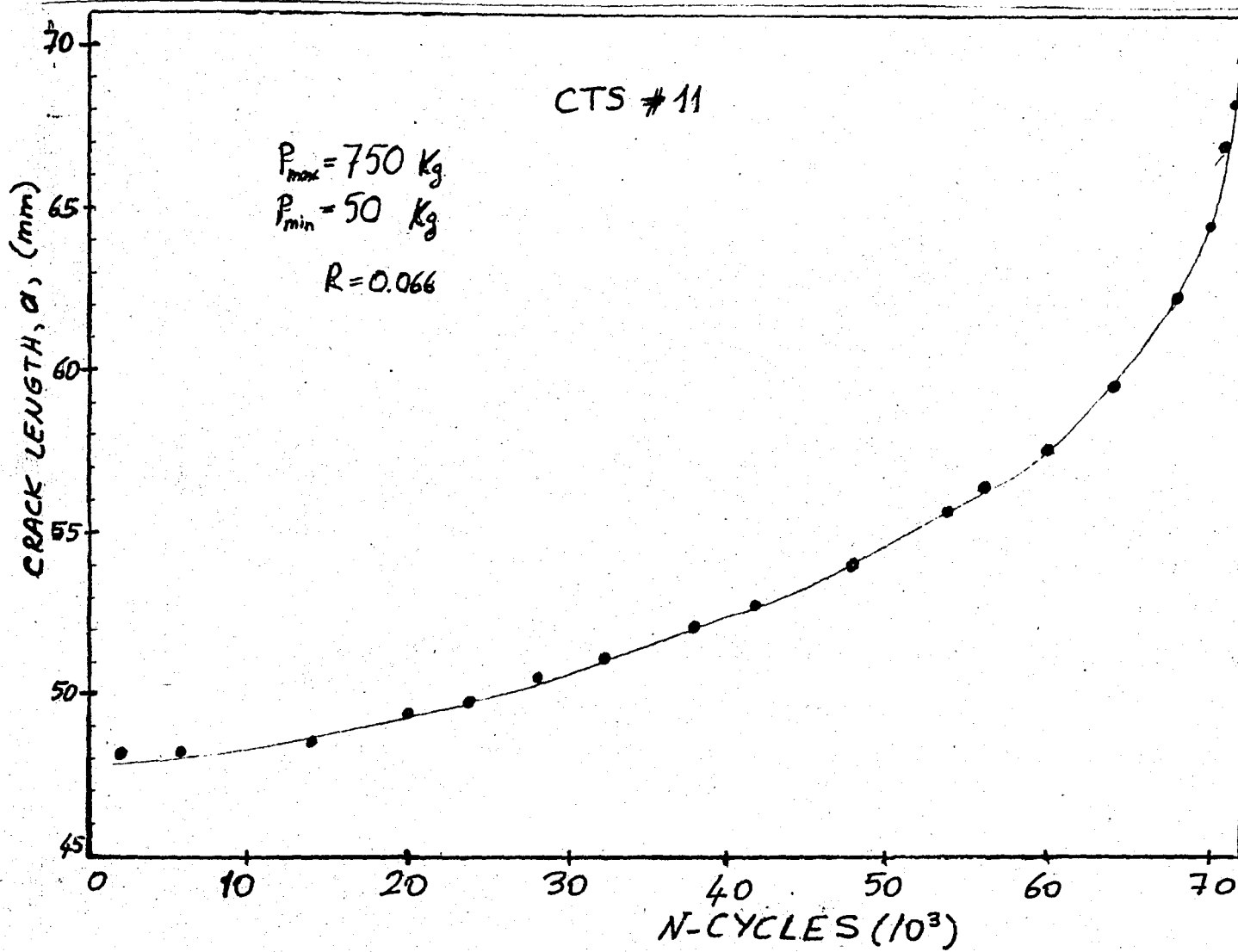


Figure 4.10: Crack length vs. number of cycles (CTS 11)

Figure 4.11 and 4.12 show the fracture surfaces of specimens 1 and 11. Figure 4.13 shows crack growth rate  $da/dN$ , plotted against applied stress intensity range,  $\Delta K$ , for the 2024-T4 Al-alloy for two specimens.



Fig.4.11:Fracture surface  
of specimen 1.

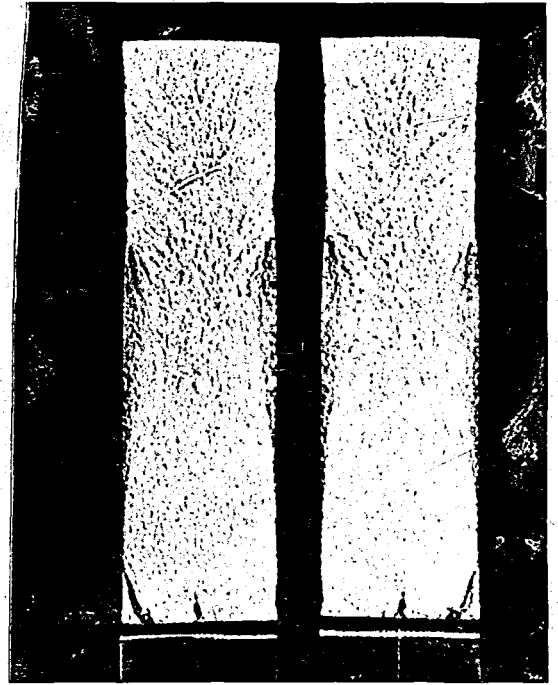


Fig.4.12:Fracture surfaces  
of specimen 11

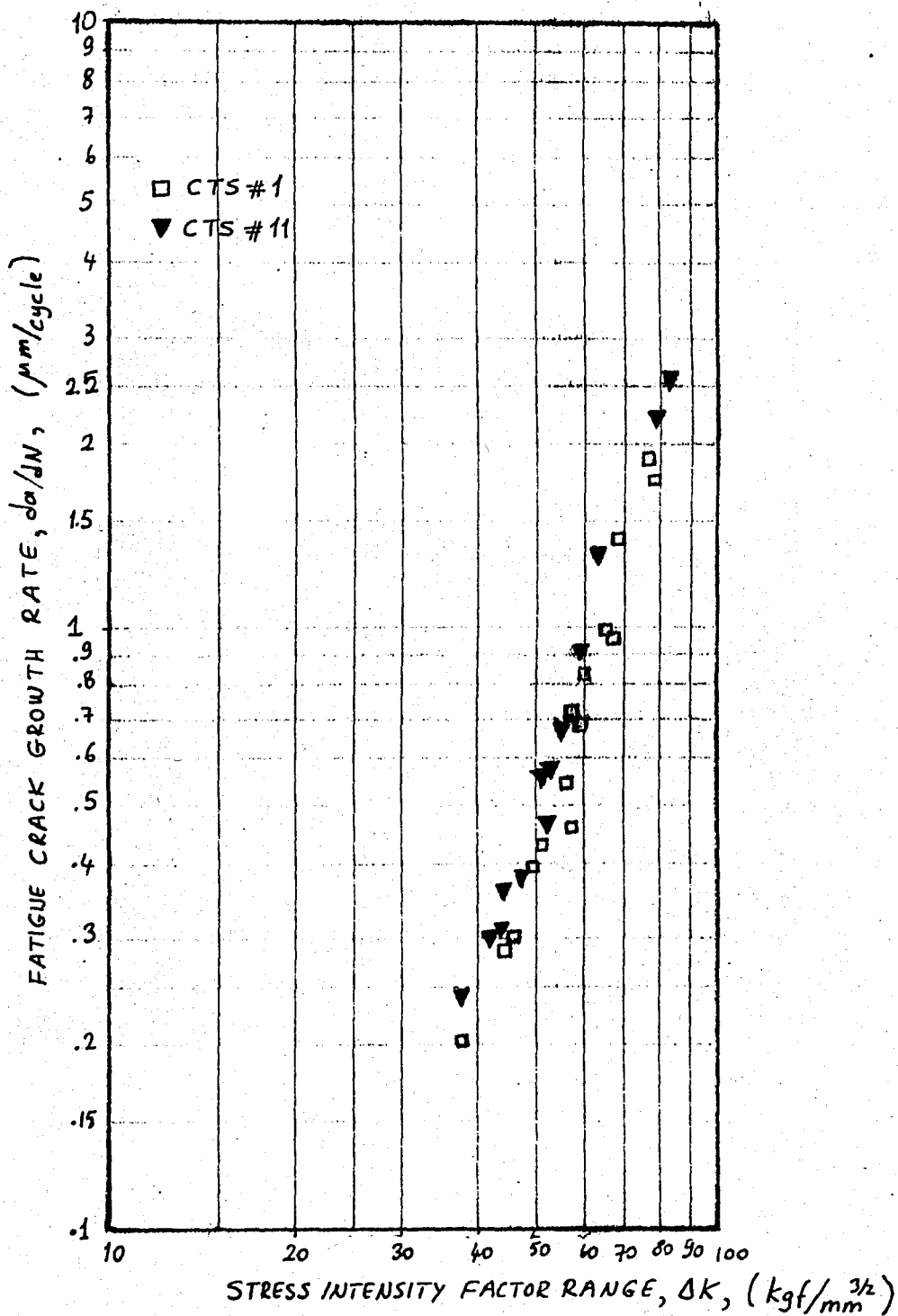


Figure 4.13: Crack growth rate as a function of stress intensity factor range for constant amplitude tests



#### 4.5.2. Group II test result

Figure 4.14 and 4.15 represent the fracture surfaces of specimens 2 and 3, respectively.

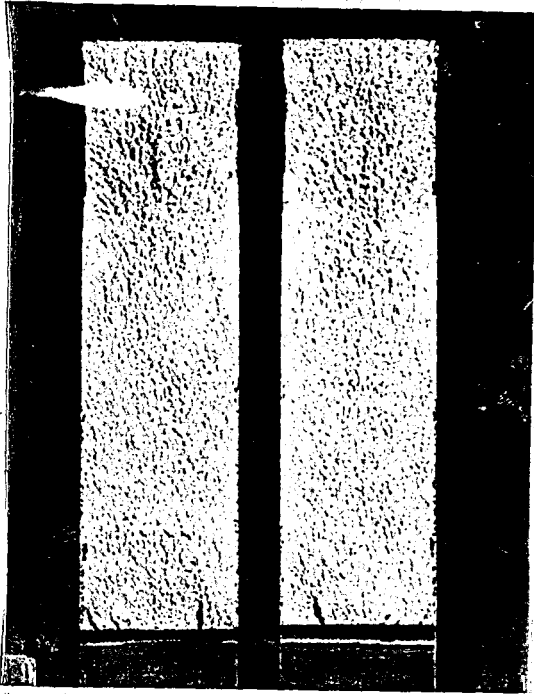


Fig.4.14:Fracture surfaces  
of specimen 2

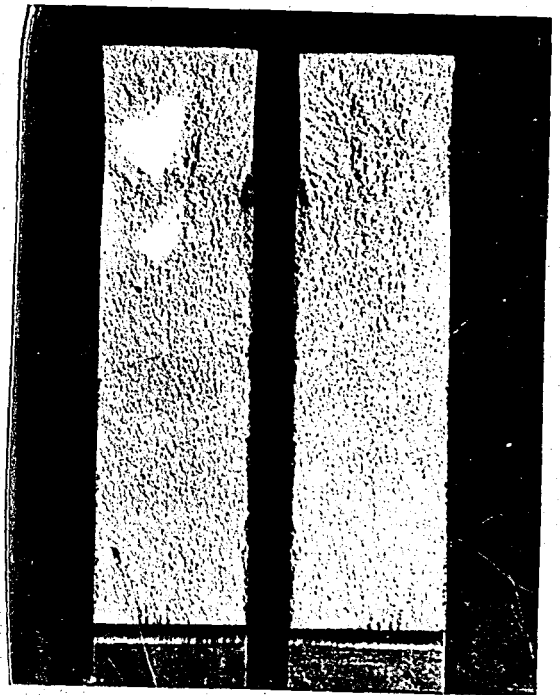


Fig.4.15:Fracture surfaces  
of specimen 3

The crack length vs. number of cycles results for these tests are presented in Fig.4.16 and 4.17. And Fig.4.18 shows fatigue crack growth rate vs. applied stress intensity range for specimen 2 and 3.

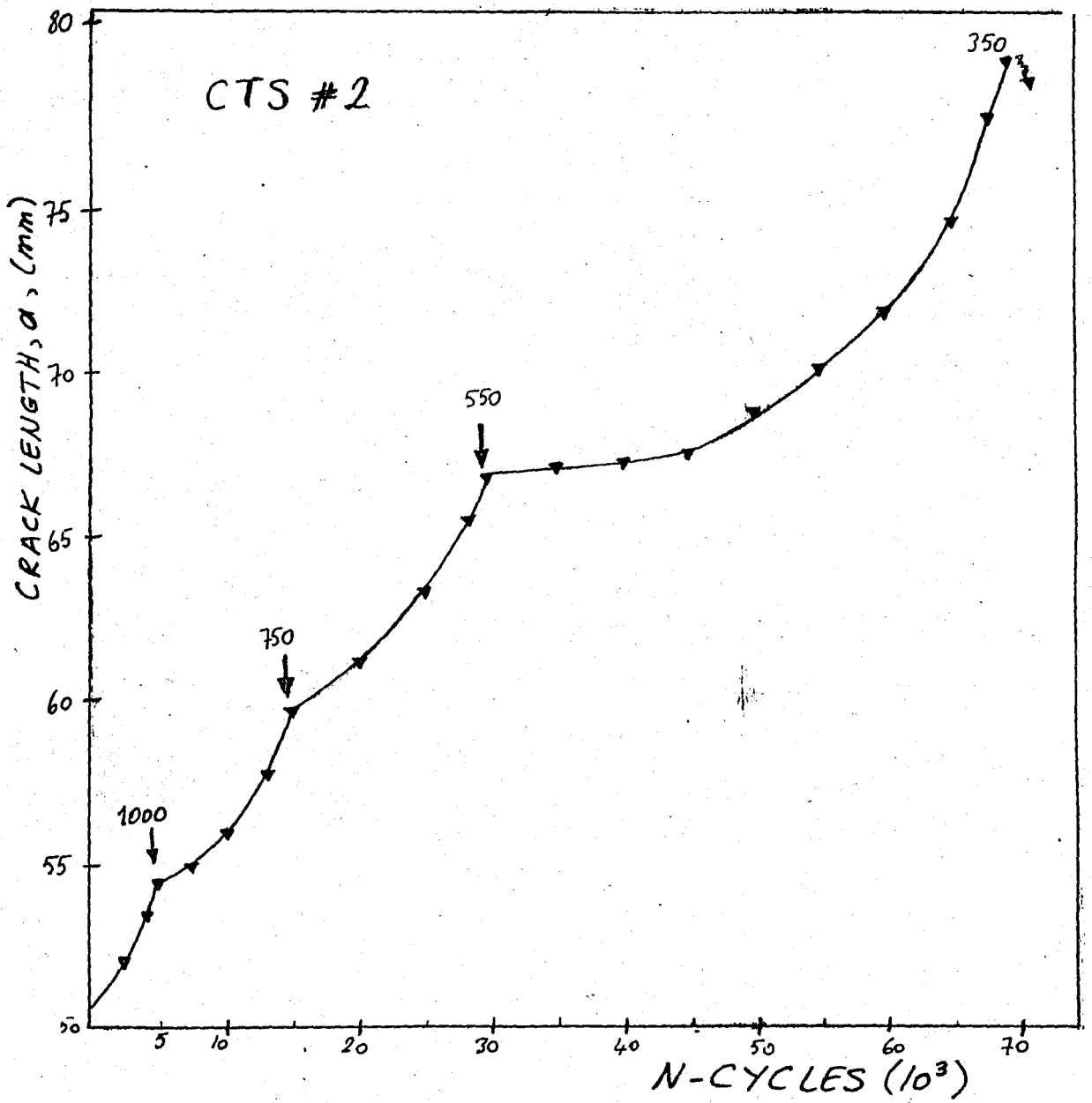


Figure 4.16: Crack length vs. applied cycles (CTS 2)

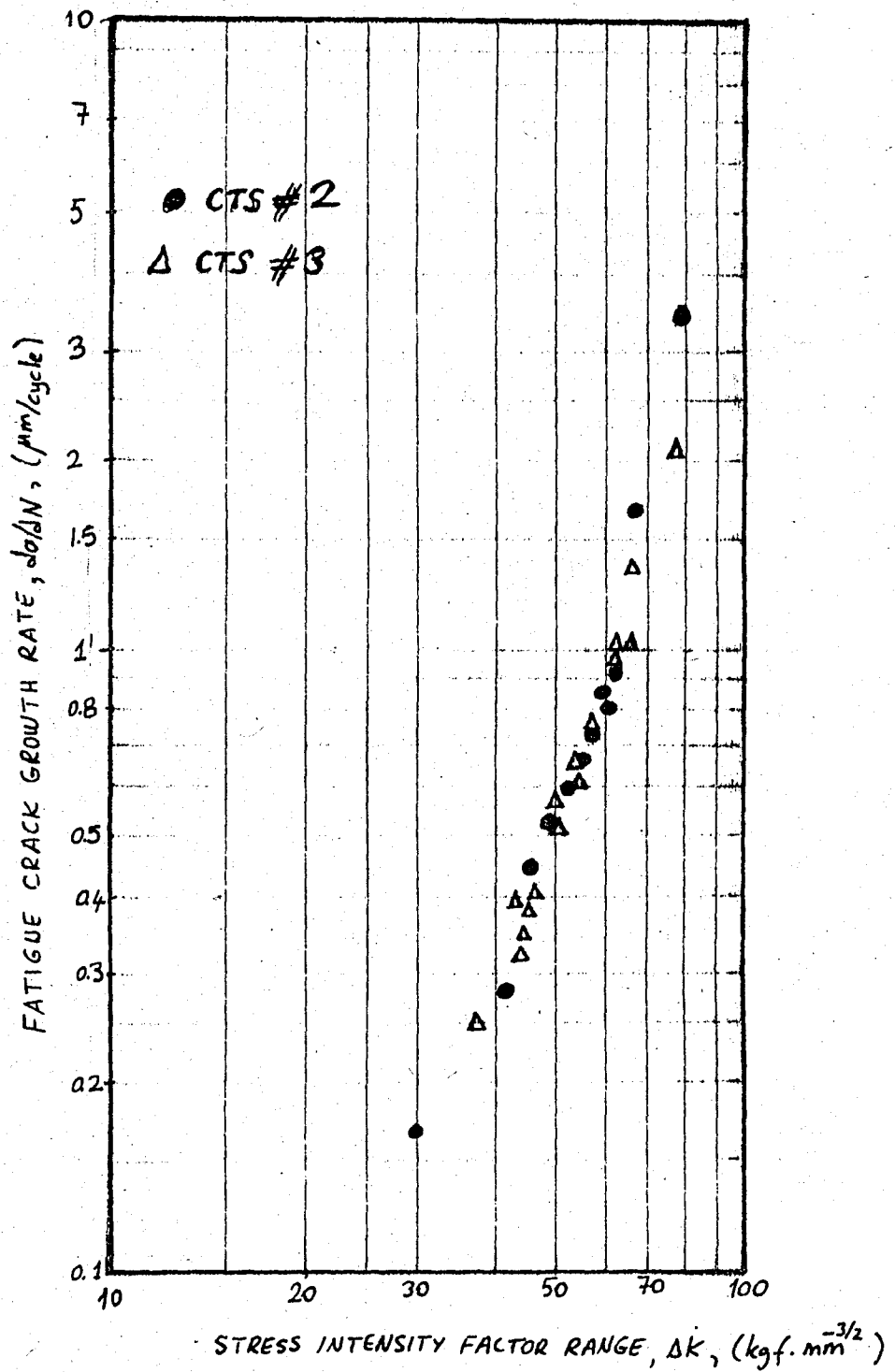


Figure 4.18: Fatigue crack growth vs. stress intensity factor range for Group II

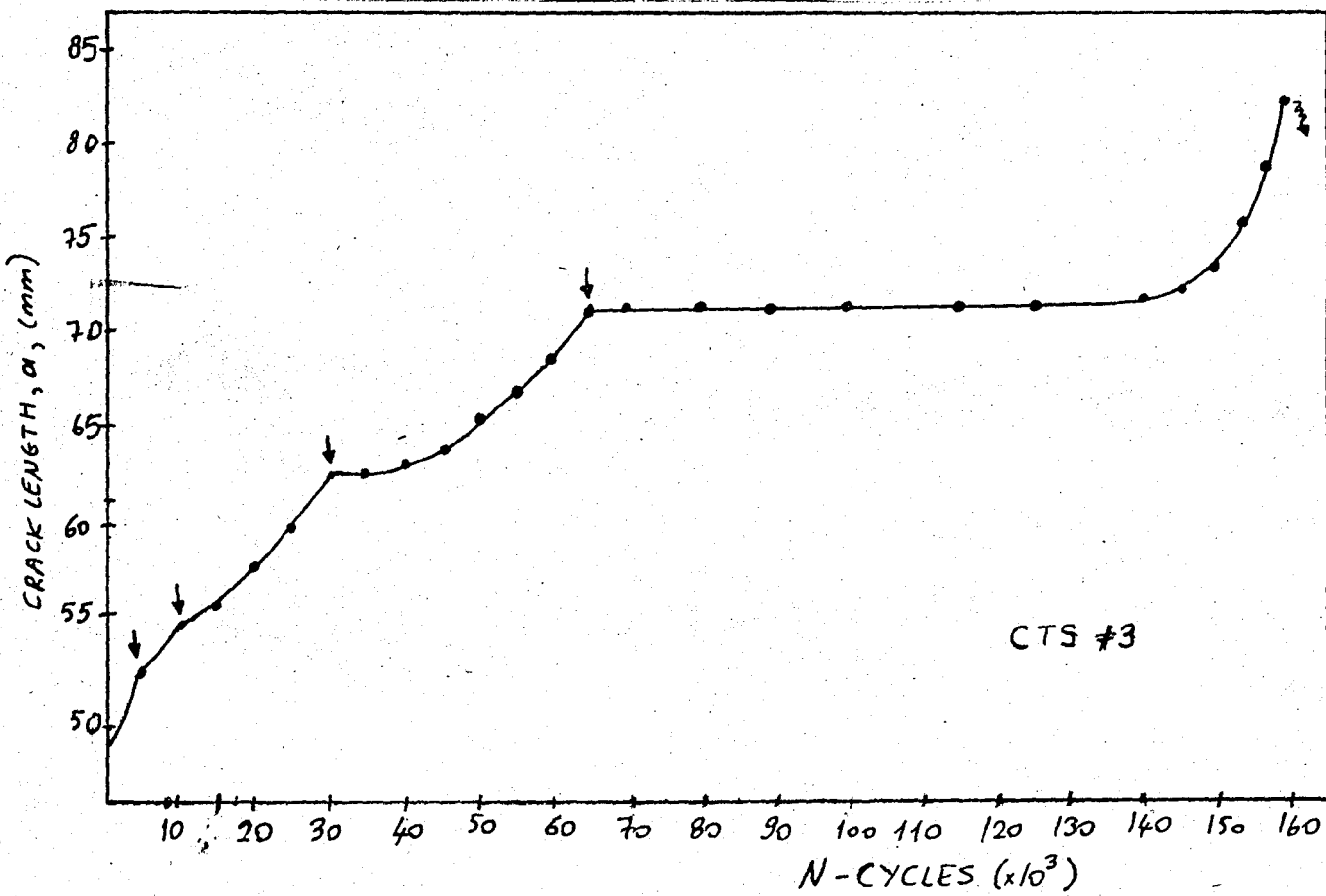


Figure 4.17: Crack length vs. applied cycles (CTS 3)

#### 4.5.3. Group III test results

The fracture surfaces of specimen 4 are seen in Figure 4.19.

And Figure 4.20 shows the crack length vs. applied cycles for specimen 4.

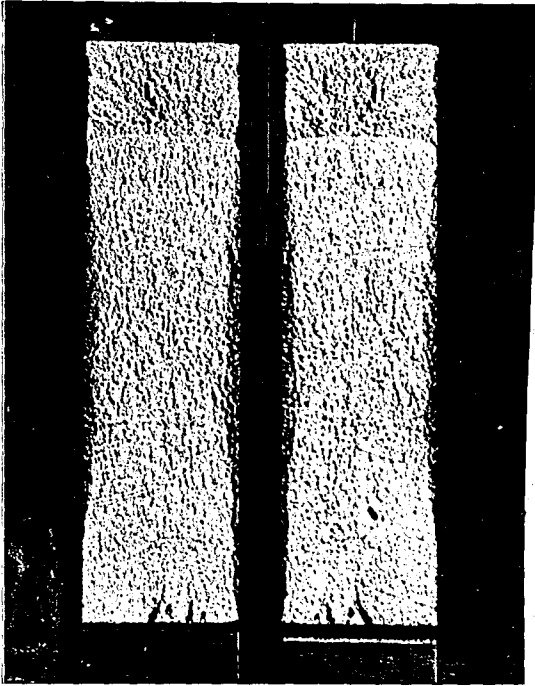


Figure 4.19: Fracture surfaces of specimen 4 (at displacement control)

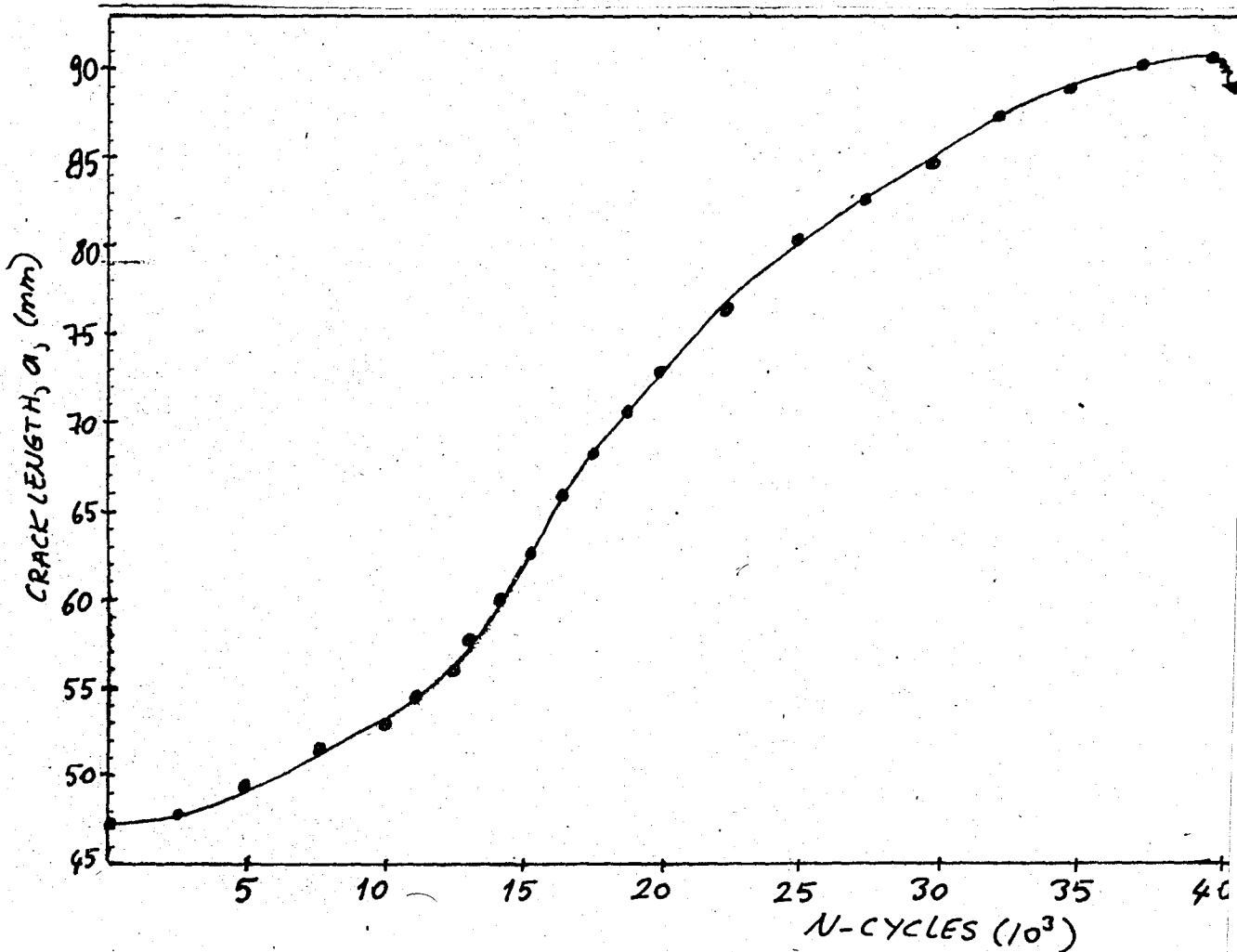


Figure 4.20: Crack Length vs. applied cycles (CTS 4)

Figure 4.21 shows fatigue crack growth rate vs. stress intensity factor range for specimen 4.

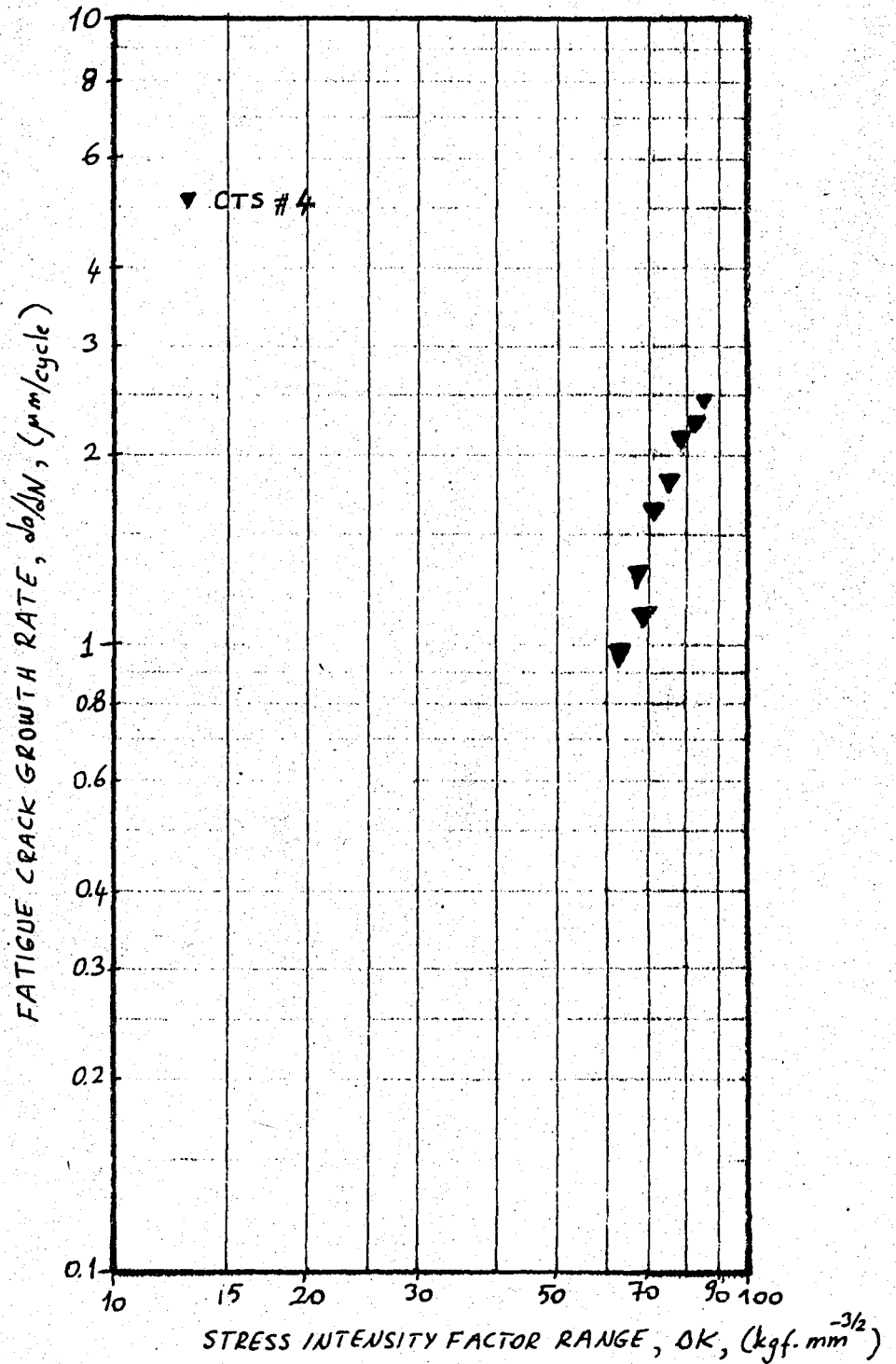


Figure 4.21: Fatigue growth rate vs. stress intensity range (CTS 4)

#### 4.5.4. Group IV test results

Figure 4.22 shows the fracture surfaces of specimen 5. Figure 4.23 represents the crack length vs. applied cycles behaviour and Figure 4.24 shows the crack growth rate vs. stress intensity factor range, for specimen 5.



Figure 4.22: Fracture surfaces of specimen 5 (Single Overload Test)

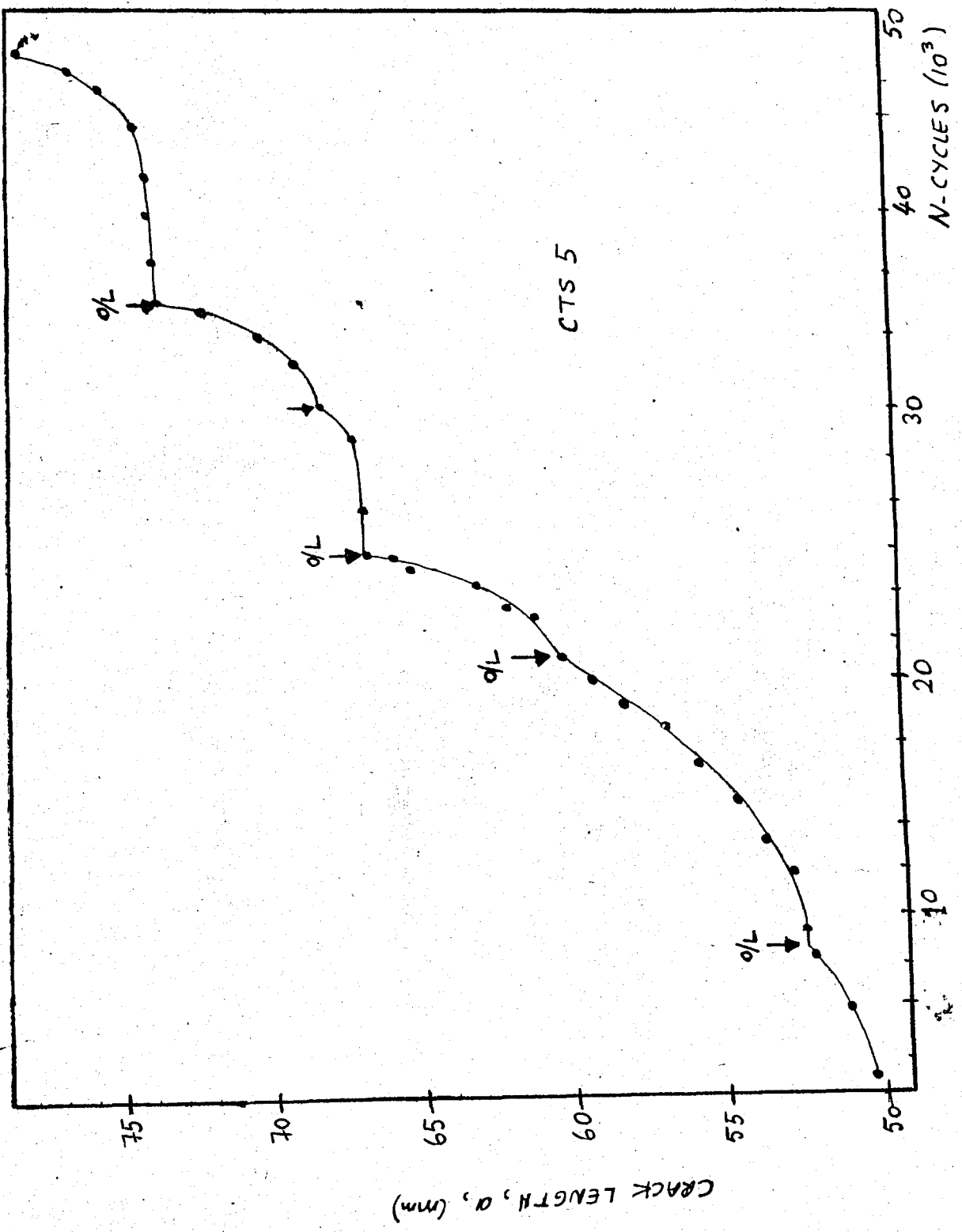


Figure 4.23: Crack length vs. applied cycles (CTS 5)



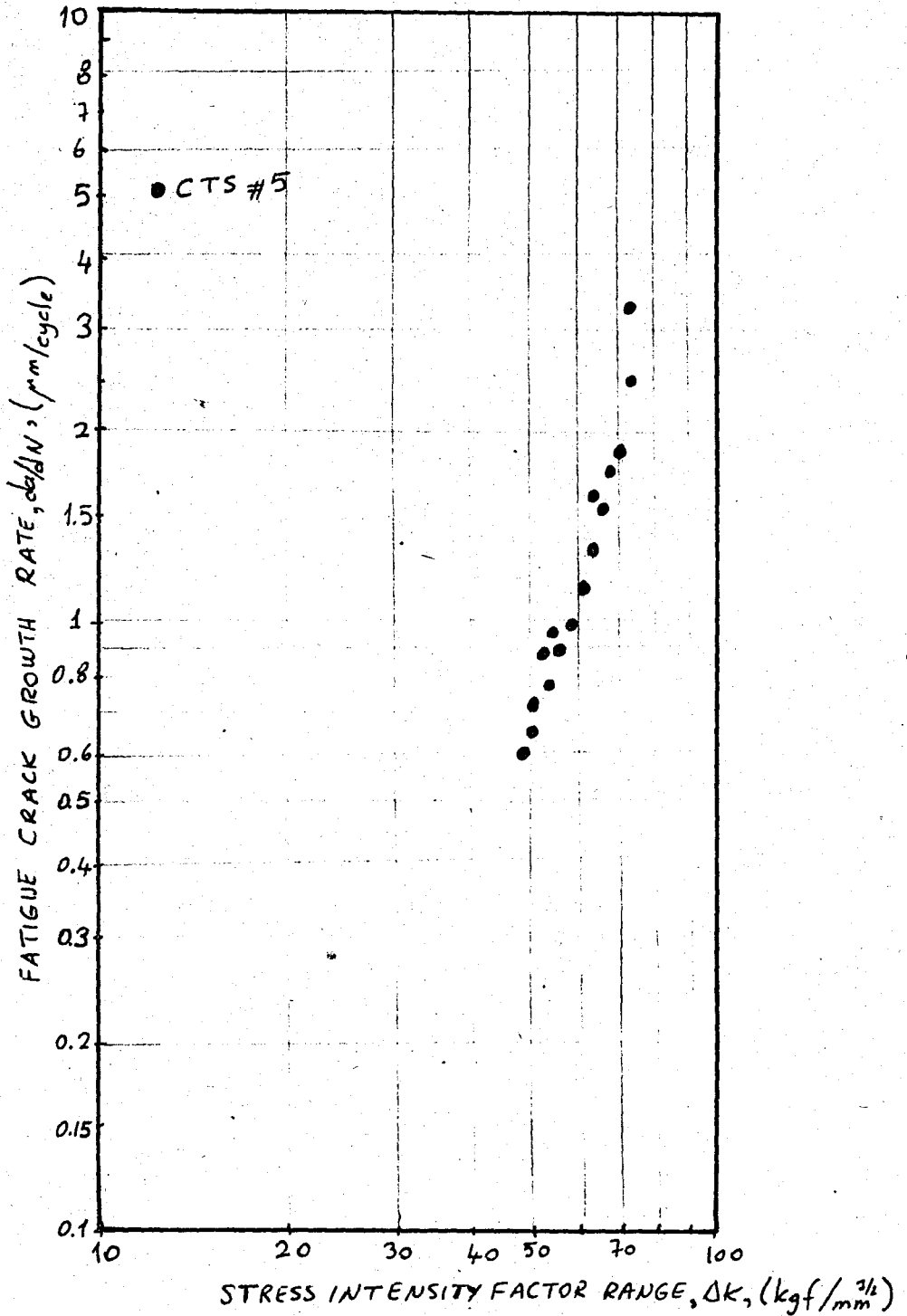


Figure 4.24: Crack growth rate vs. stress intensity factor range (CTS 5)

#### 4.5.5. Group V test results

The objective of these tests were to obtain detailed crack growth measurements during and subsequent to the application of single overloads, and to define the effects of those overloads on subsequent crack growth behaviour. The data were analyzed by plotting crack length vs. number of cycles and crack growth rate vs. stress intensity factor range.

Figures 4.25, 4.26 and 4.27 present overall  $a$  vs.  $N$  data for three specimens subjected to single overload applications with different overload ratios. The application of tensile overloads caused crack growth rate following the overload to be much less than it would have been without the overload. Also in these figures, the  $a$ - $N$  curve obtained from experiments was compared to predicted  $a$ - $N$  versus based on Willenborg Model.

Subsequent to the application of an overload, the behaviour of the crack growth on the specimen surfaces was somewhat erratic.

Figures 4.28, 4.29 and 4.30 present the fracture surfaces of specimens 6, 8 and 9, respectively.

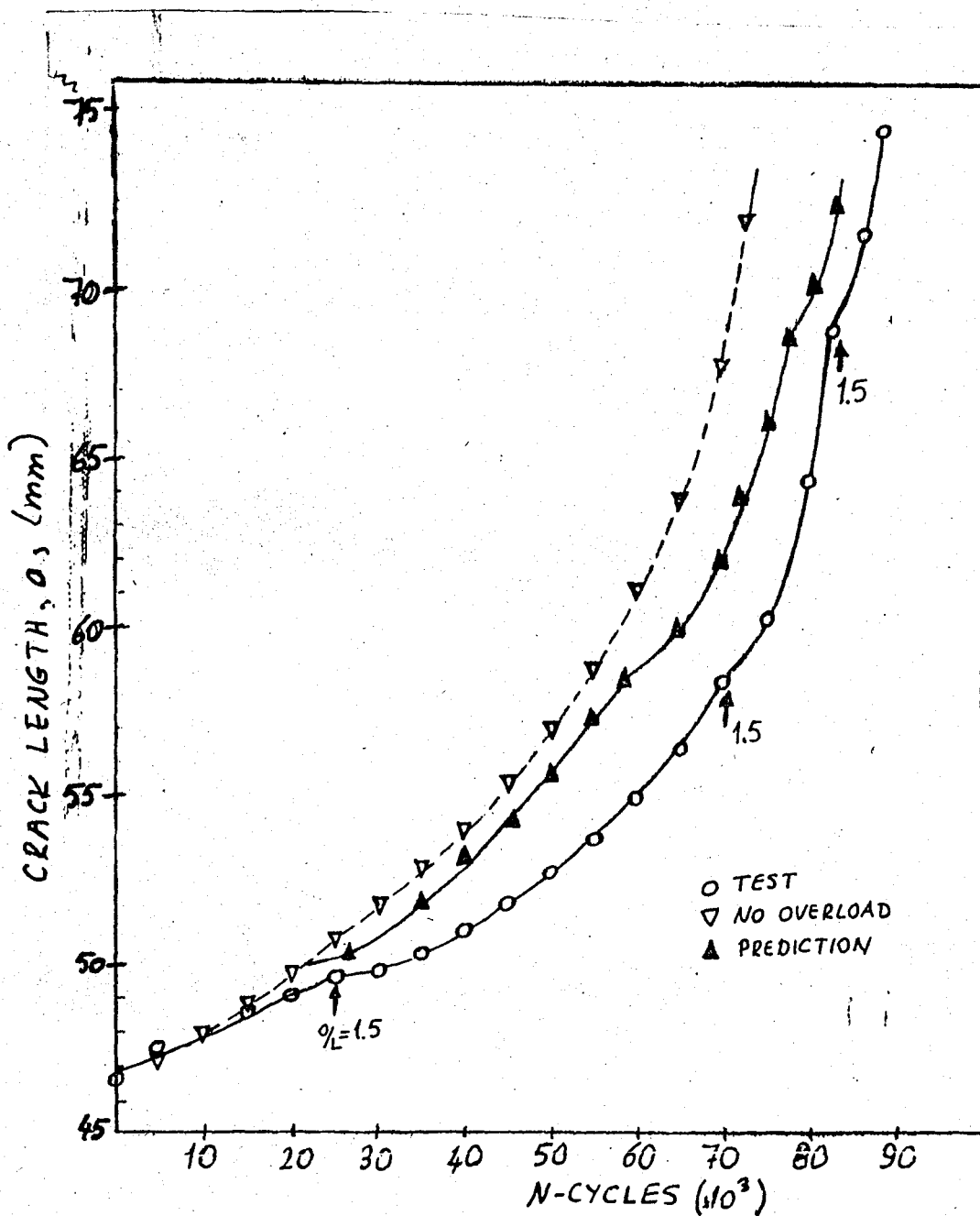


Figure 4.25: Crack length vs. applied cycles for overload test:  $O/L=1.5$  (CTS 6)

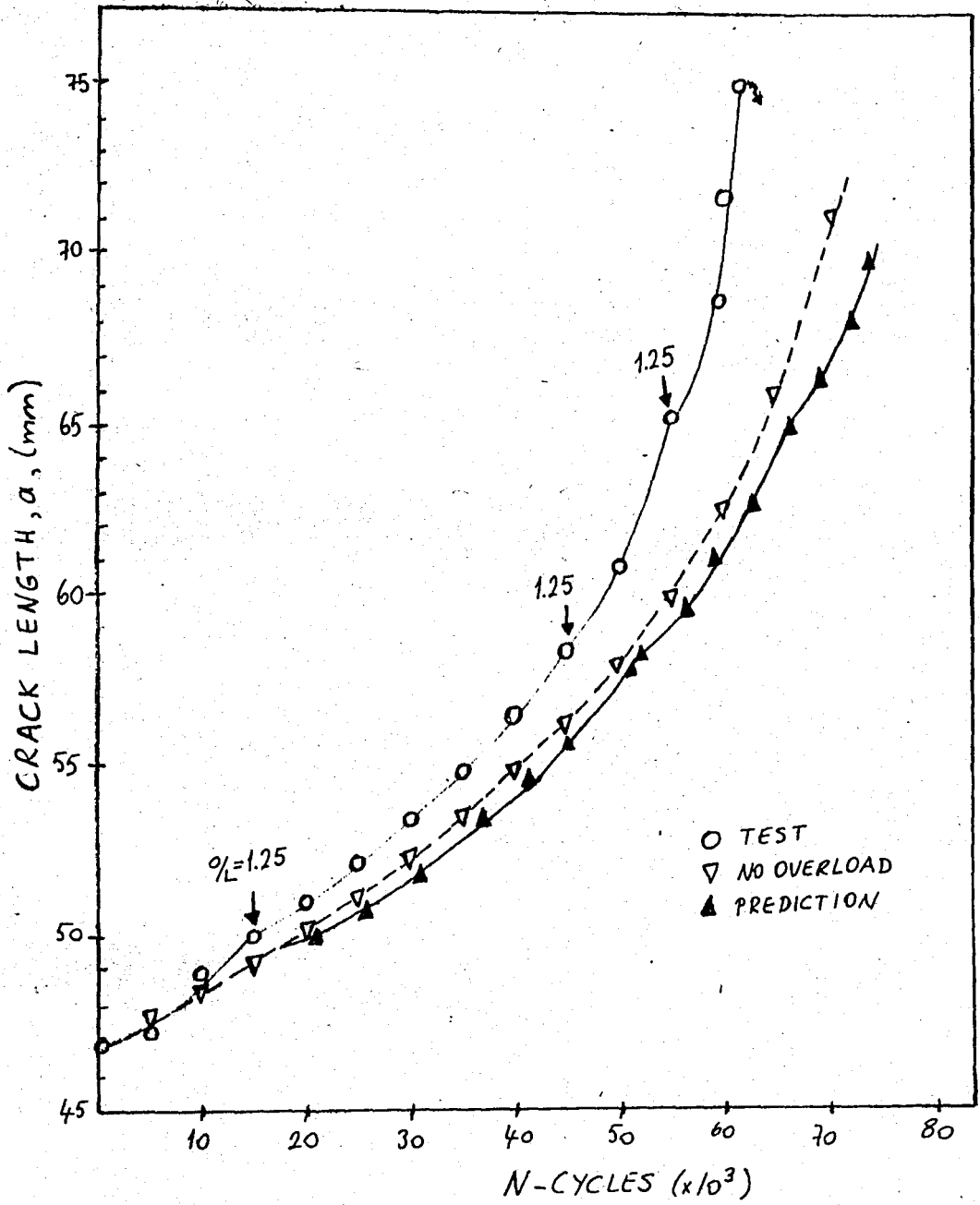


Figure 4.26: Crack length vs. applied cycles for overload test:  $O/L=1.25$  (CTS 8)

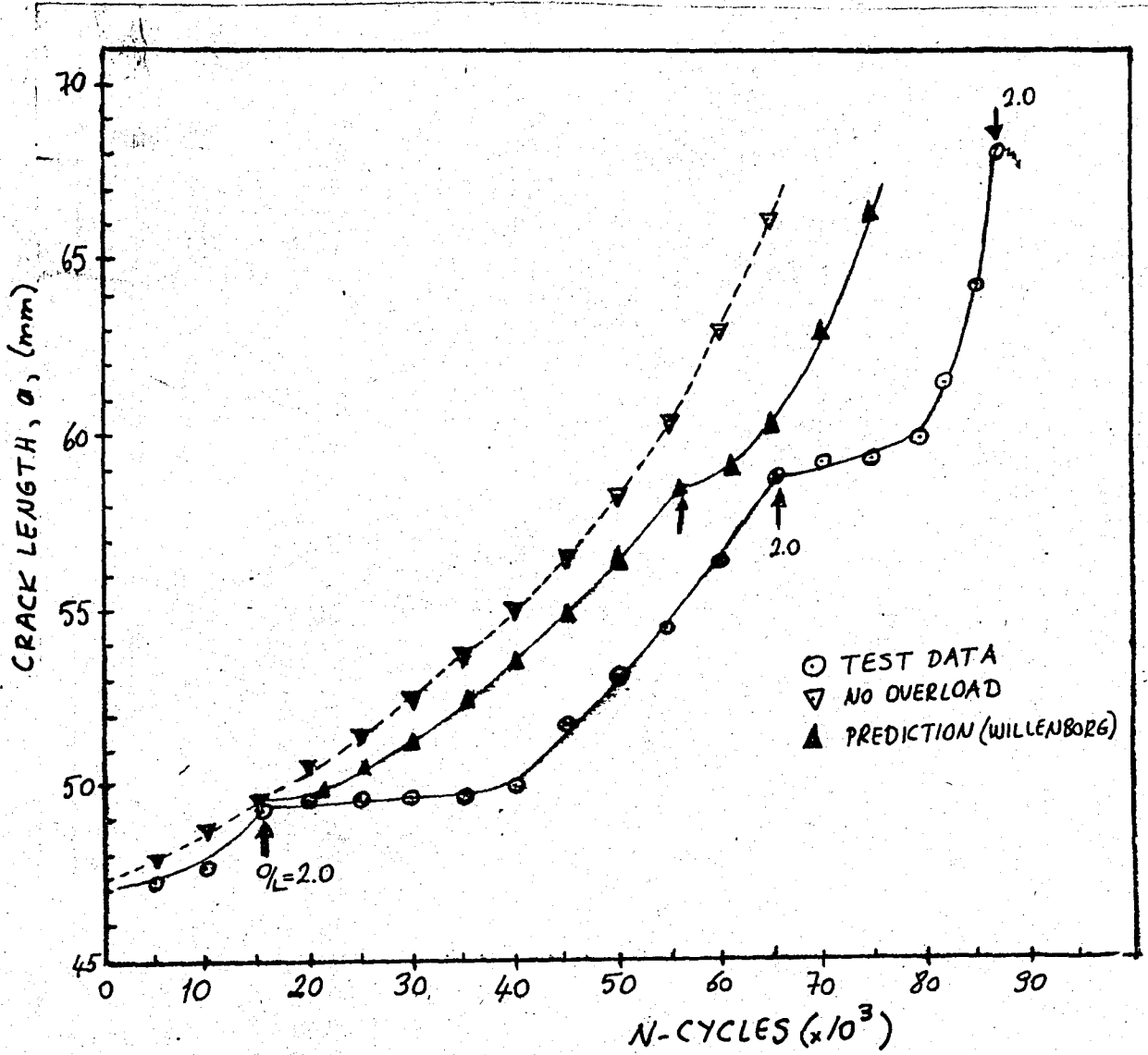


Figure 4.27: Crack length vs. applied cycles for overload test ( $a/L=2.0$ ) (CTS 9)

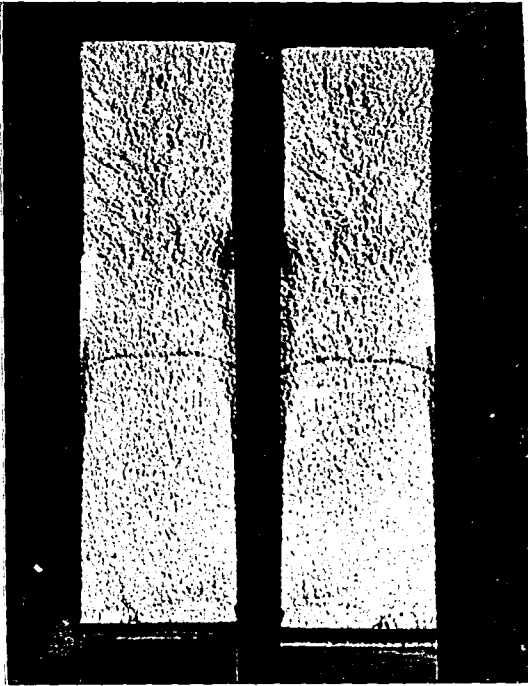


Fig. 4.28: Fracture surfaces of specimen 6 ( $O/L=1.5$ )

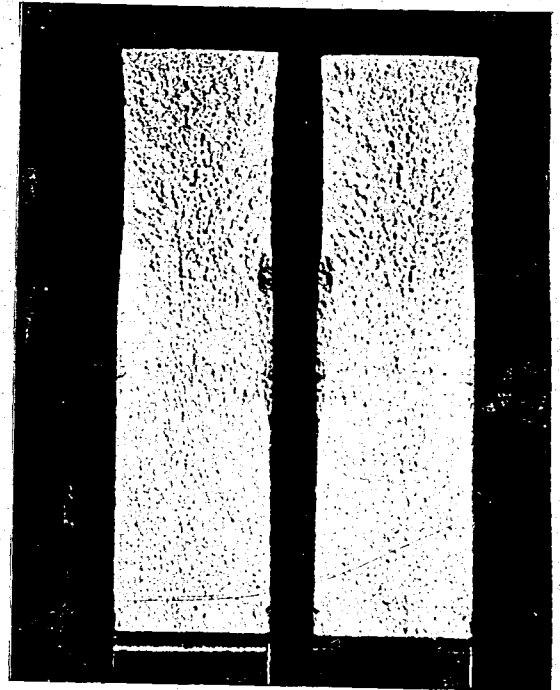


Fig. 4.29: Fracture surfaces of specimen 8 ( $O/L=1.25$ )

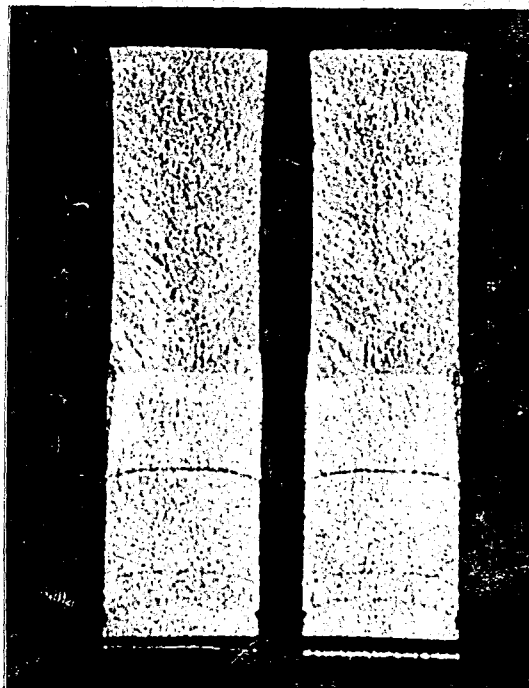


Fig. 4.30: Fracture surfaces of specimen 9 ( $O/L=2.0$ )

In Figure 4.31, the fracture surfaces of specimens 6, 8 and 9 are placed so that comparisons can be made. The a-N curves of these three specimens can be seen in Figure 4.32.



Figure 4.31: Fracture surfaces of three specimens (6, 8 and 9, respectively)

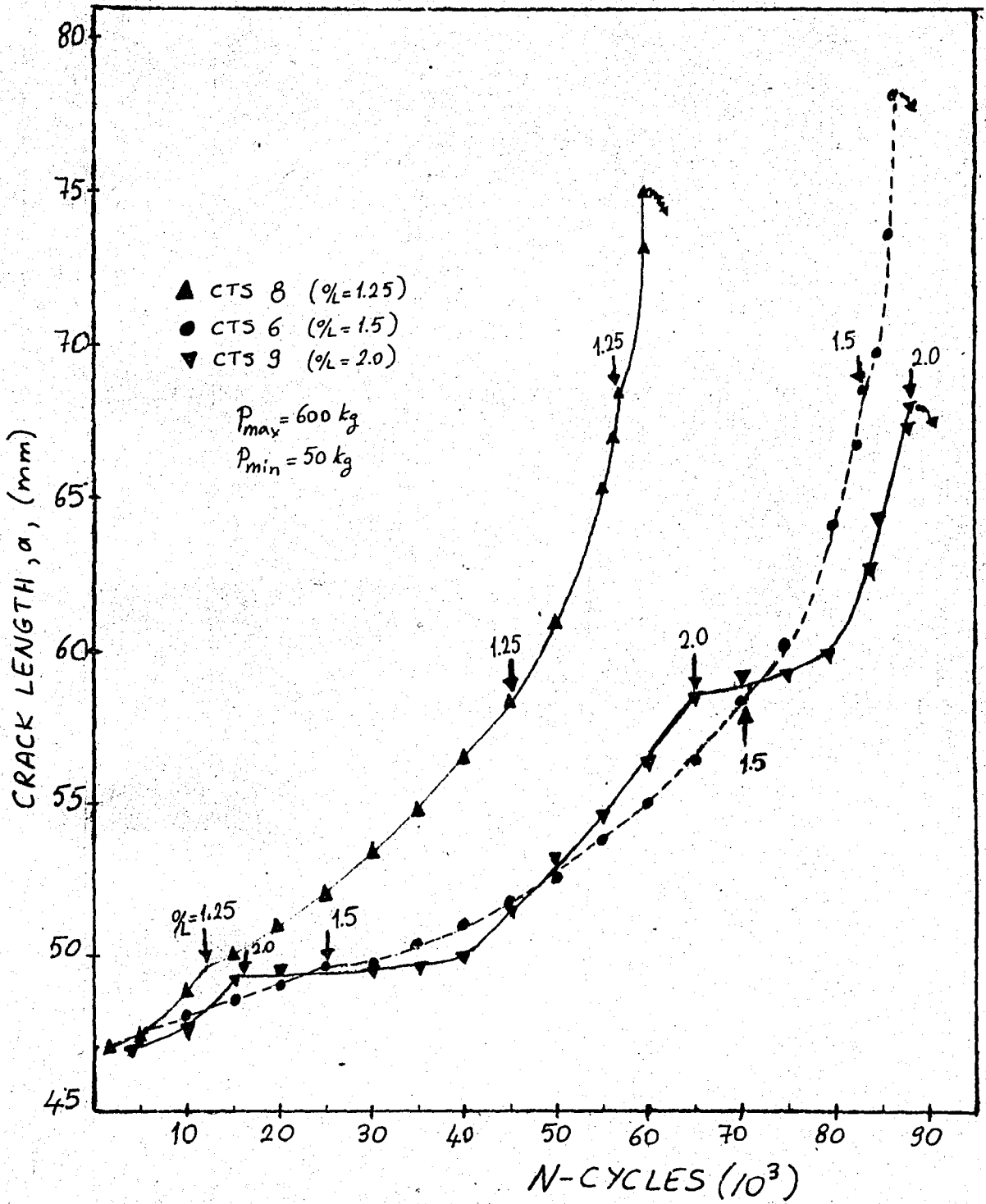


Figure 4.32: Crack length vs. applied cycles for Group V specimens



The crack growth rate as a function of stress intensity factor range is presented in Figure 4.33.

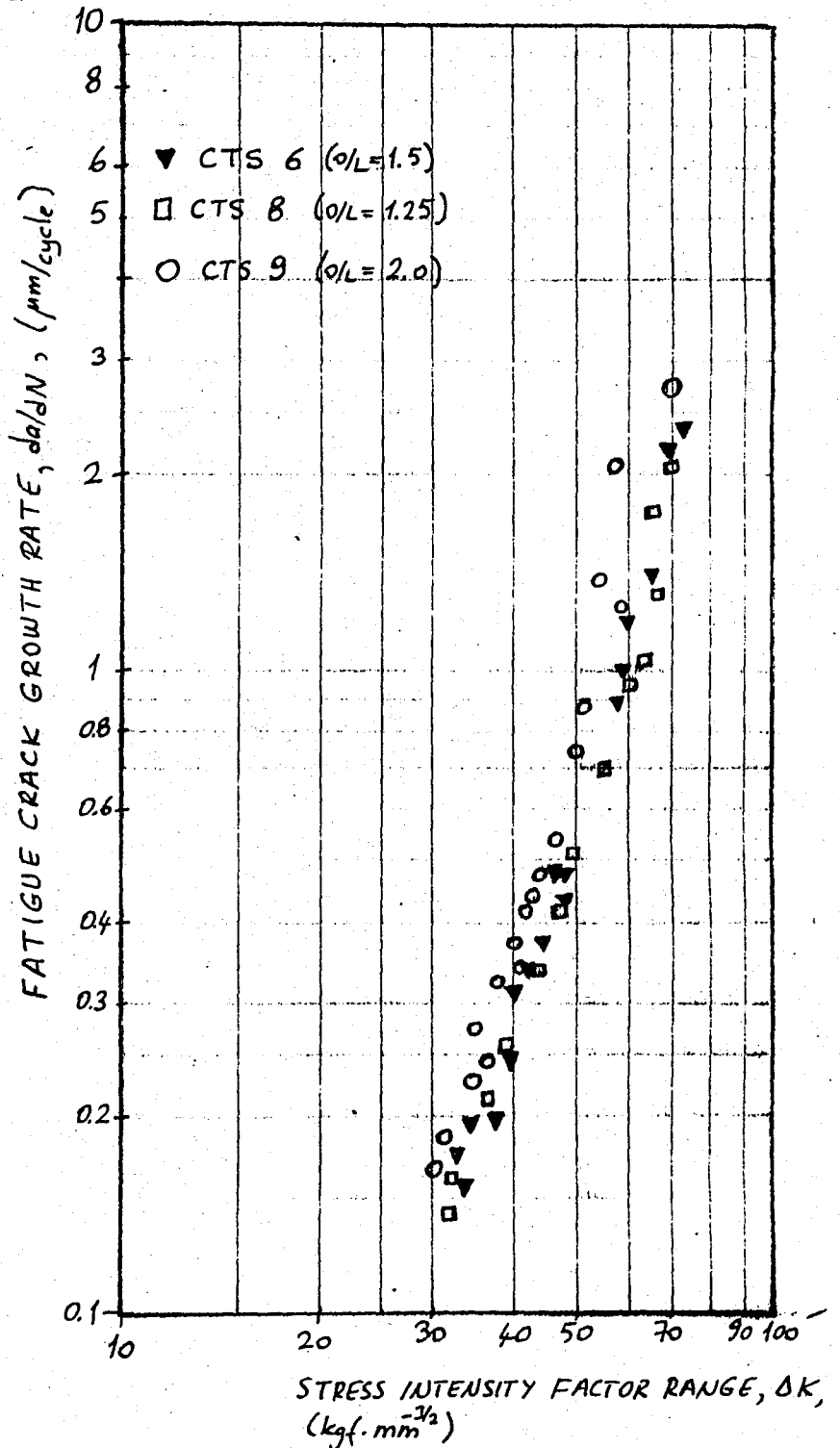


Figure 4.33@ Crack growth rate vs. stress intensity factor range for overload tests

#### 4.5.6. Group VI test results

Specimens 7 and 10 were tested for fracture toughness testing. Figure 4.34 shows the fracture surfaces of specimen 7.

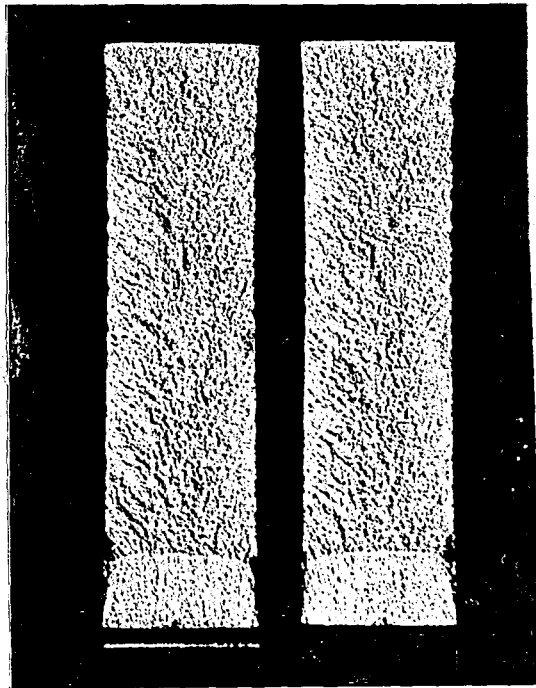


Figure 4.34: Fracture surfaces of specimen 7 (After Fracture Toughness Test)

#### 4.6. Discussion of Results

##### 4.6.1. Constant Amplitude Test Results

Figure 4.13 shows crack growth rate,  $da/dN$ , plotted against applied stress intensity range,  $\Delta K$ , for the 2024 - T4 aluminum for a variety of stress ratios. It is evident from the figure that, as the stress ratio,  $R$ , is increased, the crack growth rate increases for the same value of  $\Delta K$ .

The data were fitted to a Paris Equation of the form:

$$\frac{da}{dN} = C (\Delta K)^n$$

$\frac{da}{dN} : (\text{mm/cycle})$   
 $\Delta K : (\text{kgf/mm}^{3/2})$

A least squares procedure was used to fit the data to above equation. And the parameters were obtained as;

$$C = 7 \times 10^{-6}$$

$$n = 2.87$$

therefore, the Paris Equation used in all tests becomes

$$\frac{da}{dN} = 7 \times 10^{-6} (\Delta K)^{2.87} \quad (\text{kgf, mm})$$

#### 4.6.2. Single Overload Test Results

Figures 4.23, 4.25, 4.26 and 4.27 present overall  $a$  vs.  $N$  data for four specimens subjected to single overload applications.

The amount of crack retardation following a single tensile overload increases as the ratio of overload max. stress intensity,  $K_{\max_{OL}}$ , to the maximum stress intensity  $K_{\max}$ , of subsequent constant amplitude loading ( or  $P_{OL}$  to  $P_{\max}$  ratio) increases. In references [43 - 50], the same trend was observed. For example, (See Figure 4.32)  $O/L \approx 1.25$  produces almost no retardation,  $O/L \approx 1.5$  produces retardation and  $O/L \approx 2.0$  produces temporary arrest followed by retarded growth, in tests of specimens 6, 8 and 9.

Figure 4.26 shows that overloads of  $O/L \approx 1.25$  have negligible effect on crack growth rates. Figures 4.25 and 4.27 show that greater overload effects can not be neglected.

The number of delay cycles also depends on the crack length at which each overload is applied. It can be seen in Figure 4.32 that, as the crack length at which the overloads were applied increases, there is an orderly increase in the number of delay cycles.

Finally, it can be concluded that the number of delay cycles is an increasing function of the crack length at which a single overload cycle is applied and of the overload ratio. Overload ratios less than approximately 1.25 produce essentially no retardation while an overload ratio greater than 2.0 is adequate to cause crack arrest.

Retardation occurs for growth through the crack tip plastic zone created by a tensile overload [43,47].

Measurement of crack growth following a tensile overload typically resemble that shown in Figure 3.5 (In References [44] and [45], this subject is studied in detail)

Crack retardation does not reach its full effect until the crack has grown some distance,  $d$ , into the plastic zone; this is called "DELAY OF RETARDATION".

Crack retardation eventually decays until growth rate before the tensile overload application is approached. Rice and Stephens [45] have found that when  $d \approx 30$  percent of the reversed plastic plane stress, yield zone size at the crack tip is:

$$r_y = \frac{1}{2\pi} \left( K_{\max_{OL}} / S_y \right)^2$$

Von Euw et al. [47] have found  $d \approx 10$  to 25 percent of total plastic zone size, or equivalently, about 50 to 100

percent of the reversed plastic zone size.

In this experimental study, "Delay of Retardation" is observed, but not calculated definitely.

Crack retardation increases if a group of consecutive overloads is applied instead of a single overload. (Group II tests). Also High to-Low load sequence can produce crack retardation. (Figures 4.16 and 4.17)

#### 4.6.3. Constant Amplitude Load, at displacement control

In Figure 4.21, fatigue crack growth rate vs. stress intensity factor range is shown. At displacement control, the stress intensity factor is

$$K_I = \frac{\delta}{B \sqrt{W}} \frac{f(a/W)}{1/k} = \frac{\delta E}{\sqrt{W}} g(a/W)$$

Saxena and Hudak [51] have found that

$$\frac{1}{k} = \frac{1}{B E} \left\{ \frac{16}{(1-(a/W)^2)} - \frac{24}{(1-a/W)} - (4.5) \ln(1-a/W) + 18.71 \right\}$$

In this case, The higher the crack length, the lower the stress intensity factor.

Using the above equations, a function of  $g(a/W)$  is obtained. (Figure 4.35)

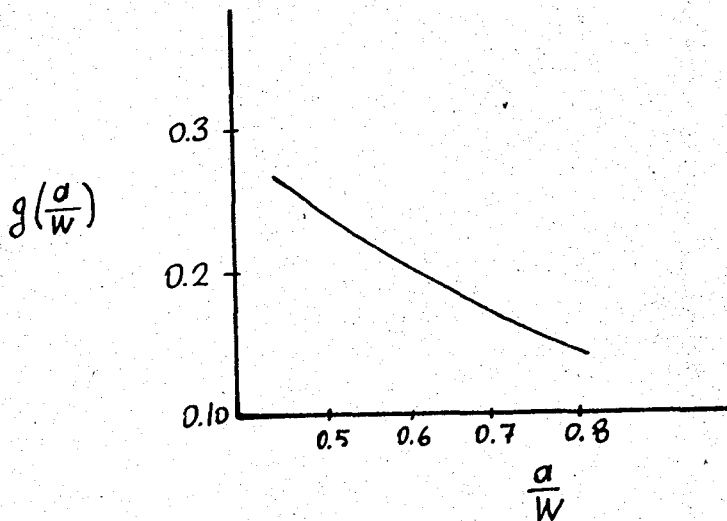


Figure 4.35: A graph for  $g(a/W)$  at displacement control

## CHAPTER V

### CONCLUSIONS

The following conclusions have been reached or verified as a direct result of investigations performed during this study:

1. A stress ratio effect on crack growth rate exists. The higher the stress ratio at a given value of  $\Delta K$ , the higher the rate of fatigue crack growth.
2. Single overload cycles less than, or equal to, 1.25 times the baseline loading, have negligible effect on subsequent crack growth rates for 2024-T4 Aluminum alloy.
3. At a given overload ratio and baseline stress ratio, delay cycles increase as a function of crack length and stress intensity factor, for Aluminum.
4. The amount of crack retardation following a single tensile overload increases, as the overload ratio increases.
5. Crack retardation increases if a group of consecutive overloads is applied instead of a single overload.



REFERENCES

1. Schijve, J., "Four Lectures on Fatigue Crack Growth" Engineering Fracture Mechanics, Vol.11, pp167-221, (1979)
2. Harrison, J.D., "An Analysis of Data on Non-propagating Fatigue Cracks on a Fracture Mechanics Basis", British Welding Journal, Vol. 2, No.3, (1970).
3. Knott, J.F., "Fundamentals of Fracture Mechanics", Butterworths, London, p 255, (1973).
4. Crooker, T.W., "The Role of Fracture Mechanics in Fatigue Design", Am. Soc. Mech. Eng., Proc.No.76-DE-5
5. Rolfe, S.T. and Barsom, J.M., "Fracture and Fatigue Control in Structures", Prentice-Hall, Inc., Englewood Cliffs, New Jersey, p 239 and 259, (1977).
6. Vardar, Ö., "Akma Sınırı Ötesinde Yorulma Çatlağı İlerlemesi", Boğaziçi Univ., Istanbul, (1980).
7. Srawley, J.E. and Brown, W.F., "Fracture Toughness Testing", ASTM (in Co-operation with NASA) , Sym. on Fracture Toughness Testing and its Applications, ASTM STP-381, pp 133-198, (1965).
8. Paris, P.C. and Sih, G.C., "Stress Analysis of Cracks", American Society for Testing and Materials, ASTM STP - 381, pp 30-83, (1965).

9. Swanson, S.R., "Random Load Fatigue Testing, A State of the Art Survey", Materials Research and Standards, Vol. 8, pp 10-44, (1968).
10. Frost, N.E., Pook, P.L. and Denton, K., "A Fracture Mechanics Analysis of Fatigue Crack Growth Data for Various Materials", Engineering Fracture Mechanics, Vol. 3, pp 109-126, (1971).
11. Paris, P.C. and Erdogan, F., "A Critical Analysis of Crack Propagation Laws", Transactions of the ASME, J. of Basic Eng., Vol. 85, pp 528-534, (1963).
12. Forman, F.G., Kearney, V.E. and Engle, R.M., "Numerical Analysis of Crack Propagation in Cyclic Loaded Structures", Trans. ASME, J. of Basic Engineering Vol. 89, p 459, (1967).
13. AGARD-LS-97, Lectures on Fracture Mechanics Design Methodology, Chapter 3, p 10, (1979).
14. Klesnil, M. and Lukas, P., "Influence of Strength and Stress History on Growth and Stabilisation of Fatigue Cracks", Engineering Fracture Mechanics, Vol. 4, pp 77-92, (1972)
15. Hartman, A. and Schijve, J., "The Effect of Environment and Load Frequency on the Crack Propagation Law for Macro Fatigue Crack Growth in Aluminum Alloys", Eng. Fracture Mech., Vol. 1, p 615, (1970).
16. Schütz, W. and Oberparleiter, W., "Ermittlung des Unteren Grenzwertes für den Rißfortschritt bei Flugzeugbauwerkstoffen", IABG-Bericht B - TF - 583.

17. Pelloux, R.M., "Review of Theories and Laws of Fatigue Crack Propagation", AFFDL - TR -70 -144, Proceedings of the Air Force Conference on Fatigue and Fracture of Aircraft Structures and Materials, pp 409 - 416, (1970).
18. Hoepfner, D.W. and Krupp, W.E., "Prediction of Component Life by Application of Fatigue Crack Growth Knowledge", Engineering Fracture Mechanics, Vol.6, pp 47-70, (1974).
19. Nelson, D.V., "Review of Fatigue Crack Growth Prediction Methods", Experimental Mech., Vol.7, 41-49 (1977)
20. Fitzgerald, J.H., "Empirical Formulations for the Analysis and Prediction of Trends for Steady-State Fatigue Crack Growth Rates", J. of Testing and Evaluation, JTEVA, Vol.5.No.5, pp343-353, (1977).
21. Schütz, W., "Calculation Methods for Fatigue Life and Crack Propagation", AGARD - AG -231, Fatigue Design of Fighters, pp 46-76, (1978).
22. Schütz, W., "The Fatigue Life Under Three Different Load Spectra - Test and Calculations", AGARD-CP-118, Sym.on Random Load Fatigue, Denmark, (1972).
23. Wood, H.A., "A Summary of Crack Growth Prediction Techniques", AGARD-LS-62, Lectures on Fatigue Life Prediction for Aircraft Structures and Materials, pp 1-31, (1973).

24. Geiger, W. and Sippel, K.O., "Fatigue Crack Propagation Under Variable Loads", AGARD-AG-257, Practical Application of Fracture Mechanics, Denmark, (1980).
25. Jonas, O. and Wei, R.P., "An Exploratory Study of Delay in Fatigue Crack Growth", Int. Journal of Fracture Mechanics, Vol.7, p116, (1971).
26. Wheeler, O.E., "Spectrum Loading and Crack Growth", Trans. ASME, J. of Basic Engineering, Vol94, pp 181-186, (1972).
27. Elber, W., "The Significance of Fatigue Crack Closure", Damage Tolerance in Aircraft Structures, ASTM STP 486, (1971).
28. Willenborg, J., Engle, R.M. and Wood, H.A., "A Crack Growth Retardation Model Using an Effective Stress Concept", Air Force Dynamics Lab., AFFDL-TM-FBR-71-L, Wright-Patterson Air Force Base, OHIO, (1971).
29. Wei, R.P. and Shih, T.T., "Delay in Fatigue Crack Growth", Int. J. of Fracture Mech., Vol. 10, 77-85, (1974).
30. McCartney, L.N., "A Theoretical Explanation of the Delaying Effects of Overloads on Fatigue Crack Propagation", Int. Journal of Fracture, Vol.14, 213-232, (1978).
31. Irwin, G.R., "Analysis of Stresses and Strains Near the End of a Crack Traversing a Plate", J. Appl. Mech. Trans. ASME, Vol. 24, p 351, (1957).
32. Nelson, D.V. and Fuchs, H.D., "Prediction of Fatigue Crack Growth Under Irregular Loading", Am. Soc. for Testing and Materials, ASTM STP 595 (1976).

33. Barsom, J.M., "Fatigue Crack Growth Under Variable Amplitude Loading in ASTM A514-B Steel", Progress in Flaw Growth and Fracture Toughness Testing, ASTM STP 536, pp 147-167, (1973).
34. Swanson, S.R., Cicci, F. and Hoppe, W., "Crack Propagation in Clad 7079-T6 Aluminum Alloy Sheet Under Constant and Random Amplitude Fatigue Loading", Fatigue Crack Propagation, ASTM STP 415, p312, (1967)
35. Engle, R.M., "CRACKS - A FORTRAN IV Digital Computer Program for Crack Propagation Analysis", AFFDL-TR-70-107, (1970).
36. Engle, R.M., "CRACKS-II User's Manual", AFFDL-TM-74-173, (1974)
37. Wood, H.A. and Haglage, T.L., "Test Results and Analysis of Crack Propagation Under Variable Amplitude Spectrum Loading", AFFDL-TM-FBR-71-2, (1971).
38. Butler, J.P., The Boeing Company, "The Material Selection and Structural Development Process for Aircraft Structural Integrity Under Fatigue Conditions", presented at the Air Force Conference on Fatigue and Fracture of Aircraft Structures and Materials, Miami Beach, Florida, (1979).
39. Bruhn, E.F., "Analysis and Design of Flight Vehicle Structures", Tri-State Offset Company, Cincinnati, OHIO, (1965).
40. Standard Method of Test for "Plane Strain Fracture Toughness of Metallic Materials", ASTM E 399-74 Annual Book of ASTM Standards, Part 10, pp 423-451 (1974)

41. Pearson, H.S. and Packman, P.F., "Fracture Testing Guidelines for Engineers", Fracture Prevention and Control", Proceedings, ASMM/Metalworking Technology Series, No.3, Ed. by D.W.Hoeppner, (1974).
42. Hudson, C.M., "Effect of Stress Ratio on Fatigue-Crack Growth in 7075-T6 and 2024-T3 Aluminum Alloy Specimens", NASA TN D-5390, (1969)
43. Bell, P.D. and Creager, M., "Crack Growth Analysis for Arbitrary Spectrum Loading", AFFDL-TR-74-129, Wright-Patterson Air Force Base, OHIO, (1974)
44. Corbly, D.M. and Packman, P.F., "On the Influence of Single and Multiple Peak Overloads on Fatigue Crack Propagation in 7075-T651 Aluminum", Engineering Fracture Mechanics, Vol.5, pp 479 (1973).
45. Rice, R.C. and Stephens, R.I., "Overload Effects on Subcritical Crack Growth in Austenitic Manganese Steel", Progress in Flaw Growth and Fracture Testing, ASTM STP 536, p 95, (1973).
46. Trebules, V.W., Hertzberg, R.W. and Roberts, R.W., "Effects of Multiple Overloads on Fatigue Crack Propagation in 2024-T3 Aluminum Alloy", ASTM STP 536 p 240, (1973)
47. Von Euw, E.F.J., Hertzberg, R.W. and Roberts, R.W., "Delay Effects in Fatigue Crack Propagation", Stress Analysis and Growth of Cracks, ASTM STP 513, p 113, (1973).

48. Himmelein, M.K. and Hillbery, B.M., "Effect of Stress Ratio and Overload Ratio on Fatigue Crack Delay and Arrest Behaviour Due to Single Peak Overloads", Mechanics of Crack Growth, ASTM STP 590, pp 321-330, (1976).
49. Bathias, C. and Vancon, M., "Mechanisms of Overload Effect on Fatigue Crack Propagation in Aluminum Alloys", Engineering Fracture Mechanics, Vol.10, pp 409-424, (1978).
50. Robin, C. and Pelloux, R.M., "Fatigue Crack Growth Retardation in an Aluminum Alloy", Materials Science and Engineering, Vol.44, pp 115-120, (1980).
51. Saxena, A. and Hudak, S.J., "Review and Extension of Compliance Information for Common Crack Growth Specimens", Int. J. Fracture, Vol. 14, No.5, pp 453-458 (1978).

APPENDIX - A

THE DATA OBTAINED FROM THE EXPERIMENTS

1. CTS 1, Constant Amplitude Test Data

$N \times 10^3$	$\Delta a$ (mm)	$\sum \Delta a$ (mm)	$a$ (mm)	$\Delta P$ (kgf)
30	5.00	5.00	50.00	950
40	0.73	5.73	50.73	550
50	0.11	5.84	50.84	
60	0.05	5.89	50.89	
70	0.08	5.97	50.97	
80	0.08	6.01	51.01	
90	0.06	6.07	51.07	
100	1.42	7.49	52.49	
110	2.36	9.85	54.85	
120	3.46	12.31	57.31	
130	3.76	16.07	61.07	
140	7.87	23.94	68.94	
141	1.79	25.79	70.73	
142	6.39	32.12	77.12	
142.08	0.69	32.81	77.81	



2. CTS 2, Block Loading with Hi-Lo Sequence

Precrack:  $\Delta N = 28000$  cycles,

$\Delta a = 5.5$  mm

$a_0 = 45$  mm

$\Delta P = 950$  kg

$a_i = 50.5$  mm

$N \times 10^3$	$\Delta a$ (mm)	$\Sigma \Delta a$ (mm)	$a$ (mm)	$\Delta P$ (kgf)	$\Delta K$ (kg/mm <sup>3/2</sup> )
1	0.2	0.8	50.7	950	62
2	0.99	1.19	51.69	"	-
3	0.74	1.93	52.43	"	-
4	1.05	2.98	53.49	"	-
5	1.02	4.00	54.5	"	63.7
6	0.1	4.1	54.60	700	-
7	0.1	4.2	54.70	"	-
8	0.14	4.34	54.84	"	-
9	0.5	4.84	55.34	"	-
10	0.58	5.42	55.92	"	49.5
11	0.78	6.20	56.70	"	-
12	0.65	6.85	57.35	"	-
13	0.72	7.57	58.07	"	-
14	0.83	8.40	58.90	"	-
15	0.81	9.21	59.71	"	62.5
16	0.07	9.28	59.78	520	-
17	0.09	9.37	59.87	"	-
18	0.18	9.55	60.05	"	-
19	0.45	10.00	60.50	"	48.9
20	0.64	10.64	61.14	"	-
21	0.46	11.10	61.60	"	-
22	0.45	11.55	62.05	"	-
23	0.48	12.03	62.53	500	-
24	0.34	12.37	62.87	"	-
25	0.55	12.92	63.42	"	52
26	0.53	13.45	63.95	"	-
27	0.72	14.17	64.67	"	-
28	0.63	14.80	65.30	"	-
29	0.73	15.53	66.03	"	-
30	0.91	16.44	66.94	"	61.3
35	0.05	16.49	66.99	300	36.8
40	0.18	16.67	67.17	"	36.86
45	0.25	16.82	67.42	"	37.6
50	1.3	18.12	68.72	"	40

$$\Delta P = P_{max} - P_{min}$$

$$P_{min} = 50 \text{ kg}$$

$N \times 10^3$	$\Delta a$ (mm)	$\sum \Delta a$ (mm)	$a$ (mm)	$\Delta P$ (kgf)	$\Delta K$ (kg/mm <sup>3/2</sup> )
55	1.32	19.44	70.04	300	42.8
60	1.67	21.11	71.71	"	46.6
61	0.46	21.57	72.17	"	
62	0.48	22.05	72.65	"	
63	0.44	22.49	73.09	"	
64	0.68	23.17	73.77	"	
65	0.68	23.85	74.45	"	54.4
66	0.70	24.55	75.10	"	
67	0.92	25.47	76.02	"	
68	1.41	26.88	77.53	"	
69	2.83	29.71	80.36	"	75

$N_f = 69230$  cycles

3. CTS 3, Block Loading with Hi-Lo Sequence

Precrack:  $\Delta N = 10800$  cycles

$\Delta a = 3.61$  mm

$a_o = 45$  mm

$\Delta P = 1150$  kg

$a_i = 48.61$  mm

$N \times 10^3$	$\Delta a$ (mm)	$\sum \Delta a$ (mm)	$a$ (mm)	$\Delta P$ (kgf)	$\Delta K$ (kg/mm <sup>3/2</sup> )
1	0.21	0.21	48.82	950	56
2	0.82	1.03	49.04	"	57.63
3	1.18	2.21	50.80	"	
4	0.85	3.06	51.65	"	
5	1.11	4.17	52.76	"	64.6
6	0.15	4.32	52.91	800	51.35
7	0.49	4.81	53.40	"	
8	0.58	5.39	53.98	"	
9	0.66	6.05	54.64	"	
10	0.73	6.78	55.37	"	56
11	0.03	6.81	55.40	550	41
12	0.04	6.85	55.44	"	
13	0.21	7.06	55.65	"	
14	0.39	7.45	56.04	"	
15	0.25	7.70	56.29	"	42.1
16	0.51	8.21	56.80	"	
17	0.28	8.49	57.08	"	
18	0.40	8.89	57.48	"	
19	0.33	9.22	57.71	"	
20	0.43	9.65	58.24	"	45.1

$N \times 10^3$	$\Delta a$ (mm)	$\sum \Delta a$ (mm)	$a$ (mm)	$\Delta P$ (kgf)	$\Delta K$ (kg/mm <sup>3/2</sup> )
21	0.33	9.98	58.57	550	46
22	0.33	10.30	58.90	"	
23	0.60	10.90	59.50	"	
24	0.48	11.30	59.98	"	
25	0.40	11.70	60.38	"	49.13
26	0.50	12.20	60.88	"	
27	0.55	12.75	61.43	"	
28	0.56	13.31	61.99	"	
29	0.59	13.90	62.58	"	
30	0.60	14.50	63.18	"	55
31	0.02	14.52	63.20	350	35
32	0.02	14.54	63.22	"	
33	0.01	14.55	63.23	"	
34	0.01	14.56	63.24	"	
35	0.01	14.57	63.25	"	35.2
38	0.01	14.58	63.26	"	
40	0.32	14.90	63.58	"	35.7
41	0.30	15.20	63.88	"	
42	0.22	15.44	64.10	"	
43	0.24	15.68	64.34	"	
44	0.21	15.89	64.55	"	
45	0.16	16.05	64.71	"	37.33
46	0.27	16.32	64.98	"	
47	0.31	16.63	65.29	"	
48	0.24	16.87	65.53	"	
49	0.32	17.19	65.85	"	
50	0.23	17.42	66.08	"	39.9
51	0.26	17.68	66.34	"	
52	0.26	17.94	66.60	"	
53	0.33	18.27	66.93	"	
54	0.28	18.55	67.21	"	
55	0.40	18.95	67.61	"	42.8
56	0.21	19.16	67.82	"	
57	0.39	19.55	68.21	"	
58	0.32	19.87	68.53	"	
59	0.35	20.22	68.88	"	
60	0.36	20.58	69.24	"	46.31
61	0.37	20.95	69.61	"	
62	0.67	21.62	70.28	"	
63	0.48	22.10	70.76	"	
64	0.57	22.67	71.33	"	
65	0.62	23.29	71.95	"	53.1
70	0.06	23.35	72.01	150	23
80	0.07	23.42	72.08	"	23
85	0.02	23.44	72.10	"	23.1

$N \times 10^3$	$\Delta a$ (mm)	$\sum \Delta a$ (mm)	$a$ (mm)	$\Delta P$ (kgf)	$\Delta K$ (kg/mm <sup>3/2</sup> )
90	0.03	23.47	72.13	150	23.15
95	0.02	23.49	72.15	"	23.2
100	0.02	23.51	72.17	"	
105	0.01	23.52	72.18	"	
110	-				
115	-				
120	-				
125	-				
130	-				
135	-				
140	-				
145	0.22	23.75	72.40	250	39.1
146	0.37	24.12	72.77	"	
147	0.35	24.47	73.12	"	
148	0.30	24.77	73.42	"	
149	0.31	25.08	73.73	"	
150	0.34	25.42	74.07	"	42.37
151	0.36	25.78	74.43	"	
152	0.52	26.30	74.95	"	
153	0.52	26.82	75.47	"	
154	0.51	27.33	75.98	"	
155	0.53	27.86	76.51	"	52.3
156	0.67	28.53	77.18	"	
157	0.79	29.32	77.97	"	
158	0.88	30.20	78.85	"	
159	1.40	31.60	80.25	"	
160	2.26	33.86	82.51	"	71.56

$N_f = 160320$  cycles

4. CTS 4, At displacement control

Precrack:  $\Delta N = 31070$  cycles

$\Delta a = 2$  mm

$\Delta P = 1150$  kg

$a_0 = 45$  mm

$a_i = 47$  mm

$N \times 10^3$	$\Delta a$ (mm)	$\Sigma \Delta a$ (mm)	$a$ (mm)	$\Delta P$ (kgf)	$\Delta K$ (kg/mm <sup>3/2</sup> )
1	0.20	0.20	47.20		
2	0.53	0.73	47.73		
3	0.64	1.37	48.37		
4	0.61	1.98	48.98		
5	0.66	2.64	49.64		
6	0.74	3.38	50.38		
7	0.73	4.11	51.11		
8	0.59	4.70	51.70		
9	0.54	5.24	52.24		
10	0.85	6.09	53.09		
11	1.33	7.42	54.42		
12	1.45	8.87	55.87		
13	1.64	10.51	57.51		
14	2.56	13.07	60.07		
15	2.71	15.78	62.78		
15.55	0.88	16.66	63.66	770	
16	1.14	17.80	64.80	710	
16.5	1.36	19.16	66.16	670	77.3
17	1.14	20.30	67.30	610	
17.5	1.00	21.30	68.30	580	
18	0.91	22.21	69.21	540	73
18.5	1.21	23.42	70.42	510	
19	1.08	24.50	71.50	475	
19.5	0.92	25.42	72.42	440	
20	0.65	26.07	73.07	405	67.3
20.5	1.01	27.08	74.08	370	
21	0.75	27.83	74.83	360	
21.5	0.65	28.48	75.48	340	
22	0.27	28.75	75.75	328	
22.5	0.57	29.32	76.32	310	

$N \times 10^3$	$\Delta a$ (mm)	$\Sigma \Delta a$ (mm)	$a$ (mm)	$\Delta P$ (kgf)	$\Delta K$ (kg/mm <sup>3/2</sup> )
23	1.57	30.89	77.89	290	
23.5	0.56	31.45	78.45	270	
24	0.57	32.02	79.02	250	
24.5	0.61	32.63	79.63	240	
25	0.65	33.28	80.28	220	56.5
25.5	0.37	33.65	80.65	212	
26	0.48	34.13	81.13	190	
26.5	0.71	34.84	81.84	172	
27	0.47	35.31	82.31	170	
27.5	0.42	35.73	82.73	162	
28	0.47	36.20	83.20	155	
28.5	0.34	36.54	83.54	140	
29	0.60	37.14	84.14	140	
29.5	0.23	37.37	84.37	135	
30	0.44	37.81	84.81	125	40.4
30.5	0.44	38.25	85.25	115	
31	0.53	38.78	85.78	100	
31.5	0.61	39.39	86.39	90	
32	0.38	39.77	86.77	85	
32.5	0.48	40.25	87.25	90	
33	0.35	40.60	87.60	90	
33.5	0.31	40.91	87.91	80	
34	0.47	41.38	88.38	70	
34.5	0.28	41.66	88.66	62	
35	0.35	42.01	89.01	65	27.3
35.5	0.25	42.26	89.26	64	
36	0.31	42.57	89.57	60	26
36.5	0.37	42.94	89.94	55	
37	0.23	43.17	90.17	52	
37.5	0.30	43.47	90.47	50	
38	0.14	43.61	90.61	50	19

Note that: ( $a \uparrow, \Delta K \downarrow$ )

5. CTS 5, Single Overload Test Data

Precrack:  $\Delta N = 19200$  cycles

$\Delta a = 5$  mm

$a_0 = 45$  mm

$\Delta P = 1150$  kg

$a_i = 50$  mm

$N \times 10^3$	$\Delta a$ (mm)	$\sum \Delta a$ (mm)	$a$ (mm)	$\Delta P$ (kgf)	$\Delta K$ (kg/mm <sup>3/2</sup> )
5	0.05	0.05	50.05	750	48
6.5	0.13	0.18	50.18	"	
7	0.31	0.49	50.49	"	
7.5	0.19	0.68	50.68	"	
8	0.28	0.96	50.96	"	
8.5	0.35	1.31	51.31	"	
9	0.36	1.67	51.67	"	
10	0.73	2.40	52.40	"	52

\* Overload (O/L=1.5) - - - - - 1150

10.5	0.13	2.53	52.53	750	53.2
11	0.03	2.56	52.56	"	
11.5	-				
12	-				
12.5	0.06	2.62	52.62	"	
13	-				
13.5	0.59	3.21	53.21	"	
14	0.41	3.62	53.62	"	
14.5	0.46	4.08	54.08	"	
15	0.50	4.58	54.58	"	55.5
15.5	0.49	5.07	55.07	"	
16	0.44	5.51	55.51	"	
16.5	0.32	5.83	55.83	"	
17	0.61	6.44	56.44	"	
17.5	0.60	7.04	57.04	"	
18	0.59	7.63	57.63	"	
18.5	0.56	8.19	58.19	"	
19	0.61	8.80	58.80	"	
19.5	0.80	9.60	59.60	"	
20	0.94	10.54	60.54	"	69

\* Overload (O/L=1.5) - - - - - 1150

$N \times 10^3$	$\Delta a$ (mm)	$\sum \Delta a$ (mm)	$a$ (mm)	$\Delta P$ (kgf)	$\Delta K$ (kg/mm <sup>3/2</sup> )
20.5	0.24	10.78	60.78	750	69.5
21	-				
21.5	0.47	11.25	61.25	"	
22	0.74	11.99	61.99	-- "	73.8
22.5	1.36	13.35	63.35	"	
23	2.08	15.43	65.43	"	
23.5	1.59	17.02	67.02	--- "	- 92
* $P_{\max} = 533$ kgf ( $\Delta P = P_{\max} - P_{\min} = 533 - 50 = 483$ kgf)					
24	0.05	17.07	67.07	483	59.2
24.5	-				
25	-				
25.5	0.03	17.10	67.10	"	
26	-				
26.5	-				
27	-				
27.5	0.22	17.32	67.32	"	
28	0.34	17.66	67.66	"	
28.5	0.83	18.49	68.49	"	63.8
* Overload (O/L = 1.5) $\Delta P = 800 - 50 = 750$ kgf					
29	0.44	18.93	68.93	483	64.4
29.5	-				
30	0.14	19.07	69.07	"	
30.5	0.51	19.58	69.58	"	
31	0.97	20.55	70.55	--- "	70.4
31.5	1.27	21.82	71.82	"	
32	2.10	23.92	73.92	--- "	85
* Overload (O/L = 1.75) $\Delta P = 630 - 50 = 580$ kgf					
32.5	0.14	24.06	74.06	310	54.8
33	0.02	24.08	74.08	"	
33.5	0.11	24.19	74.19	"	
34	0.02	24.21	74.21	"	
34.5	0.02	24.23	74.23	--- "	55.26
35.5	-				
36	0.02	24.25	74.25	"	
36.5	-				
37	0.07	24.32	74.32	"	
37.5	0.04	24.36	74.36	"	
38.5	0.14	24.50	74.50	--- "	56.2
39.5	1.15	25.65	75.65	"	
40	1.19	26.84	76.84	"	
40.5	1.82	26.82	78.66	"	

$N_f = 40560$  cycles



6. CTS 6, Single Overload Test Data

Pre-crack:  $\Delta N = 7360$  cycles

$\Delta a = 1.5$  mm

$\Delta P = 1150$  kg

$a_0 = 45$  mm

$a_i = 46.5$  mm

Overload Ratio: (O/L) = 1.5

$P_{max_{OL}} = 900$  kg

$P_{max} = 600$  kg (Baseline load)

$P_{min} = 50$  kg

$N \times 10^3$	$\Delta a$ (mm)	$\sum \Delta a$ (mm)	$a$ (mm)	$\Delta P$ (kgf)	$\Delta K$ (kg/mm <sup>3/2</sup> )
1.5	0.01	0.01	46.51	550	32
3.5	0.07	0.08	46.58	"	
4.5	0.01	0.09	46.59	"	
---					
---					
---					
312	0.36	0.45	46.95	"	32.3
313	0.15	0.60	47.10	"	
313.5	0.13	0.73	47.23	"	
314	0.18	0.91	47.41	"	
314.5	0.08	0.99	47.49	"	
315	0.12	1.11	47.61	"	33
316	0.09	1.20	47.70	"	
317	0.09	1.29	47.79	"	
318	0.06	1.35	47.85	"	
319	0.05	1.40	47.90	"	
320	0.18	1.58	48.08	"	33.36
321	0.09	1.67	48.17	"	
321.5	0.04	1.71	48.21	"	
322	0.07	1.78	48.28	"	
323.5	0.07	1.91	48.41	"	
324	0.05	1.96	48.46	"	
324.5	0.06	2.02	48.52	"	
325	0.05	2.07	48.57	"	33.85

$N \times 10^3$	$\Delta a$ (mm)	$\sqrt{\Delta a}$ (mm)	$a$ (mm)	$\Delta P$ (kgf)	$\Delta K$ (kg/mm <sup>3/2</sup> )
325.5	0.07	2.14	48.64	550	
326	0.07	2.21	48.71	"	
327.5	0.07	2.28	48.78	"	
328	0.06	2.34	48.84	"	
328.5	0.07	2.41	48.91	"	
329.5	0.06	2.47	48.97	"	
330	0.10	2.57	49.07	"	34.3
331	0.08	2.65	49.15	"	
331.5	0.05	2.70	49.20	"	
332.5	0.08	2.78	49.28	"	
333.5	0.13	2.99	49.49	"	
335	0.13	3.12	49.62	"	34.8

\* Overload (O/L=1.5) →  $\Delta P$  900-50 = 850 kgf

335.2	0.05	3.17	49.67	550	
335.4	0.03	3.20	49.70	"	
339	0.03	3.23	49.73	-----	34.9
339.5	0.03	3.26	49.76	"	
341.2	0.09	3.35	49.85	"	
341.5	0.05	3.40	49.90	"	
341.7	0.03	3.43	49.93	"	
342.2	0.05	3.48	49.98	"	
342.5	0.07	3.55	50.05	"	
343	0.06	3.61	50.11	"	
343.2	0.04	3.66	50.15	"	
343.7	0.07	3.72	50.22	"	
344	0.02	3.74	50.24	"	
344.2	0.03	3.77	50.27	"	
345	0.09	3.86	50.36	-----	35.56
345.5	0.07	3.93	50.43	"	
346	0.09	4.02	50.52	"	
347	0.08	4.10	50.60	"	
347.5	0.06	4.16	50.66	"	
348	0.07	4.23	50.73	"	
348.5	0.05	4.28	50.78	"	
349	0.06	4.34	50.84	"	
349.5	0.08	4.44	50.92	"	
350	0.06	4.50	50.98	-----	36.3
350.5	0.06	4.56	51.04	"	
351	0.08	4.64	51.12	"	
351.5	0.14	4.78	51.26	"	
352	0.10	4.88	51.36	"	
352.5	0.09	4.97	51.45	"	
353	0.08	5.05	51.53	"	
353.5	0.04	5.09	51.57	"	

$N \times 10^3$	$\Delta a(\text{mm})$	$\sum \Delta a(\text{mm})$	$a(\text{mm})$	$\Delta P(\text{kgf})$	$\Delta K(\text{kg/mm}^{3/2})$
354	0.07	5.16	51.64	550	
354.5	0.07	5.23	51.71	"	
355	0.07	5.30	51.78	"	37.03
355.5	0.10	5.40	51.88	"	
356	0.06	5.46	51.94	"	
356.5	0.06	5.52	52.00	"	
357	0.08	5.60	52.08	"	
358	0.20	5.80	52.28	"	
359	0.16	5.96	52.44	"	
360	0.20	6.16	52.64	"	38.5
361	0.16	6.32	52.80	"	
362	0.16	6.48	52.96	"	
363	0.30	6.78	53.26	"	
364	0.20	6.98	53.46	"	
365	0.19	7.14	53.65	"	
366	0.19	7.33	53.84	"	
367	0.29	7.62	54.13	"	
368	0.23	7.85	54.36	"	
369	0.22	8.07	54.58	"	41.06
370	0.33	8.40	54.91	"	
371	0.26	8.66	55.17	"	
372	0.34	9.00	55.51	"	
373	0.18	9.18	55.69	"	
374	0.39	9.57	56.08	"	
375	0.33	9.90	56.41	"	43.63
376	0.35	10.25	56.76	"	
377	0.35	10.60	57.11	"	
378	0.39	10.99	57.50	"	
379	0.32	11.31	57.82	"	
380	0.48	11.79	58.30	"	46.2
381	0.54	12.33	58.84	"	47.2

\* Overload (O/L=1.5)

381.2	0.04	12.37	58.88	"	47.21
381.5	0.09	12.46	58.97	"	
381.7	0.02	12.48	58.99	"	
382	-	-	-	"	
382.5	0.15	12.63	59.14	"	
382.7	0.10	12.73	59.24	"	
383	0.04	12.77	59.28	"	
383.2	0.03	12.80	59.31	"	

$N \times 10^3$	$\Delta a(\text{mm})$	$\sum \Delta a(\text{mm})$	$a(\text{mm})$	$\Delta P(\text{kgf})$	$\Delta K(\text{kg}/\text{mm}^{3/2})$
383.5	0.12	12.92	59.43	550	
383.7	0.11	13.03	59.54	"	
384	0.16	13.19	59.70	"	
384.2	0.08	13.27	59.78	"	
384.5	0.22	13.49	60.00	"	
384.7	0.16	13.65	60.16	"	
385	0.09	13.74	60.25	"	49.86
385.5	0.39	14.13	60.64	"	
386	0.24	14.37	60.88	"	
386.5	0.33	14.70	61.21	"	
387	0.47	15.17	61.68	"	53.27
387.5	0.35	15.52	62.03	"	
388	0.42	15.94	62.45	"	
388.5	0.51	16.45	62.96	"	
389	0.50	16.95	63.46	"	
389.5	0.29	17.24	63.75	"	
390	0.52	17.76	64.27	"	59.4
390.5	0.53	18.29	64.80	"	
391	0.61	18.90	65.41	"	
391.5	0.69	19.59	66.10	"	
392	0.75	20.34	66.85	"	
392.5	0.95	21.29	67.80	"	
393	0.98	22.27	68.78	"	73.33

\* Overload ( $O/L = 1.5$ )

393.2	0.46	22.73	69.24	"	
393.5	0.12	22.85	69.36	"	
393.7	0.26	23.11	69.62	"	
394	0.08	23.19	69.70	"	77
394.2	0.35	23.54	70.05	"	
394.5	0.83	24.37	70.88	"	
394.7	0.95	25.32	71.83	"	
394.85	1.06	26.38	72.89	"	
395	1.47	27.85	74.36	"	99
395.1	2.92	30.77	77.28	"	

$N_f = 395110$  cycles

7. NTS 8, Single Overload Test Data

Pre-crack:  $\Delta N = 12150$  cycles

$\Delta a = 2$  mm

$\Delta P = 950$  kg

$a_o = 45$  mm

$a_i = 47$  mm

Overload Ratio: (O/L) = 1.25

$P_{max_{OL}} = 750$  kg

$P_{max} = 600$  kg

$P_{min} = 50$  kg

$N \times 10^3$	$\Delta a$ (mm)	$\Sigma \Delta a$ (mm)	$a$ (mm)	$\Delta P$ (kgf)	$\Delta K$ (kg/mm <sup>3/2</sup> )
1	-				32.34
10	-				
15	-				
18	-				
19	0.12	0.12	47.12	550	
20	0.20	0.32	47.32	"	32.6
21	0.40	0.72	47.72	"	
21.5	0.17	0.89	47.89		
22	0.17	1.06	48.06	"	33.2
22.5	0.13	1.19	48.19	"	
23	0.20	1.39	48.39	"	33.5
23.5	0.22	1.61	48.61	"	
24	0.12	1.73	48.73	"	33.73
24.5	-				
25	0.24	1.97	48.97	"	
25.5	0.18	2.15	49.15	"	34.3
26	-				
26.5	-				
27	0.20	2.35	49.35	"	
27.5	-				
28	0.16	2.51	49.51	"	34.5
28.5	0.11	2.62	49.62	"	34.8

\* Overload (O/L) = 1.25  $\Delta P = 750 - 50 = 700$  kgf

$N \times 10^3$	$\Delta a$ (mm)	$\sum \Delta a$ (mm)	$a$ (mm)	$\Delta P$ (kgf)	$\Delta K$ (kg/mm <sup>3/2</sup> )
28.8	0.13	2.75	49.75	550	34.8
29.2	0.06	2.81	49.81	"	
29.4	-				
29.6	0.03	2.84	49.84	"	
29.8	0.10	2.94	49.94	"	
30	0.06	3.00	50.00	---	35.2
30.2	-				
30.4	0.03	3.03	50.03	"	
30.6	-				
30.8	-				
31	0.03	3.06	50.06	"	
31.2	-				
31.5	0.13	3.19	50.19	"	
31.8	-				
32	0.08	3.27	50.27	"	
32.3	0.16	3.43	50.43	---	35.5
32.5	-				
33	0.15	3.58	50.58	"	
33.5	0.10	3.68	50.68	"	
34	0.10	3.78	50.78	"	
34.5	0.15	3.93	50.93	"	
35	0.09	4.02	51.02	---	36.3
35.5	0.09	4.11	51.11	"	
36	0.11	4.22	51.22	"	
36.5	0.11	4.33	51.33	---	35.93
37	0.19	4.52	51.52	"	
37.5	0.13	4.65	51.65	"	
38	0.11	4.76	51.76	"	
38.5	0.13	4.89	51.89	"	
39	0.09	4.98	51.98	"	
39.5	0.08	5.06	52.06		37.4
40	0.08	5.14	52.14	---	37.42
40.5	0.15	5.29	52.29	"	
41	0.11	5.40	52.40	"	
42	0.27	5.67	52.67	"	
43	0.26	5.93	52.93	---	38.8
44	0.23	6.16	53.16	"	
45	0.29	6.45	53.45	---	39.2
46	0.26	6.71	53.71	"	
47	0.29	7.00	54.00	---	40
48	0.25	7.25	54.25	"	
49	0.31	7.56	54.56	---	40.55
50	0.31	7.87	54.87	"	
51	0.27	8.14	55.14	"	41.25
52	0.31	8.45	55.45	"	
53	0.38	8.83	55.83	---	42
54	0.25	9.08	56.08	"	
55	0.39	9.47	56.47	"	43.6
56	0.31	9.78	56.78	"	
57	0.38	10.16	57.16	---	44.36
58	0.49	10.65	57.65	"	

$N \times 10^3$	a(mm)	a(mm)	a(mm)	P(kgf)	K(kg/mm <sup>3/2</sup> )
59	0.36	11.01	58.01	550	45.83
60	0.36	11.37	58.37	"	
61	0.53	11.90	58.90	"	47.5
* Overload (O/L) = 1.25					
61.2	0.06	11.96	58.96	"	
61.4	0.05	12.01	59.01	"	
61.6	0-				
61.8	0.06	12.07	59.07	"	
62	0.09	12.16	59.16	"	
62.2	0.16	12.32	59.32	"	48.4
62.4	0.15	12.47	59.47	"	
62.6	0.07	12.54	59.54	"	
62.8	0.11	12.65	59.65	"	
63	0.17	12.82	59.82	"	49.13
63.2	0.05	12.87	59.87	"	
63.4	0.13	13.00	60.00	"	49.35
63.6	0.12	13.12	60.12	"	
63.8	0.13	13.25	60.25	"	
64	0.13	13.38	60.38	"	
64.5	0.37	13.75	60.75	"	
65	0.24	13.99	60.99	"	51.3
65.5	0.31	14.30	61.30	"	
66	0.55	14.85	61.85	"	
66.5	0.35	15.20	62.20	"	54.26
67	0.35	15.55	62.55	"	
67.5	0.28	15.83	62.83	"	55.36
68	0.43	16.26	63.26	"	56.5
68.5	0.47	16.73	63.73	"	
69	0.37	17.10	64.10	"	59
70	1.32	18.42	65.42	"	62.33
71	1.50	19.92	66.92	"	67
72	1.90	21.82	68.82	"	73.33

\* Overload (O/L) = 1.25

72.2	0.48	22.30	69.30	"	75
72.4	0.55	22.85	69.85	"	
72.6	0.70	23.55	70.55	"	80.66
72.8	1.34	24.89	71.89	"	86.9
73	1.40	26.29	73.29	"	92
73.1	1.82	28.11	75.11	"	102.6

$N_f = 73150$  cycles

8. CTS 9, Single Overload Test Data

Precrack:  $\Delta N = 12170$  cycles

$\Delta a = 2.12$  mm

$a_0 = 45$  mm

$\Delta P = 950$  kg

$a_i = 47.12$  mm

Overload Ratio: (O/L) = 2.0

$P_{max} = 1200$  kg

$P_{max} = 600$  kg

$P_{min} = 50$  kg

$N \times 10^3$	$\Delta a$ (mm)	$\Sigma \Delta a$ (mm)	$a$ (mm)	$\Delta P$ (kgf)	$\Delta K$ (kg/mm <sup>3/2</sup> )
1	-				
5	-				
10	-				
15	-				
20	-				
23	-				
24	0.26	0.26	47.38	550	32.2
25	0.16	0.42	47.54	"	
26	0.30	0.72	47.84	"	33
27	0.48	1.20	48.32	"	
28	0.21	1.41	48.53	"	33.73
29	0.49	1.90	49.02	"	34
30	0.25	2.15	49.27	"	
31	0.20	2.35	49.47	"	34.4

\* Overload (O/L) = 2.0  $\Delta P = 1200 - 50 = 1150$  kgf

31.2	0.05	2.40	49.52	550	34.63
31.6	0.04	2.44	49.56	"	
32	-				
40	-				
50	-				
53	-				
54	0.13	2.57	49.69	"	34.8
55	0.24	2.81	49.93	"	
56	0.40	3.21	50.33	"	
57	0.31	3.52	50.64	"	
58	0.33	3.85	50.97	"	36.29
59	0.3	4.15	51.27	"	
60	0.42	4.57	51.69	"	
61	0.13	4.70	51.82	"	36.6
62	0.30	5.00	52.12	"	



$N \times 10^3$	$\Delta a$ (mm)	$\Sigma \Delta a$ (mm)	$a$ (mm)	$\Delta P$ (kgf)	$\Delta K$ (kg/mm <sup>3/2</sup> )
63	0.35	5.35	52.47	550	37.5
64	0.37	5.72	52.84	"	38
65	0.29	6.01	53.13		
66	0.14	6.15	53.27		
67	0.19	6.34	53.46	- - -	39.2
68	0.36	6.70	53.82	"	
69	0.38	7.08	54.20		
70	0.32	7.40	54.52	- - - - -	40.5
71	0.30	7.70	54.82	"	
72	0.38	8.08	55.20	"	
73	0.48	8.56	55.68	"	42
74	0.23	8.79	55.91	"	
75	0.44	9.23	56.35	"	42.9
76	0.31	9.54	56.66	"	44
77	0.48	10.02	57.14	"	44.36
78	0.45	10.47	57.59	"	44.73
79	0.49	10.96	58.08	"	45.83
80	0.41	11.37	58.49	"	46.80
81	0.45	11.82	58.94	"	46.87
* Overload (O/L) = 2.0					
81.2	0.28	12.10	59.22	"	48
81.5	0.06	12.16	59.28	"	
82	0.09	12.25	59.37	"	48.03
85	-			"	
90	-			"	
92	-			"	
93	0.09	12.34	59.46	"	
94	0.13	12.47	59.59	"	48.56
95	0.25	12.72	59.84	"	49
96	0.50	13.22	60.34	"	49.86
97	0.75	13.97	61.09	"	51.33
98	1.13	15.10	62.22	"	53.9
99	1.02	16.12	63.24	"	56.46
100	1.16	17.28	64.40	"	60
100.5	0.75	18.03	65.15	"	61.6
101	0.53	18.56	65.68	"	63
101.5	0.77	19.33	66.45	"	66
102	0.97	20.30	67.42	"	68.5
102.15	0.60	20.90	68.02	"	

$N_f = 102150$  cycles

APPENDIX - B

FRACTURE TOUGHNESS TEST PROCEDURE

The following specific items of the ASTM criteria for Fracture Toughness Tests;

1. Precrack length requirement: Minimum precrack length must be 0.050 in. (0.127 mm) and must be greater than 5% of total crack length (a) at all points along the crack front.

2. The maximum stress intensity of the final 2.5 % crack length, a, divided by the modulus must be less than  $0.0012^{1/2}$ .

3. The maximum stress intensity during the final precracking divided by the yield must be less than  $0.6 K_Q/S_y$ .

4. The minimum specimen thickness must <sup>be</sup> greater than or equal to 2.5 times the square of the ratio of  $K_Q$  to the yield stress

$$B \geq 2.5 (K_Q/S_y)^2$$

$K_{IC}$  Test Procedure:

1. Determine critical specimen size dimensions

$$B, a \geq 2.5 (K_{IC}/S_y)^2$$

$$W \geq 5.0 (K_{IC}/S_y)^2$$

2. Select a test specimen and prepare shop drawings

There are two standard specimen designs, namely the slow-bend test specimen and the compact tension specimen. It was tested the compact tension specimen (CTS). The initial machined crack length,  $a$ , should be  $0.45 W$  so that the crack can be extended by fatigue to approximately  $0.5 W$ .

3. Fatigue crack the test specimen

Because a fatigue crack is considered to be the sharpest crack that can be reproduced in the laboratory, the machine notch is extended by fatigue. The fatigue crack should extend at least  $0.05W$  ahead of the machined notch to eliminate any effects of the geometry of the machined notch.

4. Obtain test fixtures and displacement gage

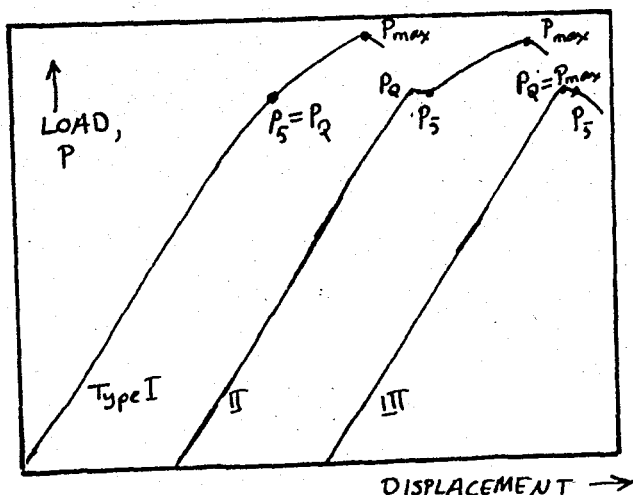
Recommended bend test and tension testing fixtures for CTS testing are described in reference [40]. These fixtures were developed to minimize friction and have been used successfully by numerous laboratories.

### 5. Test Procedure

The displacement gage should be seated in the knife-edges to maintain registry between the knife-edges and the gage groove. The specimens should be loaded at a rate such that the rate of increase of stress intensity is within the range  $30 - 150 \text{ ksi}\sqrt{\text{in}}/\text{min}$ ., corresponding to a loading rate for the 1 in. thick specimen between 4500 and 22500 lb/min. A photograph showing a typical compact tension test set-up is presented in Figure 4.8.

### 6. Analysis of P- $\Delta$ records

If a material exhibited perfectly elastic behaviour until fracture, the load-displacement curve would be merely a straight line until fracture. The principal types of load-displacement curves observed are presented in below figure.



To establish that a valid  $K_{IC}$  has been determined, it is necessary first to calculate a conditional result,  $K_Q$ , which involves a construction on the test record.

7. Calculation of conditional  $K_{IC}$  ( $K_Q$ )

After determining  $P_Q$  for the compact tension specimen, calculate  $K_Q$  using the following expression.

$$K_Q = \frac{P_Q}{B\sqrt{W}} \left[ 29.6 \left( \frac{a}{W} \right)^{1/2} - 185.5 \left( \frac{a}{W} \right)^{3/2} + 655.7 \left( \frac{a}{W} \right)^{5/2} - 1017 \left( \frac{a}{W} \right)^{7/2} + 638.9 \left( \frac{a}{W} \right)^{9/2} \right]$$

$P_Q$  = load

$B$  = thickness of specimen

$W$  = width of specimen

$a$  = crack length

8. Final check for  $K_{IC}$

Calculate  $2.5(K_Q/S_y)^2$  where  $S_y = 0.2$  % offset yield strength in tension. If this quantity is less than both the thickness and the crack length of the specimen, then  $K_Q$  is equal to  $K_{IC}$ . Otherwise it is necessary to use a larger specimen to determine  $K_{IC}$  in order to satisfy this requirement.